

*Midwest State's Regional Pooled Fund Program
Research Project Number SPR-3(017)*

CRASH TESTING OF SOUTH DAKOTA'S CABLE GUARDRAIL TO W-BEAM TRANSITION

Submitted by

Ronald K. Faller, Ph.D., P.E.
Research Assistant Professor

Dean L. Sicking, Ph.D., P.E.
Associate Professor and MwRSF Director

John R. Rohde, Ph.D., P.E.
Associate Professor

James C. Holloway, M.S.C.E., E.I.T.
Facilities Operations Manager

Eric A. Keller, B.S.M.E., E.I.T.
Computer Design Technician II

John D. Reid, Ph.D.
Assistant Professor

MIDWEST ROADSIDE SAFETY FACILITY

University of Nebraska-Lincoln
1901 "Y" Street, Building "C"
Lincoln, Nebraska 68588-0601
(402) 472-6864

Submitted to

SOUTH DAKOTA DEPARTMENT OF TRANSPORTATION

Office of Research
700 East Broadway Avenue
Pierre, South Dakota 57501-2586

MwRSF Research Report No. TRP-03-80-98

December 4, 1998

Technical Report Documentation Page

1. Report No. SD98-16		2.		3. Recipient's Accession No.	
4. Title and Subtitle Crash Testing of South Dakota's Cable Guardrail to W-Beam Transition		5. Report Date December 4, 1998		6.	
7. Author(s) Faller, R.K., Sicking, D.L., Rohde, J.R., Holloway, J.C., Keller, E.A., and Reid, J.D.		8. Performing Organization Report No. TRP-03-80-98			
9. Performing Organization Name and Address Midwest Roadside Safety Facility (MwRSF) University of Nebraska-Lincoln 1901 Y St., Bldg. C Lincoln, NE 68588-0601		10. Project/Task/Work Unit No.		11. Contract © or Grant (G) No. SPR-3(017)	
12. Sponsoring Organization Name and Address South Dakota Department of Transportation Office of Research 700 East Broadway Avenue Pierre, South Dakota 57501-2586		13. Type of Report and Period Covered Final Report 1998		14. Sponsoring Agency Code	
15. Supplementary Notes Prepared in cooperation with U.S. Department of Transportation, Federal Highway Administration					
16. Abstract (Limit: 200 words) A cable guardrail to W-beam transition system, used by the South Dakota Department of Transportation, was crash tested to determine whether the system meets current safety standards. The three-strand cable guardrail with reduced post spacing was attached to a standard W-beam guardrail which incorporated a breakaway cable terminal (BCT) on the upstream end. Three full-scale crash tests were successfully performed according to the Test Level 3 requirements specified in NCHRP Report 350: <i>Recommended Procedures for the Safety Performance Evaluation of Highway Features</i> . Two tests - one using a small car and one with a pickup truck - were used to evaluate the potential for vehicle snagging in the region where the cable guardrail transitions into the W-beam guardrail. One additional pickup truck crash test was performed to evaluate the potential for snagging and pocketing when the pickup impacts the cable guardrail upstream of the BCT terminal and deflects the cable guardrail such that the pickup contacts the terminal in a critical manner. The South Dakota cable guardrail to W-beam transition successfully met current safety standards and is recommended for use along the National Highway System.					
17. Document Analysis/Descriptors Highway Safety, Guardrail Longitudinal Barrier, Approach Guardrail Transition		Roadside Appurtenances, Crash Test, Compliance Test		18. Availability Statement No restrictions. Document available from: National Technical Information Services, Springfield, Virginia 22161	
19. Security Class (this report) Unclassified	20. Security Class (this page) Unclassified	21. No. of Pages 123	22. Price		

DISCLAIMER STATEMENT

The contents of this report reflect the views of the authors who are responsible for the facts and the accuracy of the data presented herein. The contents do not necessarily reflect the official views or policies of the South Dakota Department of Transportation nor the Federal Highway Administration. This report does not constitute a standard, specification, or regulation.

ACKNOWLEDGMENTS

The authors wish to acknowledge several sources that made a contribution to this project: (1) the South Dakota Department of Transportation for sponsoring this project; (2) MwRSF personnel for constructing the barriers and conducting the crash tests; and the Nebraska Department of Roads for its cooperation in administering the research agreement. A special thanks is also given to the following individuals who made a contribution to the completion of this research project.

Midwest Roadside Safety Facility

K.L. Krenk, B.S.M.E., Field Operations Manager
M.L. Hanau, Laboratory Mechanic I
Undergraduate and Graduate Assistants

Nebraska Department of Roads

Leona Kolbet, Research Coordinator
Ken Sieckmeyer, Transportation Planning Manager

South Dakota Department of Transportation

David Huft, Research Engineer, Office of Research
Daris Ormesher, Office of Research
Daniel Strand, Office of Research
Tim Bjorneberg, P.E., Chief Road Design Engineer, Office of Roadway Design
Dean Hoelscher, Office of Roadway Design
Paul Knofczynski, P.E., Office of Roadway Design
Mike Young, P.E., Operations Support
Charles Olsen, Mitchell Operations
Jeff Gustafson, P.E., Mitchell Operations

Federal Highway Administration

Roland Stanger, P.E., Traffic and Safety Engineer

Dunlap Photography

James Dunlap, President and Owner

TABLE OF CONTENTS

	Page
TECHNICAL REPORT DOCUMENTATION PAGE	i
DISCLAIMER STATEMENT	ii
ACKNOWLEDGMENTS	iii
TABLE OF CONTENTS	v
List of Figures	vi
List of Tables	viii
1 INTRODUCTION	1
1.1 Problem Statement	1
1.2 Objective	1
1.3 Scope	1
2 BACKGROUND	3
3 TEST REQUIREMENTS AND EVALUATION CRITERIA	4
3.1 Test Requirements	4
3.2 Evaluation Criteria	4
4 CABLE GUARDRAIL TO W-BEAM TRANSITION	7
5 TEST CONDITIONS	17
5.1 Test Facility	17
5.2 Vehicle Tow and Guidance System	17
5.3 Test Vehicles	17
5.4 Data Acquisition Systems	19
5.4.1 Accelerometers	19
5.4.2 Rate Transducer	19
5.4.3 High-Speed Photography	20
5.4.4 Pressure Tape Switches	21
6 COMPUTER SIMULATION	32
7 CRASH TEST NO. 1	33
7.1 Test SDC-1	33
7.2 Test Description	33
7.3 Barrier Damage	35
7.4 Vehicle Damage	35

7.5 Occupant Risk Values	36
7.6 Discussion	36
8 CRASH TEST NO. 2	49
8.1 Test SDC-2	49
8.2 Test Description	49
8.3 Barrier Damage	50
8.4 Vehicle Damage	51
8.5 Occupant Risk Values	51
8.6 Discussion	52
9 CRASH TEST NO. 3	64
9.1 Test SDC-3	64
9.2 Test Description	64
9.3 Barrier Damage	65
9.4 Vehicle Damage	66
9.5 Occupant Risk Values	66
9.6 Discussion	66
10 SUMMARY AND CONCLUSIONS	76
11 RECOMMENDATIONS	78
12 REFERENCES	79
13 APPENDICES	81
APPENDIX A - DESIGN DETAILS FOR CABLE GUARDRAIL TO W-BEAM TRANSITION	82
APPENDIX B - ACCELEROMETER DATA ANALYSIS, SDC-1	97
APPENDIX C - RATE TRANSDUCER DATA ANALYSIS, SDC-1	104
APPENDIX D - ACCELEROMETER DATA ANALYSIS, SDC-2	106
APPENDIX E - RATE TRANSDUCER DATA ANALYSIS, SDC-2	113
APPENDIX F - ACCELEROMETER DATA ANALYSIS, SDC-3	115
APPENDIX G - RATE TRANSDUCER DATA ANALYSIS, SDC-3	122

List of Figures

	Page
1. Overall Layout of Cable Guardrail to W-Beam Transition	9
2. Overall Layout of Cable Guardrail to W-Beam Transition (Continued)	10
3. Overall Layout of Cable Guardrail to W-Beam Transition (Continued)	11
4. Cable Guardrail to W-Beam Transition	12
5. Transition Cable Brackets	13
6. Cable Guardrail to W-Beam Transition - Upstream and Downstream Views	14
7. Upstream Cable Anchorage	15
8. Downstream Cable Anchorage	16
9. Test Vehicles, Tests SDC-1, SDC-2, and SDC-3	22
10. Vehicle Dimensions, Test SDC-1	23
11. Vehicle Dimensions, Test SDC-2	24
12. Vehicle Dimensions, Test SDC-3	25
13. Vehicle Target Locations, Test SDC-1	26
14. Vehicle Target Locations, Test SDC-2	27
15. Vehicle Target Locations, Test SDC-3	28
16. Location of High-Speed Cameras, Test SDC-1	29
17. Location of High-Speed Cameras, Test SDC-2	30
18. Location of High-Speed Cameras, Test SDC-3	31
19. Summary of Test Results and Sequential Photographs, Test SDC-1	38
20. Additional Sequential Photographs, Test SDC-1	39
21. Full-Scale Crash Test, Test SDC-1	40
22. Full-Scale Crash Test, Test SDC-1	41
23. Full-Scale Crash Test, Test SDC-1	42
24. Impact Location, Test SDC-1	43
25. Cable Guardrail to W-Beam Transition Damage, Test SDC-1	44
26. Breakaway Cable Terminal Damage, Test SDC-1	45
27. Upstream Cable Anchorage Damage, Test SDC-1	46
28. Downstream Cable Anchorage Damage, Test SDC-1	47
29. Vehicle Damage, Test SDC-1	48
30. Summary of Test Results and Sequential Photographs, Test SDC-2	53
31. Additional Sequential Photographs, Test SDC-2	54
32. Full-Scale Crash Test, Test SDC-2	55
33. Full-Scale Crash Test, Test SDC-2	56
34. Full-Scale Crash Test, Test SDC-2	57
35. Impact Location, Test SDC-2	58
36. Cable Guardrail to W-Beam Transition Damage, Test SDC-2	59
37. Breakaway Cable Terminal Damage, Test SDC-2	60
38. Upstream Cable Anchorage Damage, Test SDC-2	61
39. Downstream Cable Anchorage Damage, Test SDC-2	62
40. Vehicle Damage, Test SDC-2	63

41. Summary of Test Results and Sequential Photographs, Test SDC-3	68
42. Additional Sequential Photographs, Test SDC-3	69
43. Full-Scale Crash Test, Test SDC-3	70
44. Full-Scale Crash Test, Test SDC-3	71
45. Impact Location, Test SDC-3	72
46. Cable Guardrail to W-Beam Transition Damage, Test SDC-3	73
47. Cable Guardrail to W-Beam Transition Damage, Test SDC-3	74
48. Vehicle Damage, Test SDC-3	75
A-1. Cable Guardrail to W-Beam Transition Design Details	83
A-2. Cable Guardrail to W-Beam Transition Design Details (Continued)	84
A-3. Cable Guardrail to W-Beam Transition Design Details (Continued)	85
A-4. Cable Guardrail to W-Beam Transition Design Details (Continued)	86
A-5. Cable Guardrail to W-Beam Transition Design Details (Continued)	87
A-6. Cable Guardrail to W-Beam Transition Design Details (Continued)	88
A-7. Cable Guardrail to W-Beam Transition Design Details (Continued)	89
A-8. Cable Guardrail to W-Beam Transition Design Details (Continued)	90
A-9. Cable Guardrail to W-Beam Transition Design Details (Continued)	91
A10. Cable Guardrail to W-Beam Transition Design Details (Continued)	92
A-11. Cable Guardrail to W-Beam Transition Design Details (Continued)	93
A-12. Cable Guardrail to W-Beam Transition Design Details (Continued)	94
A-13. Cable Guardrail to W-Beam Transition Design Details (Continued)	95
A-14. Cable Guardrail to W-Beam Transition Design Details (Continued)	96
B-1. Graph of Longitudinal Deceleration, Test SDC-1	98
B-2. Graph of Longitudinal Occupant Impact Velocity, Test SDC-1	99
B-3. Graph of Longitudinal Occupant Displacement, Test SDC-1	100
B-4. Graph of Lateral Deceleration, Test SDC-1	101
B-5. Graph of Lateral Occupant Impact Velocity, Test SDC-1	102
B-6. Graph of Lateral Occupant Displacement, Test SDC-1	103
C-1. Graph of Roll, Pitch, and Yaw Angular Displacements, Test SDC-1	105
D-1. Graph of Longitudinal Deceleration, Test SDC-2	107
D-2. Graph of Longitudinal Occupant Impact Velocity, Test SDC-2	108
D-3. Graph of Longitudinal Occupant Displacement, Test SDC-2	109
D-4. Graph of Lateral Deceleration, Test SDC-2	110
D-5. Graph of Lateral Occupant Impact Velocity, Test SDC-2	111
D-6. Graph of Lateral Occupant Displacement, Test SDC-2	112
E-1. Graph of Roll, Pitch, and Yaw Angular Displacements, Test SDC-2	114
F-1. Graph of Longitudinal Deceleration, Test SDC-3	116
F-2. Graph of Longitudinal Occupant Impact Velocity, Test SDC-3	117
F-3. Graph of Longitudinal Occupant Displacement, Test SDC-3	118
F-4. Graph of Lateral Deceleration, Test SDC-3	119
F-5. Graph of Lateral Occupant Impact Velocity, Test SDC-3	120
F-6. Graph of Lateral Occupant Displacement, Test SDC-3	121
G-1. Graph of Roll, Pitch, and Yaw Angular Displacements, Test SDC-3	123

List of Tables

	Page
1. NCHRP Report 350 Evaluation Criteria for 820C and 2000P Crash Tests	6
2. Summary of Safety Performance Evaluation Results	77

1 INTRODUCTION

1.1 Problem Statement

South Dakota has successfully used a cable guardrail to W-beam transition for many years. The design permits installation of a minimum amount of W-beam near the object to be protected, and allows use of three-cable guardrail further away from the obstacle. Because the three-cable system traps much less snow than W-beam guardrail systems, overall safety as well as economy is much improved. The cable guardrail to W-beam transition has not been crash tested and evaluated according to the guidelines provided in the National Cooperative Highway Research Program Report No. 350, *Recommended Procedures for the Safety Performance Evaluation of Highway Features* (1), therefore, the cable guardrail to W-beam transition must be crash tested and shown to meet current impact safety standards in order for its use to be continued on federal-aid highways.

1.2 Objective

The objective of this research study was to evaluate the safety performance of the South Dakota Department of Transportation's (SDDOT's) cable guardrail to W-beam transition according to the Test Level 3 (TL-3) evaluation criteria provided in NCHRP Report No. 350.

1.3 Scope

The proposed research was to begin by performing a limited, BARRIER VII computer analysis of the existing guardrail system to determine the critical impact point (CIP) for the proposed crash tests. The computer analysis would also be used to identify any structural weaknesses that may exist in the system. Following this analysis, if serious questions arose over the potential performance of the system, South Dakota representatives were to be contacted for further design considerations as well as contract modifications for any additional design effort. If these initial simulation efforts

predicted a reasonable probability of success, three full-scale crash tests were to be performed.

2 BACKGROUND

In 1987, the cable guardrail to W-beam transition was successfully crash tested at Southwest Research Institute (SwRI) according to the criteria provided by the National Cooperative Highway Research Program Report No. 230, *Recommended Procedures for the Safety Performance Evaluation of Highway Appurtenances* (2). Crash testing was successfully performed with large passenger sedans on the transition system for impacts both upstream of the W-beam breakaway cable terminal (BCT) and directly at the terminal end (3-5). The maximum dynamic rail deflections for the large sedan crash tests was 1.8 m (6 ft).

In 1989, three additional crash tests were performed by SwRI on three-strand cable guardrail supported by 6.0-kg/m (4-lb/ft) Franklin steel posts with attached soil plates according to the NCHRP 230 safety standards (6-8). The test results revealed that a three-strand cable guardrail system constructed on a 6:1 front slope could safely redirect large passenger sedans as well as small cars. The maximum dynamic rail deflections for the large sedan and small car crash tests were 3.0 m (9.8 ft) and 1.9 m (6.2 ft), respectively.

More recently, the standard G1 three-strand cable guardrail system was successfully crash tested by the Texas Transportation Institute according to the TL-3 conditions of NCHRP 350 (9). The ¾-ton pickup truck, with a gross static mass of 2,075 kg (4,575 lbs), impacted the guardrail at a speed of 95.1 km/hr (59.1 mph) and an angle of 26.7 degrees, resulting in a maximum dynamic rail deflection of 2.4 m (7.8 ft).

3 TEST REQUIREMENTS AND EVALUATION CRITERIA

3.1 Test Requirements

Longitudinal barriers, such as approach guardrail transitions, must satisfy the requirements provided in NCHRP Report 350 to be accepted for use on new construction projects or as a replacement for existing transition designs not meeting current safety standards. According to Test Level 3 (TL-3) of NCHRP Report 350, approach guardrail transitions must be subjected to two full-scale vehicle crash tests: (1) a 2,000-kg (4,409-lb) pickup truck impacting at a speed of 100.0 km/hr (62.1 mph) and at an angle of 25 degrees; and (2) an 820-kg (1,808-lb) small car impacting at a speed of 100.0 km/hr (62.1 mph) and at an angle of 20 degrees.

Although only two crash tests are generally required for evaluating approach guardrail transitions, it was believed that three full-scale vehicle crash tests would be needed to evaluate the safety performance of the cable guardrail to W-beam transition. Two tests - one using an 820-kg (1,808-lb) small car and one with a 2,000-kg (4,409-lb) pickup truck - were believed necessary to evaluate the potential for vehicle snagging in the region where the cable guardrail transitions into the W-beam guardrail. One additional pickup truck crash test was anticipated to evaluate the potential for snagging and pocketing when the pickup impacts the cable guardrail upstream of the BCT terminal and deflects the cable guardrail such that the pickup contacts the BCT terminal in a critical manner.

3.2 Evaluation Criteria

Evaluation criteria for full-scale vehicle crash testing are based on three appraisal areas: (1) structural adequacy; (2) occupant risk; and (3) vehicle trajectory after collision. Criteria for structural adequacy are intended to evaluate the ability of the barrier to contain, redirect, or allow controlled

vehicle penetration in a predictable manner. Occupant risk evaluates the degree of hazard to occupants in the impacting vehicle. Vehicle trajectory after collision is a measure of the potential for the post-impact trajectory of the vehicle to cause subsequent multi-vehicle accidents, thereby subjecting occupants of other vehicles to undue hazard or to subject the occupants of the impacting vehicle to secondary collisions with other fixed objects. These three evaluation criteria are defined in Table 1. The full-scale vehicle crash tests were conducted and reported in accordance with the procedures provided in NCHRP Report No. 350.

Table 1. NCHRP Report 350 Evaluation Criteria for 820C and 2000P Crash Tests.

Evaluation Factors	Evaluation Criteria	Test Designation	
		2000P	820C
Structural Adequacy	A. Test article should contain and redirect the vehicle; the vehicle should not penetrate, underride, or override the installation although controlled lateral deflection of the test article is acceptable.	X	X
Occupant Risk	D. Detached elements, fragments or other debris from the test article should not penetrate or show potential for penetrating the occupant compartment, or present an undue hazard to other traffic, pedestrians, or personnel in a work zone. Deformations of, or intrusions into, the occupant compartment that could cause serious injuries should not be permitted.	X	X
	F. The vehicle should remain upright during and after collision although moderate roll, pitching, and yawing are acceptable.	X	X
	H. Longitudinal and lateral occupant impact velocities (m/s) should satisfy the following: <div style="display: flex; justify-content: space-around;"><div><u>Preferred</u> 9</div><div><u>Maximum</u> 12</div></div>		X
	I. Longitudinal and lateral occupant ridedown accelerations (G's) should satisfy the following: <div style="display: flex; justify-content: space-around;"><div><u>Preferred</u> 15</div><div><u>Maximum</u> 20</div></div>		X
Vehicle Trajectory	K. After collision it is preferable that the vehicle's trajectory not intrude into adjacent traffic lanes.	X	X
	L. The occupant impact velocity in the longitudinal direction should not exceed 12 m/s and the occupant ridedown acceleration in the longitudinal direction should not exceed 20 G's.	X	X
	M. The exit angle from the test article preferably should be less than 60 percent of test impact angle, measured at time of vehicle loss of contact with test device.	X	X

4 CABLE GUARDRAIL TO W-BEAM TRANSITION

The overall layout of the cable guardrail to W-beam transition system is shown in Figures 1 through 3. Photographs of the transition system are shown in Figures 4 through 8. Additional design details are provided in Figures A-1 through A-14 of Appendix A. The cable guardrail to W-beam transition consisted of three major systems: (1) a cable guardrail system; (2) a breakaway cable terminal with W-beam guardrail; and (3) a simulated bridge railing for anchorage of the W-beam guardrail at the downstream end.

The 88.32-m (289-ft 9-in.) long cable guardrail system was constructed using three 19.0-mm ($\frac{3}{4}$ -in.) diameter steel cables with the center of the top, middle, and bottom cables mounted to a height above the ground of 686 mm (27 in.), 610 mm (24-in.), and 533 mm (21 in.), respectively. The three-strand cable guardrail system was supported by thirty-two S76x8.5 (S3x5.7) steel posts - twenty-three placed in soil and nine placed in the existing concrete tarmac. Post nos. 1C through 23C were configured with soil plates measuring 6.4-mm ($\frac{1}{4}$ -in.) thick by 203-mm (8-in.) wide by 610-mm (24-in.) long. The center-to-center spacings for post nos. 1C through 16C, 16C through 28C, and 28C through 32C were 1,219 mm (4 ft), 4,877 mm (16 ft), and 1,829 mm (6 ft), respectively. The soil embedment depth for post nos. 1C through 23C was 838 mm (33 in.). The steel posts were placed in a compacted coarse, crushed limestone material that met Grading B of AASHTO M147-65 (1990) as found in NCHRP Report 350. Two concrete anchor assemblies were used in the cable system - a steel turnbuckle cable end assembly at the upstream end and a spring cable end assembly at the downstream end. Two steel transition cable brackets were located downstream from post no. 1C - one at 8,611 mm (28 ft - 3 in.) and one at 189 mm (15 ft - 9 in.).

A 11.43-m (37-ft 6-in.) long breakaway cable terminal (BCT) and a 7.62-m (25-ft) long

strong-post W-beam guardrail were constructed behind the cable guardrail system using 2.66-mm (12-gauge) W-beam guardrail mounted at 686 mm (27 in.), as measured from the ground to the top of the W-beam. The W-beam guardrail and BCT terminal were supported by eleven posts spaced on 1,905-mm (6-ft 3-in.) on centers. Post nos. 1W through 2W were 140-mm (5½-in.) wide by 190-mm (7½-in.) deep by 1,080-mm (3-ft 6½-in.) long and were placed in steel foundation tubes. Post nos. 3W through 11W were 152-mm (6-in.) wide by 203-mm (8-in.) deep by 1,829-mm (6-ft) long with a soil embedment depth of approximately 1,118 mm (44 in.). Timber spacers, measuring 152-mm (6-in.) wide by 203-mm (8-in.) deep by 356-mm (14-in.) long were used to block the W-beam away from the face of the post nos. 3W through 11W. The timber posts were placed in a compacted coarse, crushed limestone material that met Grading B of AASHTO M147-65 (1990) as found in NCHRP Report 350. Lap-splice connections between the W-beam rail sections were configured to reduce vehicle snagging at the splice during the crash tests.

A simulated thrie beam bridge railing system was located at the downstream end of the W-beam guardrail system in order to replicate actual field conditions and provide a mechanism for developing the tensile capacity of the W-beam guardrail. The thrie beam bridge railing was attached to the W-beam guardrail using an 1,905-mm (6-ft 3-in.) long W-beam to thrie beam transition section.

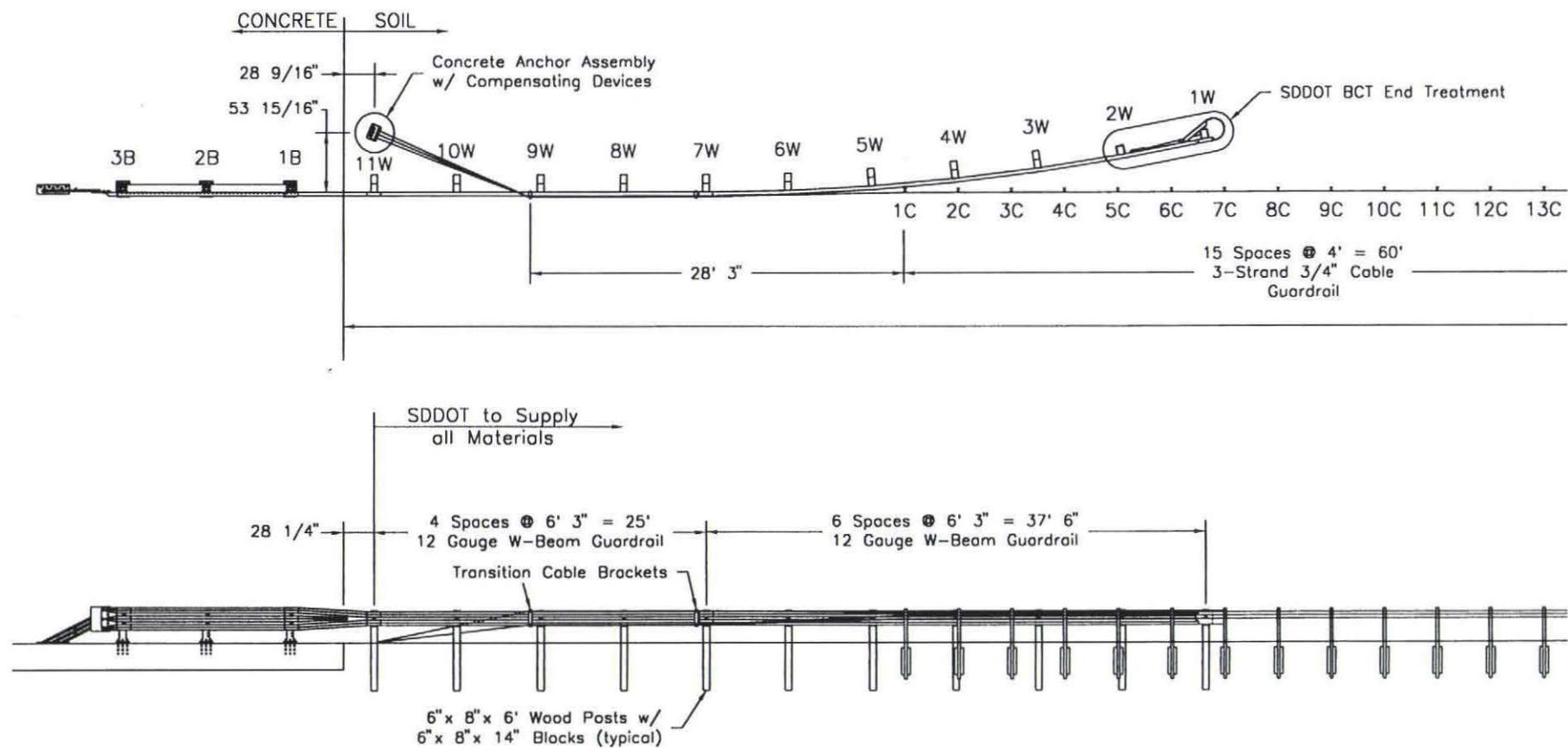
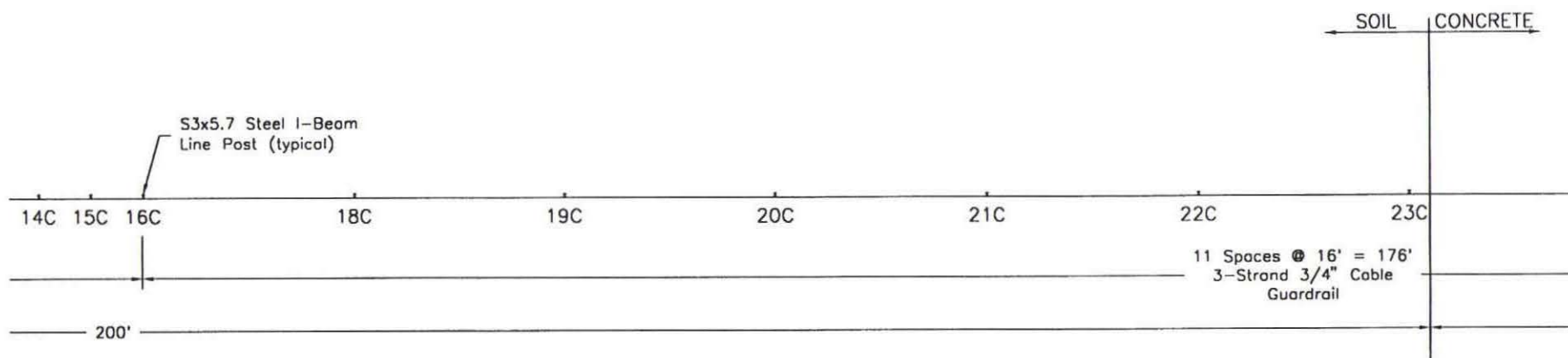


Figure 1. Overall Layout of Cable Guardrail to W-beam Transition.



10

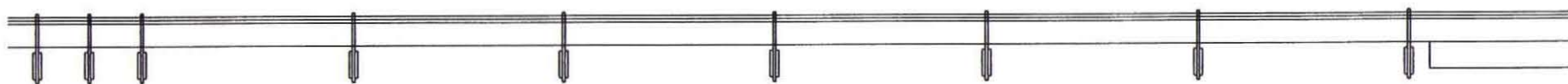
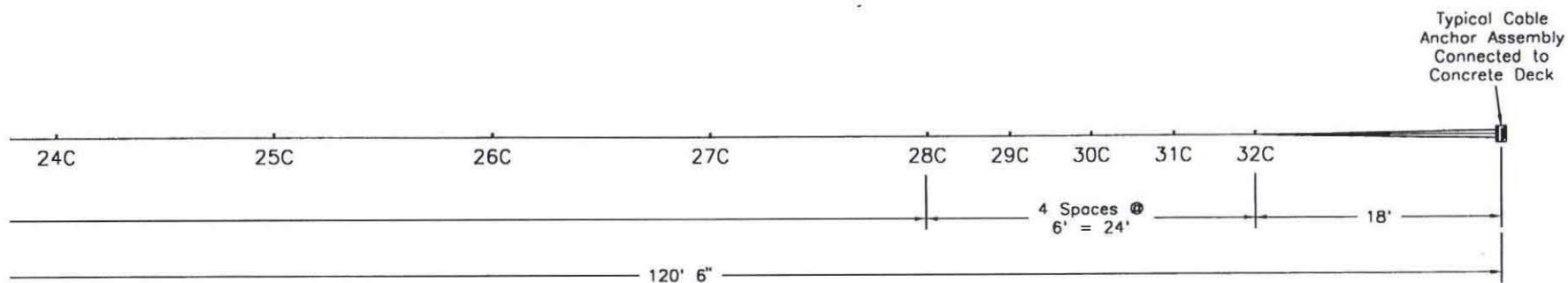


Figure 2. Overall Layout of Cable Guardrail to W-beam Transition (Continued).



11

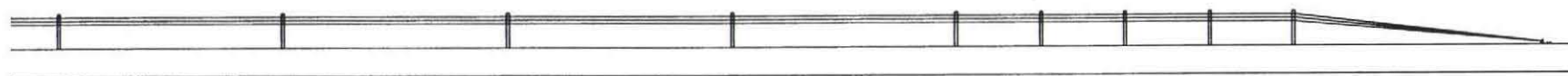


Figure 3. Overall Layout of Cable Guardrail to W-beam Transition (Continued).

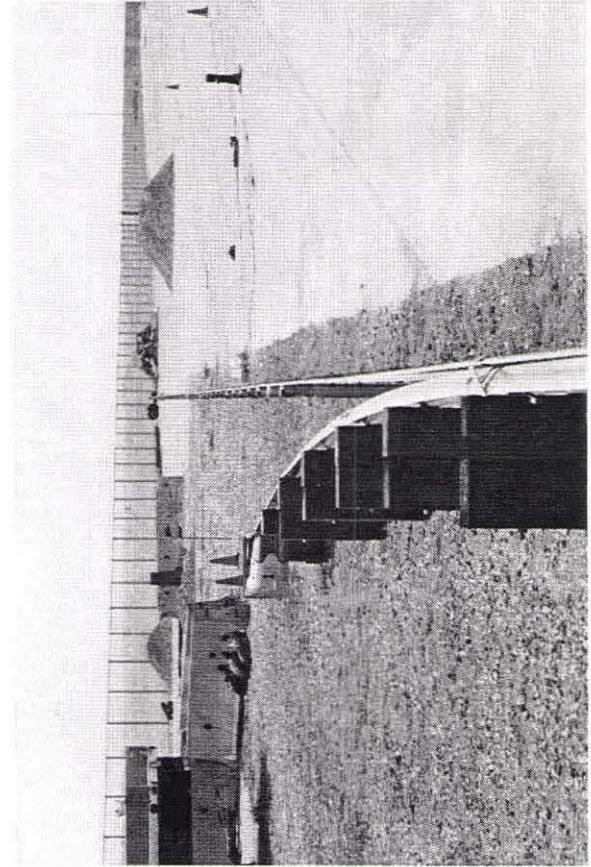
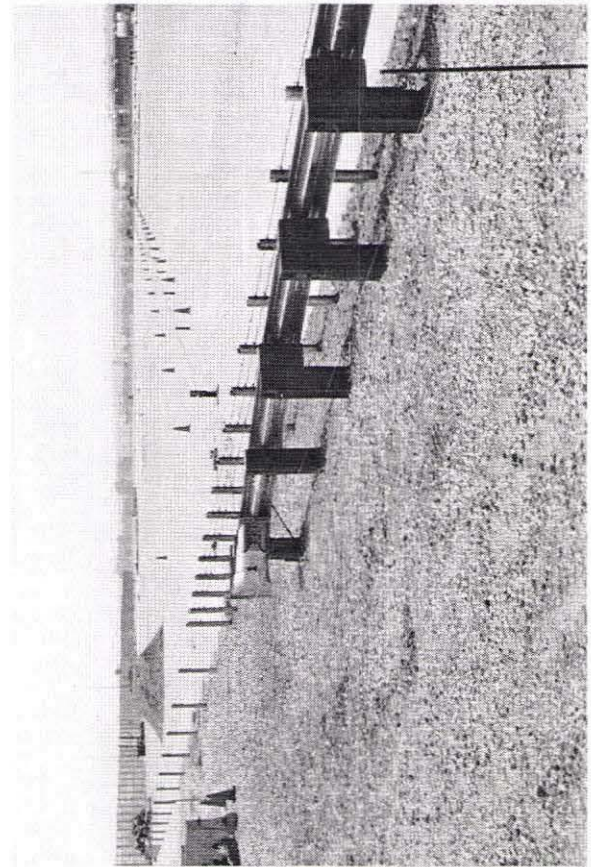
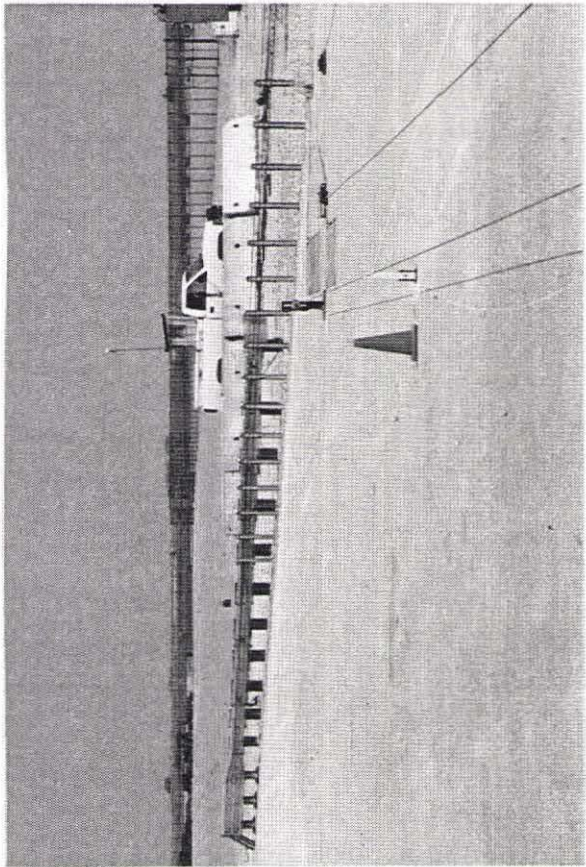
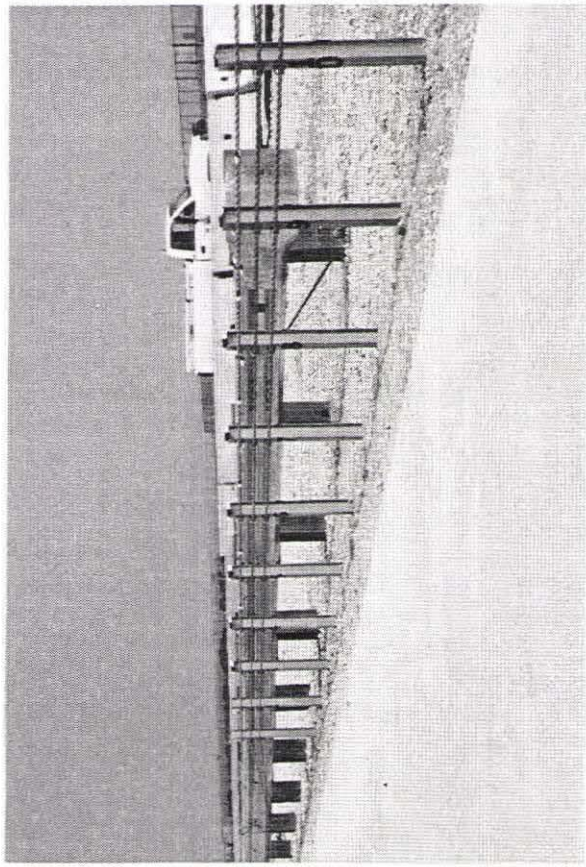


Figure 4. Cable Guardrail to W-Beam Transition.

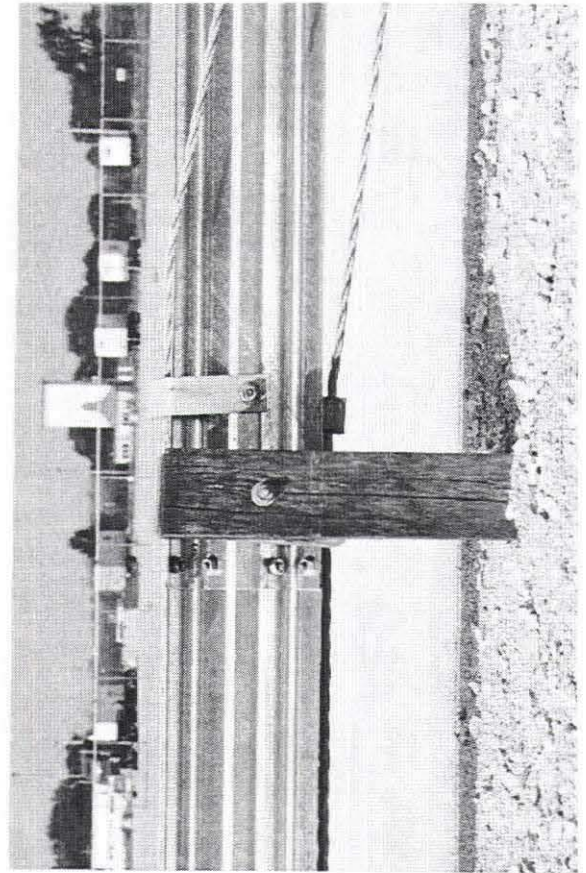
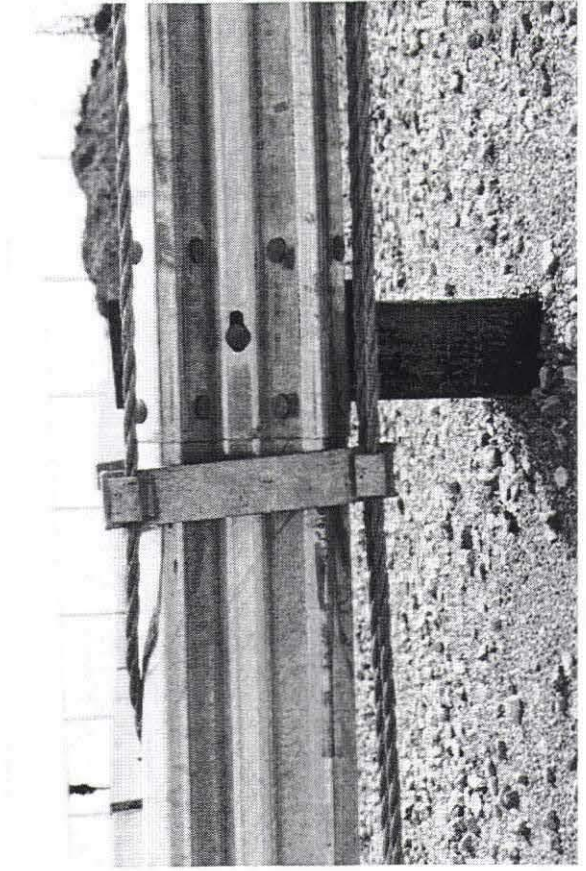
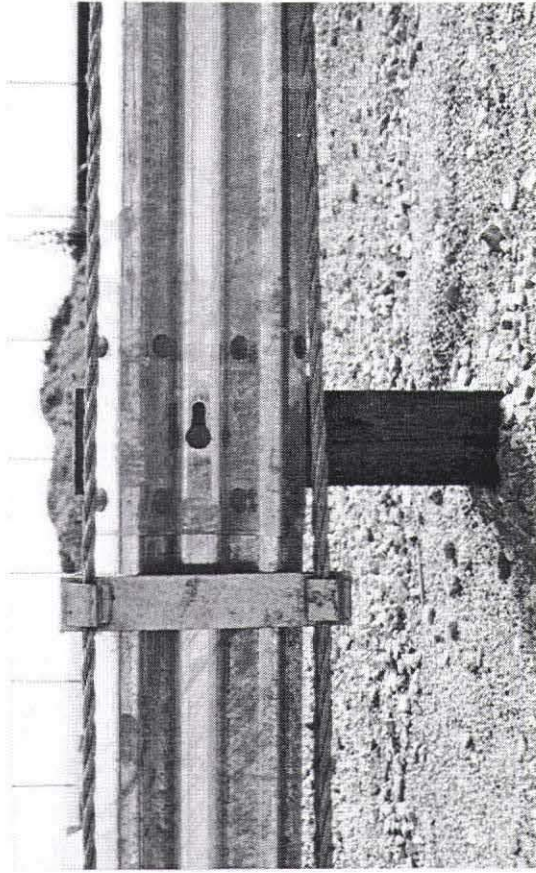
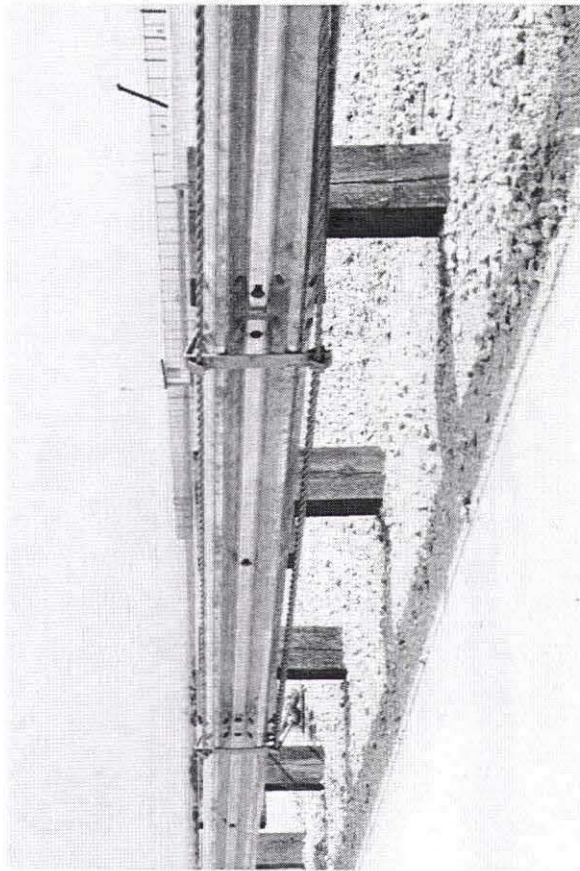


Figure 5. Transition Cable Brackets.

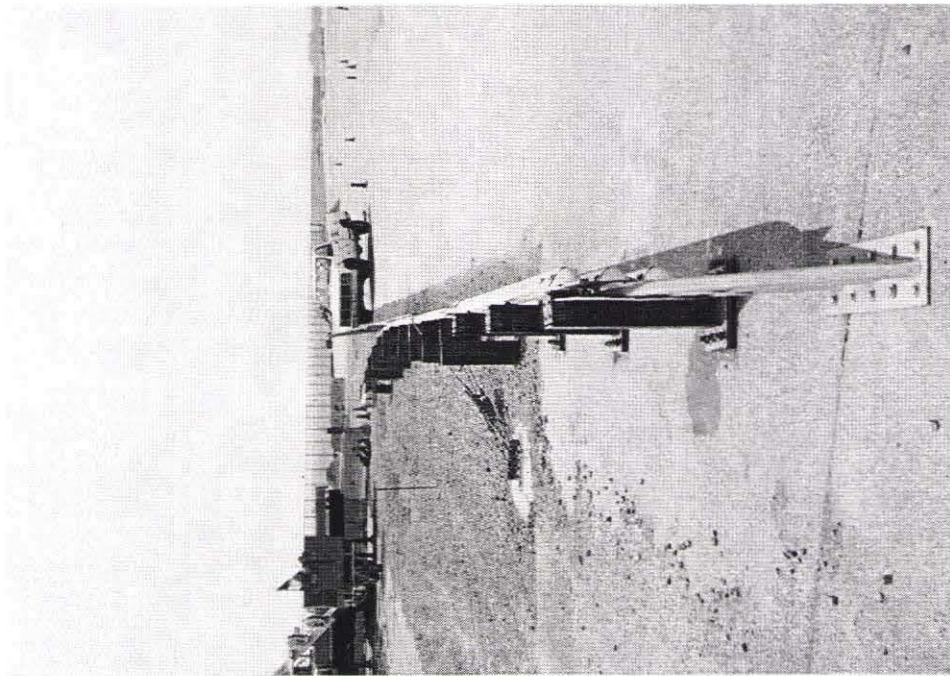
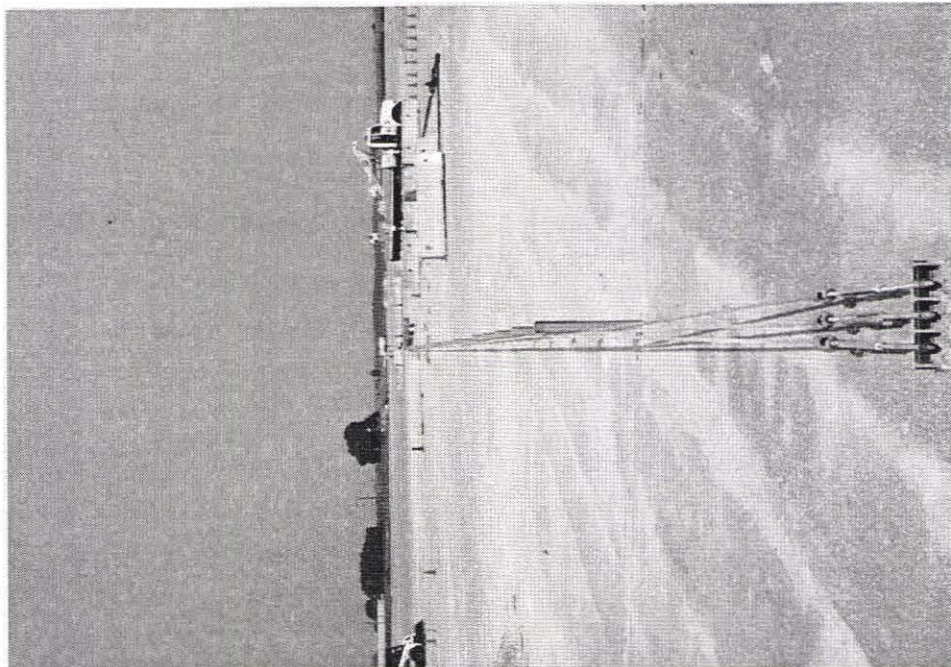


Figure 6. Cable Guardrail to W-Beam Transition - Upstream and Downstream Views.

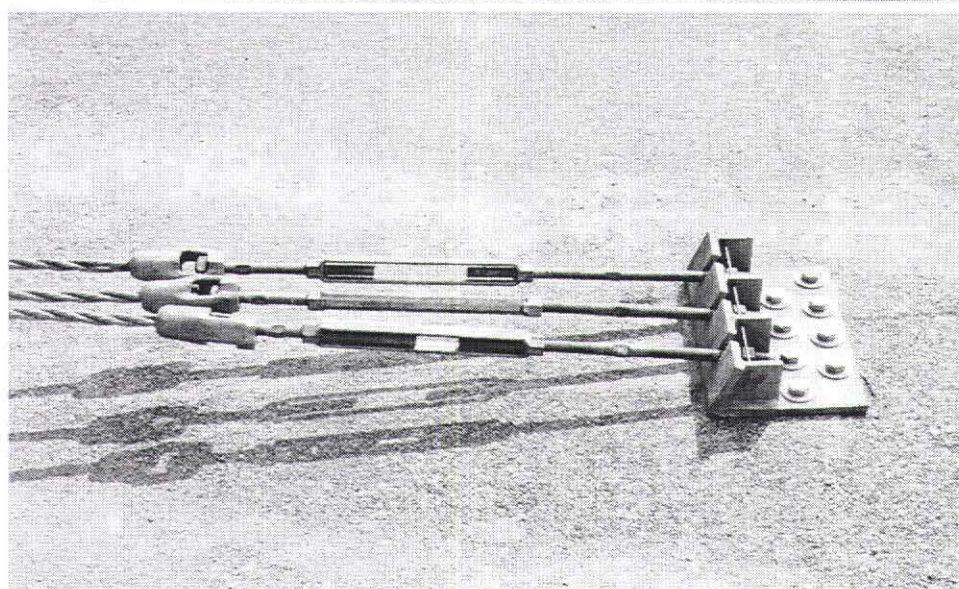
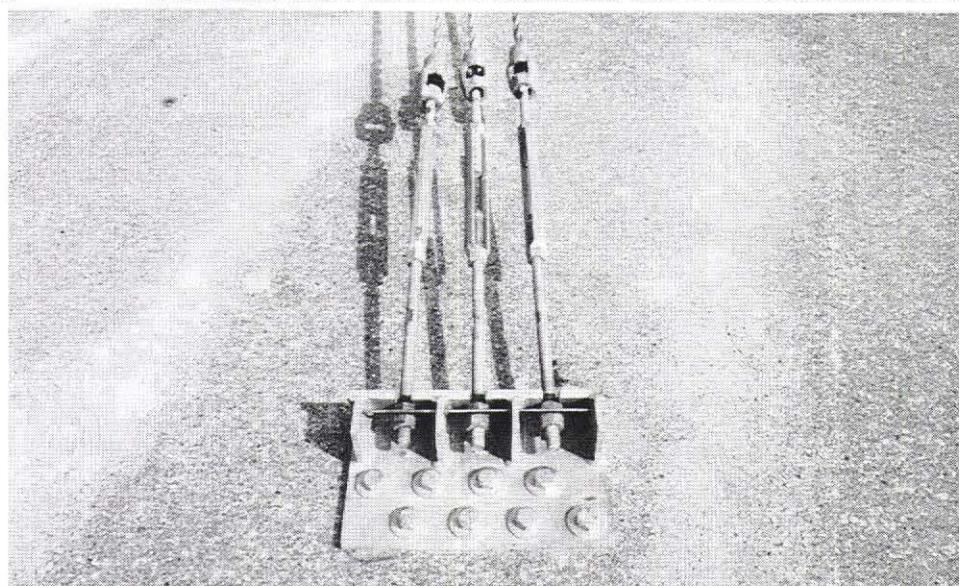
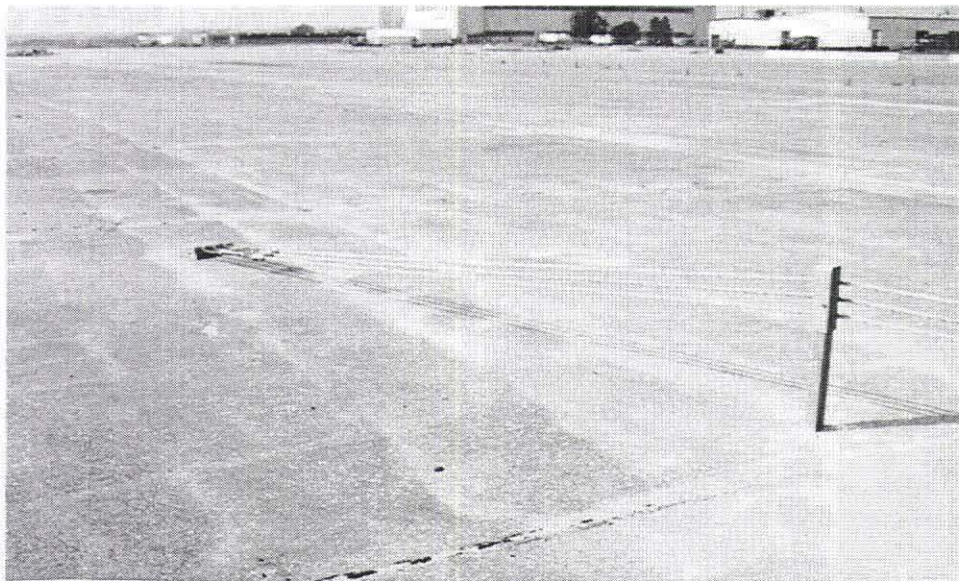


Figure 7. Upstream Cable Anchorage.

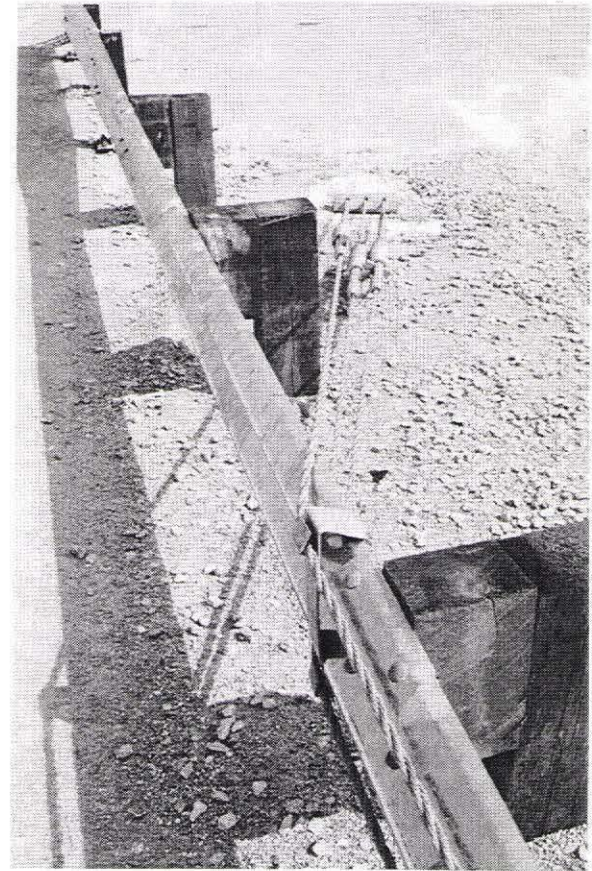
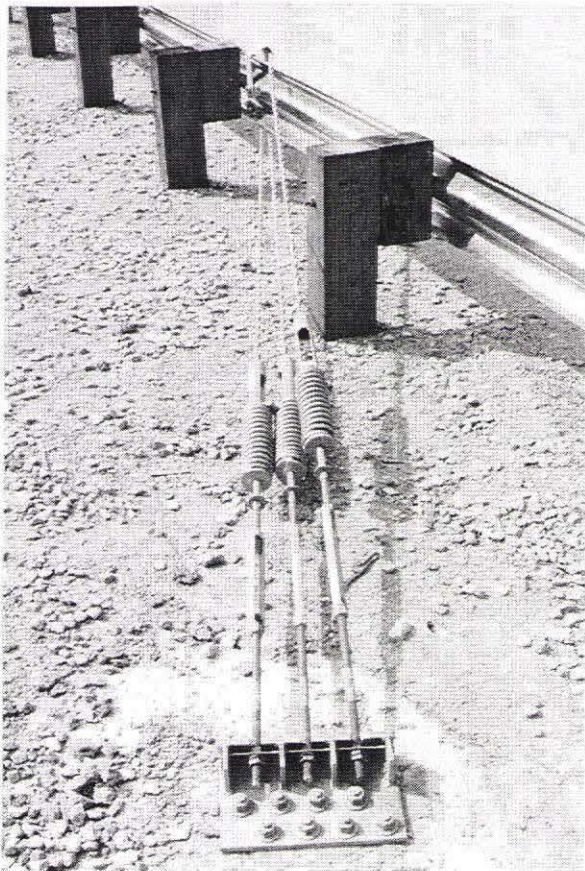
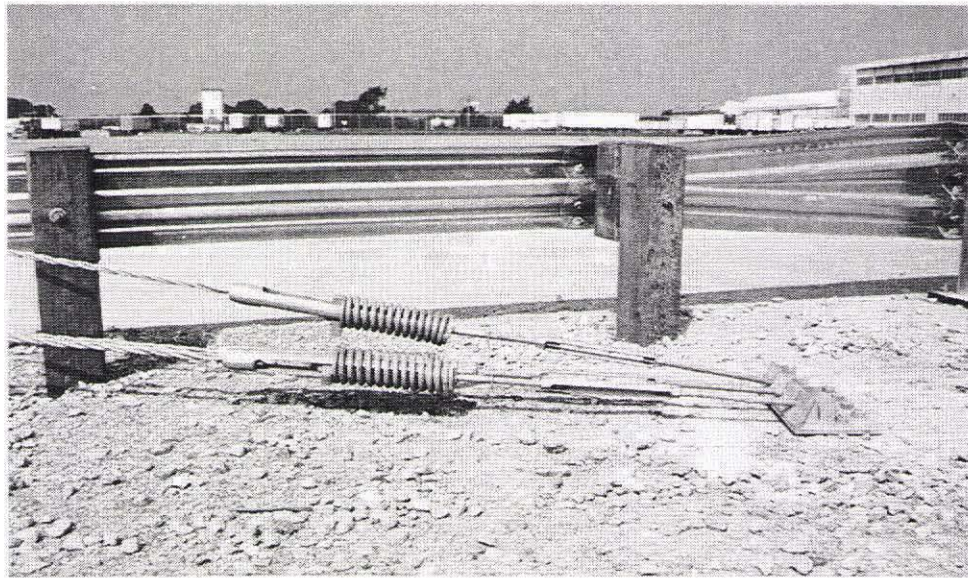


Figure 8. Downstream Cable Anchorage.

5 TEST CONDITIONS

5.1 Test Facility

The testing facility is located at the Lincoln Air-Park on the NW end of the Lincoln Municipal Airport and is approximately 8.0 km (5 mi.) NW of the University of Nebraska-Lincoln. The site is protected by an 2.44-m (8-ft) high chain-link security fence.

5.2 Vehicle Tow and Guidance System

A reverse cable tow system with a 1:2 mechanical advantage was used to propel the test vehicles. The distance traveled and the speed of the tow vehicle were one-half that of the test vehicle. The test vehicle was released from the tow cable before impact with the guardrail system. A digital speedometer, located on the tow vehicle, was used to increase the accuracy of the test vehicle impact speed.

A vehicle guidance system developed by Hinch (10) was used to steer the test vehicle. A guide-flag, attached to the front-left wheel and the guide cable, was sheared off before impact. The 9.5-mm diameter guide cable was tensioned to approximately 13.3 kN (3,000 lbs), and supported by hinged stanchions in the lateral and vertical directions and spaced at 30.48 m (100 ft) initially and at 15.24 m (50 ft) toward the end of the guidance system. The hinged stanchions stood upright while holding up the guide cable, but as the vehicle was towed down the line, the guide-flag struck and knocked each stanchion to the ground.

5.3 Test Vehicles

For test SDC-1, a 1993 GMC 2500 (¾-ton) pickup truck was used as the test vehicle. The test inertial and gross static weights were 2,013 kg (4,438 lbs). The test vehicle is shown in Figure 9, and vehicle dimensions are shown in Figure 10.

For test SDC-2, a 1994 GMC 2500 (¾-ton) pickup truck was used as the test vehicle. The test inertial and gross static weights were 2,023 kg (4,459 lbs). The test vehicle is shown in Figure 9, and vehicle dimensions are shown in Figure 11.

For test SDC-3, a 1991 Geo Metro was used as the test vehicle. The test inertial and gross static weights were 802 kg (1,769 lbs) and 878 kg (1,935 lbs), respectively. The test vehicle is shown in Figure 9, and vehicle dimensions are shown in Figure 12.

The Suspension Method (11) was used to determine the vertical component of the center of gravity for the test vehicles. This method is based on the principle that the center of gravity of any freely suspended body is in the vertical plane through the point of suspension. The vehicle was suspended successively in three positions, and the respective planes containing the center of gravity were established. The intersection of these planes pinpointed the location of the center of gravity. The longitudinal component of the center of gravity was determined using the measured axle weights. The location of the final centers of gravity are shown in Figures 10 through 12.

Square, black and white-checkered targets were placed on each vehicle to aid in the analysis of the high-speed film, as shown in Figures 9 and 13 through 15. One target was placed on the center of gravity on the driver's side door, the passenger's side door, and on the roof of the vehicle. The remaining targets were located for reference so that they could be viewed from the high-speed cameras for film analysis.

The front wheels of the test vehicle were aligned for camber, caster, and toe-in values of zero so that the vehicles would track properly along the guide cable. Two 5B flash bulbs were mounted on both the hood and roof of the vehicles to pinpoint the time of impact with the bridge railing on the high-speed film. The flash bulbs were fired by a pressure tape switch mounted on the front face

of the bumper. A remote controlled brake system was installed in the test vehicle so the vehicle could be brought safely to a stop after the test.

5.4 Data Acquisition Systems

5.4.1 Accelerometers

One triaxial piezoresistive accelerometer system with a range of ± 200 G's was used to measure the acceleration in the longitudinal, lateral, and vertical directions at a sample rate of 10,000 Hz. The environmental shock and vibration sensor/recorder system, Model EDR-4M6, was developed by Instrumented Sensor Technology (IST) of Okemos, Michigan and includes three differential channels as well as three single-ended channels. The EDR-4 was configured with 6 Mb of RAM memory and a 1,500 Hz lowpass filter. Computer software, "DynaMax 1 (DM-1)" and "DADiSP" were used to digitize, analyze, and plot the accelerometer data.

A backup triaxial piezoresistive accelerometer system with a range of ± 200 G's was also used to measure the acceleration in the longitudinal, lateral, and vertical directions at a sample rate of 3,200 Hz. The environmental shock and vibration sensor/recorder system, Model EDR-3, was developed by Instrumented Sensor Technology (IST) of Okemos, Michigan. The EDR-3 was configured with 256 Kb of RAM memory and a 1,120 Hz lowpass filter. Computer software, "DynaMax 1 (DM-1)" and "DADiSP" were used to digitize, analyze, and plot the accelerometer data.

5.4.2 Rate Transducer

A Humphrey 3-axis rate transducer with a range of 250 deg/sec in each of the three directions (pitch, roll, and yaw) was used to measure the rates of motion of the test vehicle. The rate transducer was rigidly attached to the vehicles near the center of gravity of the test vehicle. Rate transducer signals, excited by a 28 volt DC power source, were received through the three single-ended

channels located externally on the EDR-4M6 and stored in the internal memory. The raw data measurements were then downloaded for analysis and plotted. Computer software, "DynaMax 1 (DM-1)" and "DADiSP" were used to digitize, analyze, and plot the rate transducer data.

5.4.3 High-Speed Photography

For test SDC-1, five high-speed 16-mm Red Lake Locam cameras, with operating speeds of approximately 500 frames/sec, were used to film the crash test. A Locam with a wide-angle 12.5-mm lens was placed above the test installation to provide a field of view perpendicular to the ground. A Locam with a zoom lens was placed downstream from the impact point and had a field of view parallel to the barrier. A Locam with a zoom lens was placed on the traffic side of the barrier and had a field of view perpendicular to the barrier. Two Locam cameras were placed downstream and behind the barrier. A schematic of all five camera locations for test SDC-1 is shown in Figure 16.

For test SDC-2, five high-speed 16-mm Red Lake Locam cameras, with operating speeds of approximately 500 frames/sec, were used to film the crash test. A Locam with a wide-angle 12.5-mm lens was placed above the test installation to provide a field of view perpendicular to the ground. A Locam with a zoom lens was placed downstream from the impact point and had a field of view parallel to the barrier. A Locam with a zoom lens was placed on the traffic side of the barrier and had a field of view perpendicular to the barrier. Two Locam cameras were placed downstream and behind the barrier. A schematic of all five camera locations for test SDC-2 is shown in Figure 17.

For test SDC-3, five high-speed 16-mm Red Lake Locam cameras, with operating speeds of approximately 500 frames/sec, were used to film the crash test. A Locam with a wide-angle 12.5-mm lens was placed above the test installation to provide a field of view perpendicular to the ground. A Locam with a zoom lens was placed downstream from the impact point and had a field of view

parallel to the barrier. A Locam with a zoom lens was placed on the traffic side of the barrier and had a field of view perpendicular to the barrier. A Locam with a zoom lens was placed upstream and behind the barrier. A Locam with a zoom lens was placed downstream and behind the barrier. A schematic of all five camera locations for test SDC-3 is shown in Figure 18.

The film was analyzed using the Vanguard Motion Analyzer. Actual camera speed and camera divergence factors were considered in the analysis of the high-speed film.

5.4.4 Pressure Tape Switches

For all three crash tests, five pressure-activated tape switches, spaced at 2-m (6.56 ft) intervals, were used to determine the speed of the vehicle before impact. Each tape switch fired a strobe light which sent an electronic timing signal to the data acquisition system as the left front tire of the test vehicle passed over it. Test vehicle speeds were determined from electronic timing mark data recorded on "Test Point" software. Strobe lights and high-speed film analysis are used only as a backup in the event that vehicle speeds cannot be determined from the electronic data.



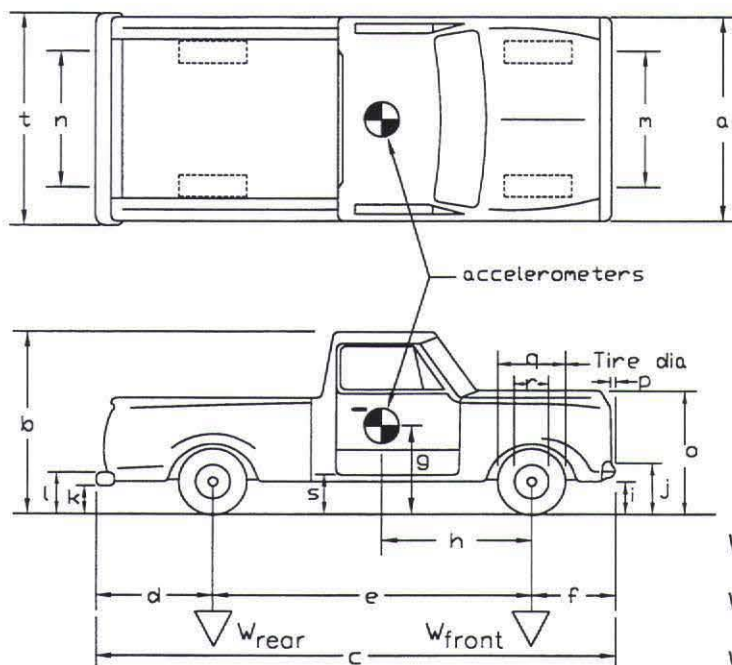
Figure 9. Test Vehicles, Tests SDC-1, SDC-2, and SDC-3.

Date: 8/11/98 Test Number: SDC-1 Model: 2500

Make: GMC Vehicle I.D.#: 1GDGC24K4PE506033

Tire Size: LT245/75R16 Year: 1993 Odometer: 173,736

*(All Measurements Refer to Impacting Side)



Vehicle Geometry - mm

a 1886 b 1842
c 5537 d 1302
e 3327 f 889
g 738 h 1394
i 445 j 667
k 597 l 800
m 1600 n 1626
o 1067 p 95
q 756 r 445
s 470 t 1849

Wheel Center Height Front 368

Wheel Center Height Rear 381

Wheel Well Clearance (FR) 895

Wheel Well Clearance (RR) 965

Engine Type V-6 gasoline

Engine Size 5.7 Liter

Transmission Type:

Automatic or Manual

FWD or RWD or 4WD

Weights - kg	Curb	Test Inertial	Gross Static
w_{front}	<u>1218</u>	<u>1170</u>	<u>1170</u>
w_{rear}	<u>954</u>	<u>843</u>	<u>843</u>
w_{total}	<u>2172</u>	<u>2013</u>	<u>2013</u>

Note any damage prior to test: Minor windshield cracking and dent in left rear panel.

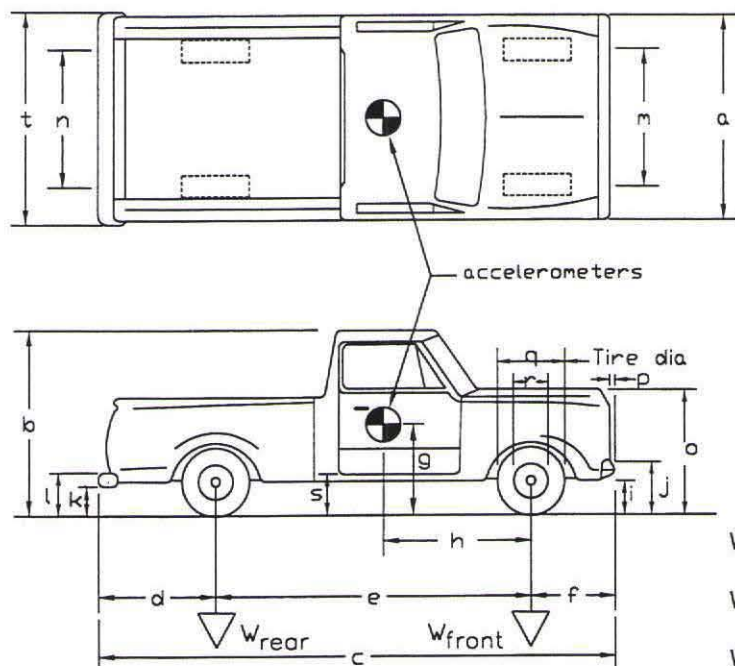
Figure 10. Vehicle Dimensions, Test SDC-1.

Date: 8/18/98 Test Number: SDC-2 Model: 2500

Make: GMC Vehicle I.D.#: 1GDGC24K9RE550015

Tire Size: 245/75R16 Year: 1994 Odometer: 185,667

*(All Measurements Refer to Impacting Side)



Vehicle Geometry - mm

a 1905 b 1835
c 5531 d 1321
e 3327 f 2153
g 738 h 1387
i 400 j 651
k 578 l 775
m 1616 n 1626
o 1022 p 64
q 772 r 445
s 470 t 1867

Wheel Center Height Front 371

Wheel Center Height Rear 368

Wheel Well Clearance (FR) 889

Wheel Well Clearance (RR) 949

Engine Type V-6 gasoline

Engine Size 5.7 Liter

Transmission Type:

Automatic or Manual

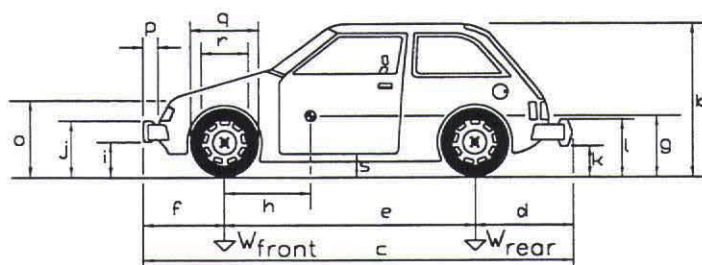
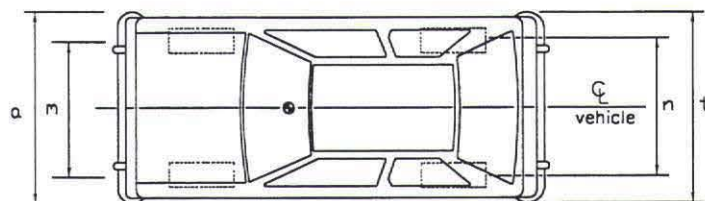
FWD or RWD or 4WD

Weights - kg	Curb	Test Inertial	Gross Static
W_{front}	<u>1181</u>	<u>1180</u>	<u>1180</u>
W_{rear}	<u>864</u>	<u>843</u>	<u>843</u>
W_{total}	<u>2045</u>	<u>2023</u>	<u>2023</u>

Note any damage prior to test: Dent in center, front bumper and right-rear box panel and right-side door.

Figure 11. Vehicle Dimensions, Test SDC-2.

Date: 8/31/98 Test Number: SDC-3 Model: Metro
 Make: GEO Vehicle I.D.#: 2C1MR246XR6739458
 Tire Size: P155/80R12 Year: 1991 Odometer: 93,969



Vehicle Geometry - mm

a 1499 b 1334
 c 3683 d 673
 e 2261 f 749
 g 546 h 933
 i 222 j 508
 k 254 l 533
 m 1349 n 1346
 o 673 p 95
 q 533 r 330
 s 305 t 1448

height of wheel center 254

Engine Type 4 cyl. gasoline

Engine size 1.0 Liter

Transmission Type:

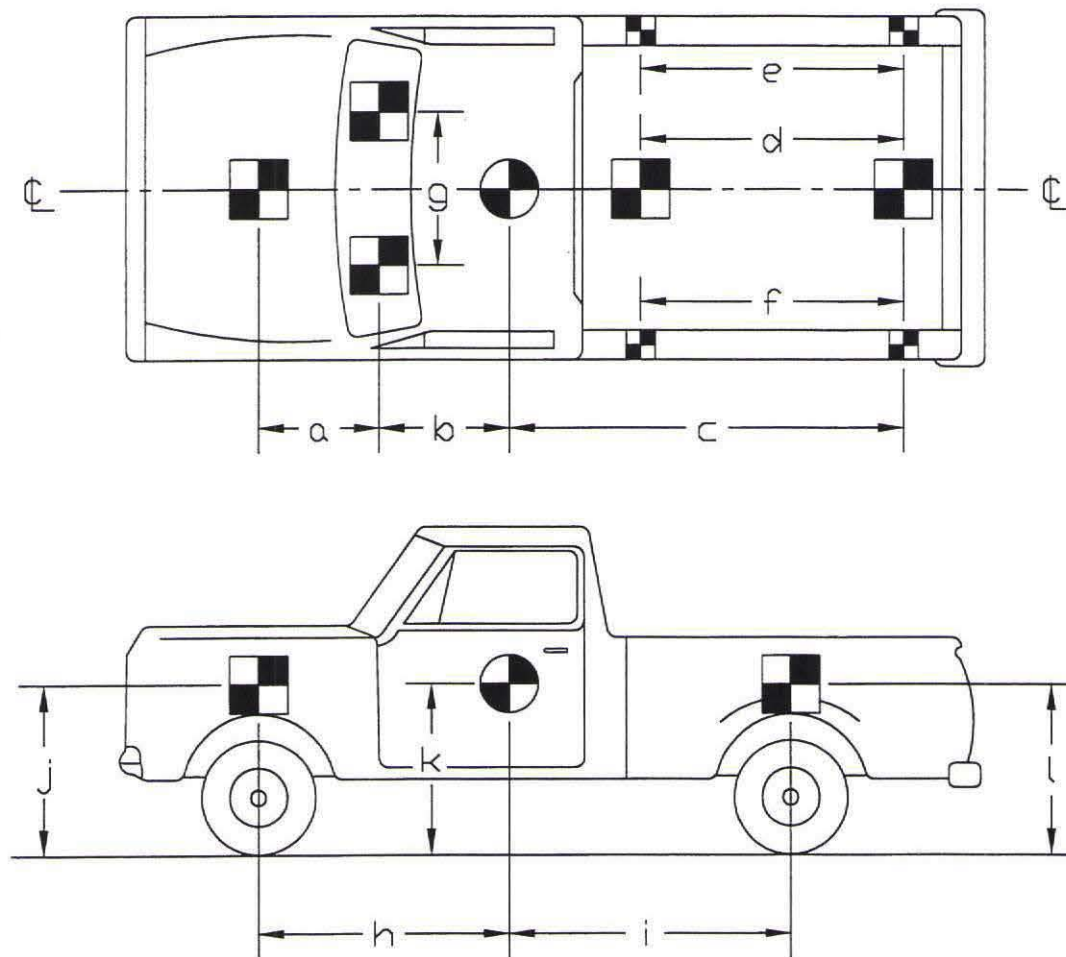
(Automatic) or Manual

(FWD) or RWD or 4WD

Weight - kg	Curb	Test Inertial	Gross Static
W_{front}	<u>463</u>	<u>471</u>	<u>506</u>
W_{rear}	<u>291</u>	<u>331</u>	<u>372</u>
W_{total}	<u>754</u>	<u>802</u>	<u>878</u>

Damage prior to test: Missing passenger side mirror.

Figure 12. Vehicle Dimensions, Test SDC-3.

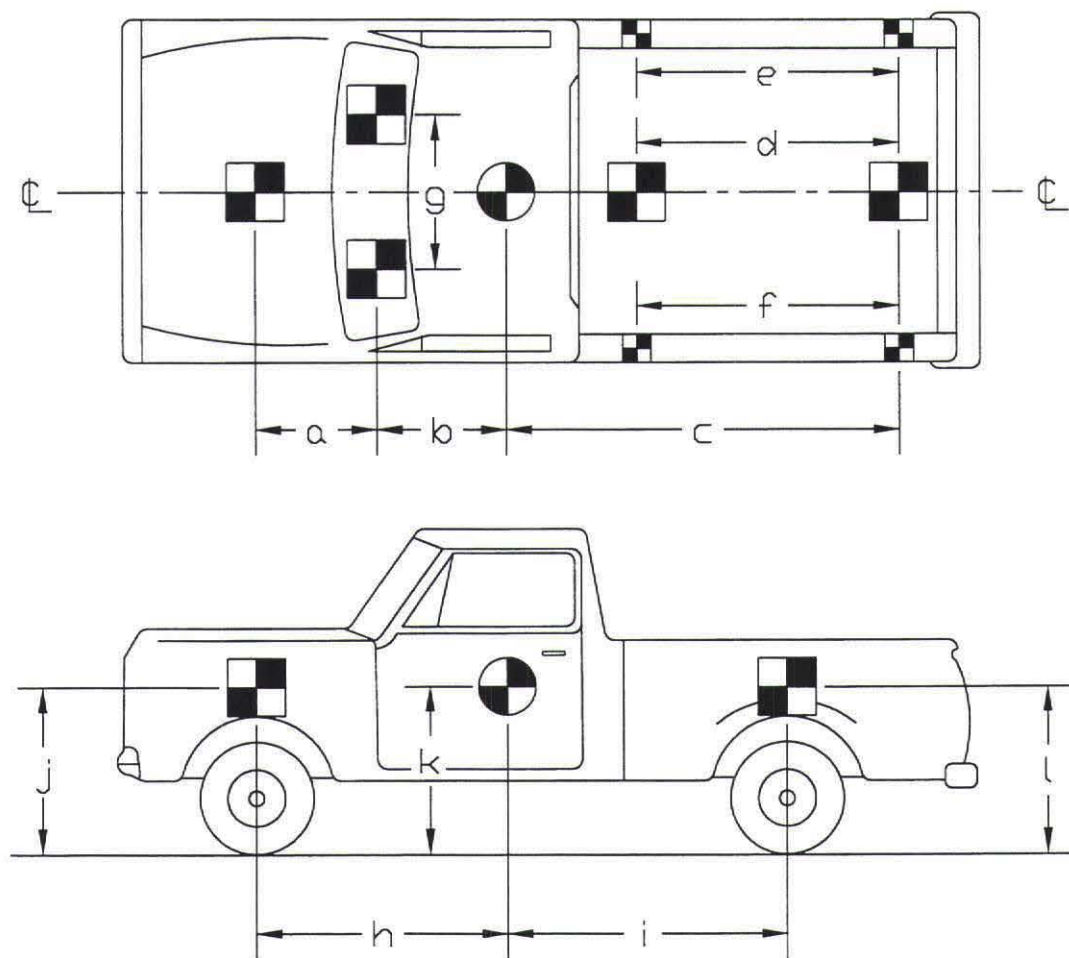


TEST #: SDC-1

TARGET GEOMETRY (mm)

a	<u>1346</u>	b	<u>584</u>	c	<u>2737</u>	d	<u>1784</u>
e	<u>2143</u>	f	<u>2146</u>	g	<u>978</u>	h	<u>1394</u>
i	<u>1969</u>	j	<u>928</u>	k	<u>738</u>	l	<u>1067</u>

Figure 13. Vehicle Target Locations, Test SDC-1.

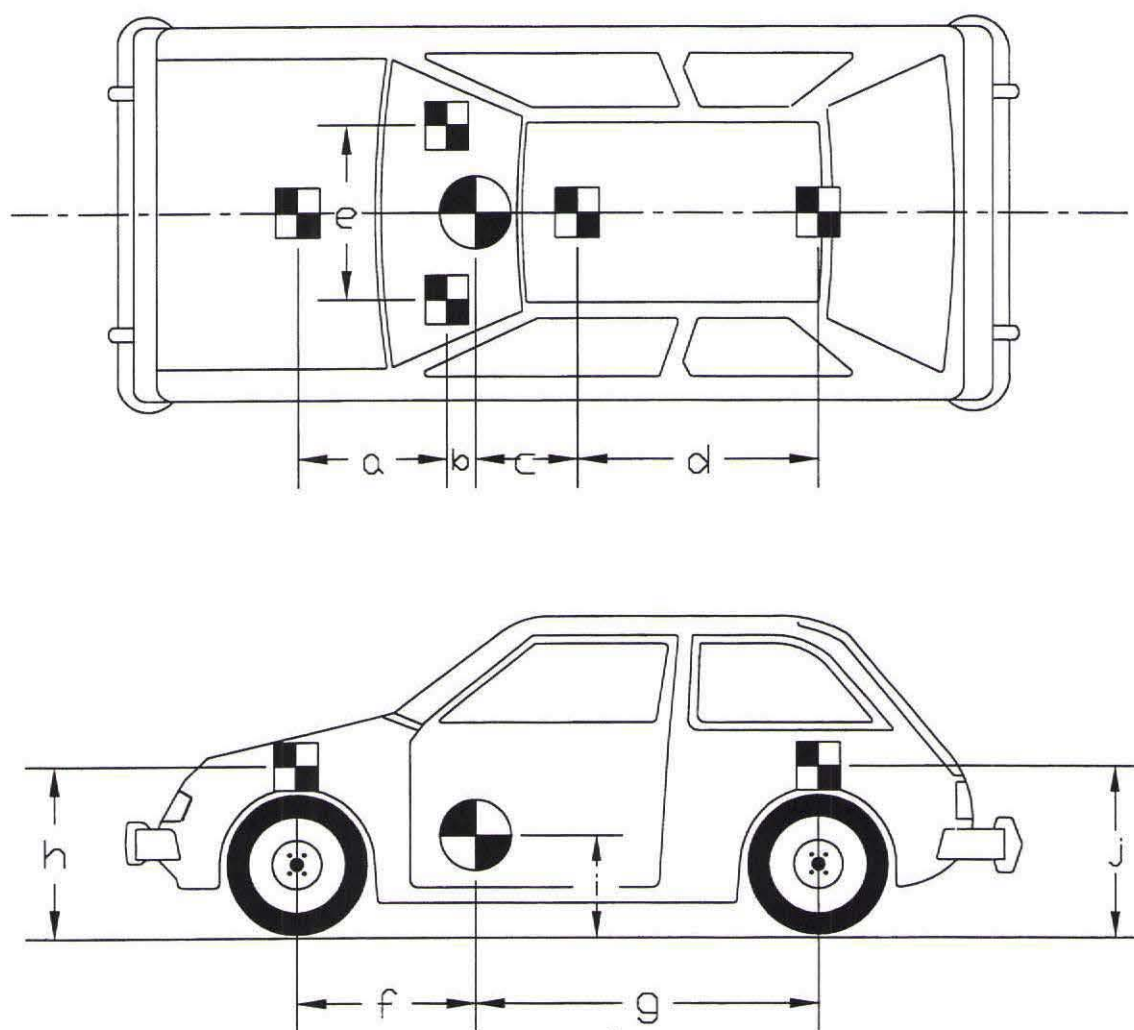


TEST #: SDC-2

TARGET GEOMETRY (mm)

a 1295 b 622 c 2642 d 1715
e 2143 f 2143 g 968 h 1387
i 1965 j 984 k 738 l 1035

Figure 14. Vehicle Target Locations, Test SDC-2.



TEST #: SDC-3

TARGET GEOMETRY (mm)

a	<u>946</u>	b	<u>216</u>	c	<u>381</u>	d	<u>1022</u>
e	<u>622</u>	f	<u>933</u>	g	<u>1340</u>	h	<u>711</u>
i	<u>546</u>	j	<u>714</u>				

Figure 15. Vehicle Target Locations, Test SDC-3.

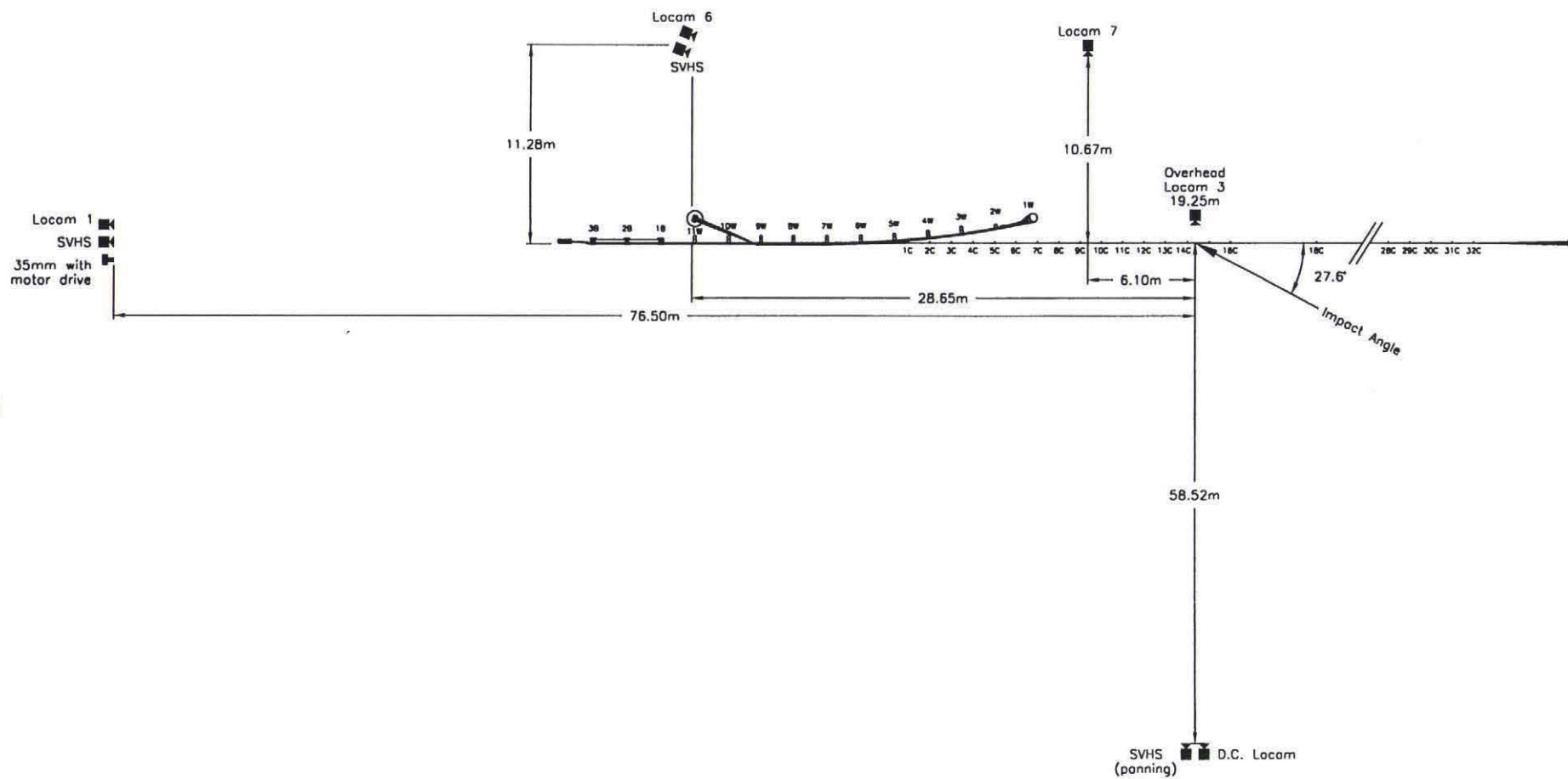


Figure 16. Location of High-Speed Cameras, Test SDC-1.

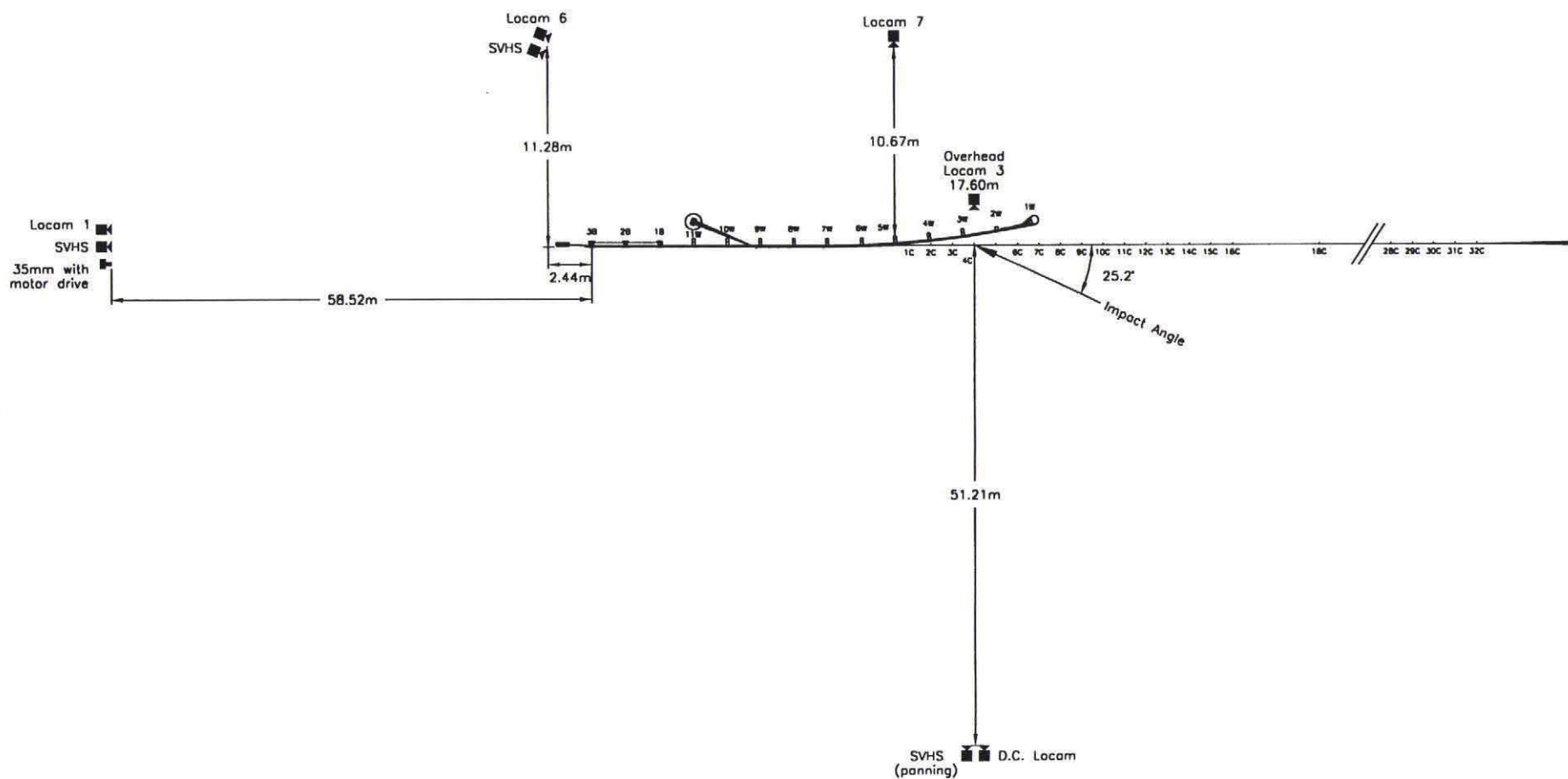


Figure 17. Location of High-Speed Cameras, Test SDC-2.

6 COMPUTER SIMULATION

Computer simulation modeling with BARRIER VII (12) was performed to determine the critical impact point (CIP) for a pickup truck impacting the cable guardrail upstream of the BCT. This CIP was based on the impact condition which produced the greatest potential for the pickup truck to pocket behind the BCT while also impacting the terminal on the front end of the vehicle. The researchers believed that this impact condition had the greatest potential for causing the cables to rupture, thus allowing the vehicle to pass behind the barrier system. The simulations were conducted modeling a 2000-kg (4,409-lb) pickup truck impacting at a speed of 100.0 km/hr (62.14 mph) and at an angle of 25 degrees.

The CIP's for the remaining two crash tests were chosen to evaluate the following: (1) the potential for a 2000-kg (4,409-lb) pickup truck, impacting slightly downstream from the end of the BCT, to climb and vault over the cable and W-beam rails as the steel posts deformed and leaned on the W-beam rail; and (2) the potential for a 820-kg (1,808-lb) small car, impacting in the region where the cables transition downward, to snag or wedge between the cables or at the connection between the two systems.

7 CRASH TEST NO. 1

7.1 Test SDC-1

The 2,013-kg (4,438-lb) pickup truck impacted the cable guardrail to W-beam transition at a speed of 101.9 km/hr (63.3 mph) and an angle of 27.6 degrees. A summary of the test results and the sequential photographs are shown in Figure 19. Additional sequential photographs are shown in Figure 20. Documentary photographs of the crash test are shown in Figures 21 through 23.

7.2 Test Description

Initial impact occurred at 438-mm (17¼-in.) upstream from post no. 14C, as shown in Figure 24. At 0.014 sec after impact, the right-front corner of the vehicle impacted post no. 14C, and subsequently was driven over by the right-front tire at 0.034 sec. The vehicle's right-front bumper contacted post nos. 13C, 12C, and 11C at 0.045 sec, 0.085 sec, and 0.115 sec after impact, respectively. It is noted that the top two cables were removed from post nos. 12C and 11C prior to the vehicle contacting them, thereby causing the posts to deform. At 0.154 sec, the right-front corner of the vehicle had moved to the same lateral offset at post no. 1W. Subsequently, post no. 10C was deformed at 0.169 sec after initial impact. At 0.241 sec, the vehicle began to redirect away from the initial impact angle. The cable guardrails contacted the head of the BCT terminal at 0.285 sec while the front end of the vehicle contacted the terminal at 0.335 sec, thus resulting in the fracturing post no. 1W at 0.365 sec after impact. At 0.321 sec, the maximum lateral dynamic cable deflection was observed to be 2.4 m (7.9 ft). At 0.399 sec, the head of the deformed BCT terminal struck the ground. The vehicle's front end was positioned between post nos. 1W and 2W with the BCT terminal and post no. 1W under the vehicle at 0.417 sec. At 0.443 sec, the right-front tire rode over the BCT end as the W-beam rail was sloping downward under the front bumper, subsequently

striking post no. 2W at 0.455 sec.

At 0.486 sec after impact, the vehicle became parallel to the barrier with a velocity of 58.7 km/hr (36.5 mph) and with the entire vehicle positioned laterally behind the original longitudinal location of the rail. At 0.499 sec, the right-front tire was positioned above the ground and with the W-beam sloped downward as the front of the vehicle passed over it. Subsequently, the left-front tire rode over post no. 9C at 0.578 sec, causing the tire to become airborne. At 0.597 sec, the middle cable lost its tensile capacity when it pulled out at the anchorage located on the upstream end. A kink formed in the W-beam rail at post no. 2W at 0.608 sec after impact, and at 0.639 sec, post no. 3W fractured as the vehicle's undercarriage passed over it. At 0.813 sec, the right-front corner of the vehicle moved downward and rolled clockwise slightly, thus allowing the right-front bumper to contact and fracture post no. 4W. The right-front tire contacted the ground near the back of the wood posts at 0.860 sec. At 1.000 sec, the vehicle's roll angles was nearly 0 degrees but with the front tires above the ground, the vehicle positioned on top of the rail, and the upper cable hooked over the right-front bumper. At 1.080 sec, the front of the vehicle is positioned at post no. 5W with the vehicle beginning to roll counter-clockwise away from the rail. At 1.122 sec, the vehicle continued to travel along the barrier with the upper cable hooked over the right-front bumper and the lower cable wrapped around the left-front tire. Subsequently, the left-front tire contacted the ground at 1.225 sec. The front of the vehicle was positioned at post nos. 6W, 7W, and 8W at 1.330 sec, 1.674 sec, and 2.186 sec, respectively.

At 1.588 sec, the vehicle reached its maximum roll angle of 32.4 degrees and counter-clockwise away from the rail. The vehicle's post-impact trajectory is shown in Figures 19 and 25. The vehicle came to rest with the right side of the vehicle positioned above the rail and the right-

front tire located 22.3-m (73-ft 2-in.) downstream from impact and 0.55 m (1 ft - 9½ in.) behind the traffic-side face of the barrier.

7.3 Barrier Damage

Damage to the barrier was extensive, as shown in Figures 25 through 28. Barrier damage consisted mostly of deformed steel posts and W-beam, fractured wood posts, ruptured or stretched cables, and deformations to the steel anchorage hardware. Steel post nos. 1C through 14C were deformed above the ground line, while post nos. 15C through 17C were rotated in the soil. Wood post nos. 1W through 4W were fractured, while post nos. 5W through 11W were all displaced, as determined either visually or by measurements taken at the ground line. The BCT head was collapsed at the nose section, and the W-beam buckled and deformed at post nos. 2W and 3W, respectively. The upper and lower cables remained intact while the middle cable was no longer anchored at the upstream end due to the failure of the threads on the connecting rod. The steel transition brackets located at post nos. 7W and 9W were deformed and only contained the lower cable following the crash test. The maximum lateral dynamic cable deflection was 2.4 m (7.9 ft), as determined from the high-speed film analysis.

7.4 Vehicle Damage

Exterior vehicle damage was moderate and occurred at several body locations, as shown in Figure 29. The vehicle's front end was crushed inward due to contact with the BCT terminal and W-beam guardrail, the right-front quarter panel was crushed, and the right-side front bumper was bent back toward the engine compartment. The engine compartment was also moved backward, and the undercarriage near the front end was deformed. Very minor deformations were found on the floorboard of the occupant compartment. Evidence of vehicle-rail interlock was also found from the

front end to the midpoint of the truck box.

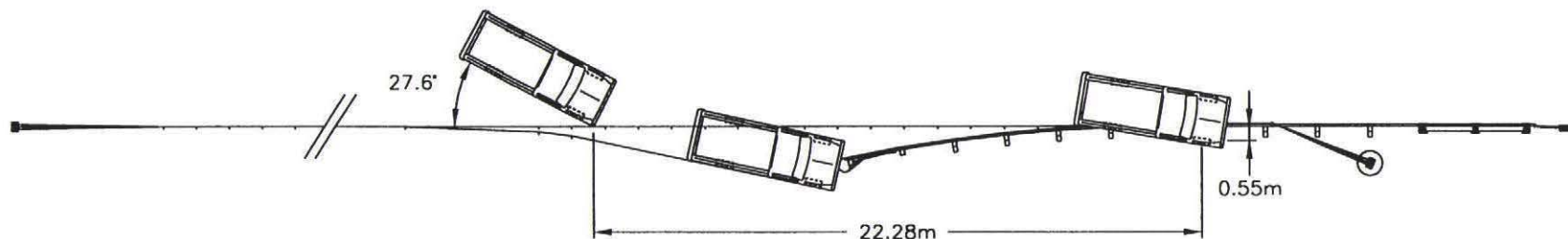
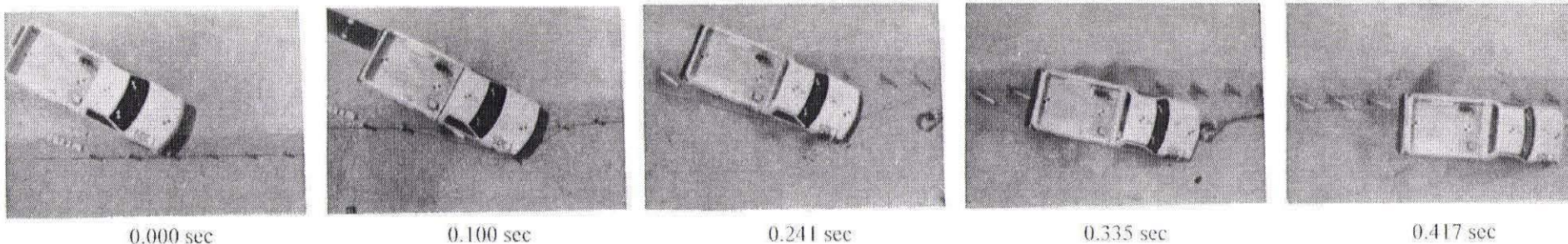
7.5 Occupant Risk Values

The normalized longitudinal and lateral occupant impact velocities were determined to be 4.62 m/sec (15.17 ft/s) and 2.99 m/sec (9.82 ft/s), respectively. The maximum 0.010-sec average occupant ridedown decelerations in the longitudinal and lateral directions were 12.21 g's and 7.36 g's, respectively. It is noted that the occupant impact velocities (OIV) and occupant ridedown decelerations (ORD) were within the suggested limits provided in NCHRP Report 350. The results of the occupant risk, determined from accelerometer data, are summarized in Figure 19. Results are shown graphically in Appendix C. The results from the rate transducer are shown graphically in Appendix D.

7.6 Discussion

The analysis of the test results for test SDC-1 showed that the barrier adequately contained and redirected the vehicle with controlled lateral displacement of the barrier. Detached elements, fragments, or other debris from the test article did not penetrate or show potential for penetrating the occupant compartment, or present undue hazard to other traffic. Minor deformations to the occupant compartment were evident but not considered excessive enough to cause serious injuries to the occupants. The vehicle remained upright both during and after the collision. Vehicle roll, pitch, and yaw angular displacements were noted, but they were deemed acceptable because they did not adversely influence occupant safety criteria or cause rollover. After collision, the vehicle's trajectory did not intrude into adjacent traffic lanes. In addition, the vehicle's exit angle was less than 60 percent of the impact angle as the vehicle was contained along the system. Therefore, test SDC-1 conducted on the cable guardrail to W-beam transition system was determined to be acceptable

according to the NCHRP Report 350 criteria.



- Test Number SDC-1
- Date 8/11/98
- Appurtenance Cable Guardrail to W-Beam Transition
- Three-Strand Cable Guardrail
 - Diameter 19.0 mm
 - Specification 3 x 7 Wire Rope
 - Top Mounting Height 686 mm (center of upper cable)
- Steel Posts
 - Post Nos. 1C - 32C W76x8.5
- W-Beam Guardrail
 - Thickness 2.66 mm
 - Top Mounting Height 686 mm
- Wood Posts
 - Spacing 1,905 mm
 - Post Nos. 1W - 2W 140 mm x 190 mm x 1,080 mm
 - Post Nos. 3W - 11W 152 mm x 203 mm x 1,829 mm
- Wood Spacer Blocks
 - Post Nos. 3W - 11W 152 mm x 203 mm x 356 mm
- Soil Type Grading B - AASHTO M 147-65 (1990)
- Vehicle Model 1993 GMC 2500 (¾-ton) 2WD
 - Curb 2,173 kg
 - Test Inertial 2,013 kg
 - Gross Static 2,013 kg

- Vehicle Speed
 - Impact 101.9 km/hr
 - Exit NA
- Vehicle Angle
 - Impact 27.6 deg
 - Exit NA
- Vehicle Snagging Minor tire and undercarriage snagging on posts
- Vehicle Pocketing Minor
- Vehicle Stability Moderate roll angle but stable
- Occupant Ridedown Deceleration (10 msec avg.)
 - Longitudinal 12.21 G's < 20 G's
 - Lateral (not required) 7.36 G's
- Occupant Impact Velocity (Normalized)
 - Longitudinal 4.62 m/s < 12 m/s
 - Lateral (not required) 2.99 m/s
- Vehicle Damage Moderate
 - TAD¹³ 1-RFQ-3, 12-FC-3
 - SAE¹⁴ 01RFEW2, 12FCLN1
- Vehicle Stopping Distance 22.3 m downstream
 - 0.55 m behind traffic-side face
- Barrier Damage Extensive
- Maximum Dynamic Deflection 2.4 m

Figure 19. Summary of Test Results and Sequential Photographs, Test SDC-1



0.000 sec



0.000 sec



0.169 sec



0.341 sec



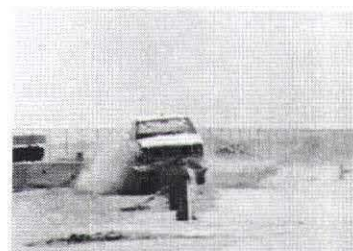
0.347 sec



0.503 sec



0.406 sec



0.651 sec



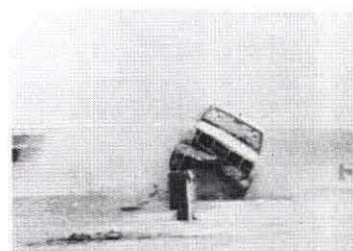
0.650 sec



1.000 sec



1.077 sec



1.835 sec

Figure 20. Additional Sequential Photographs, Test SDC-1

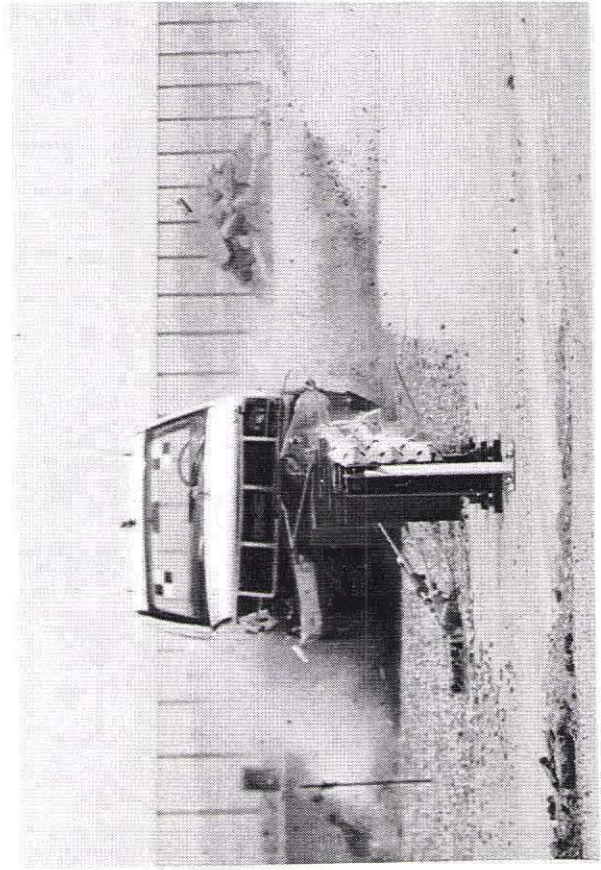
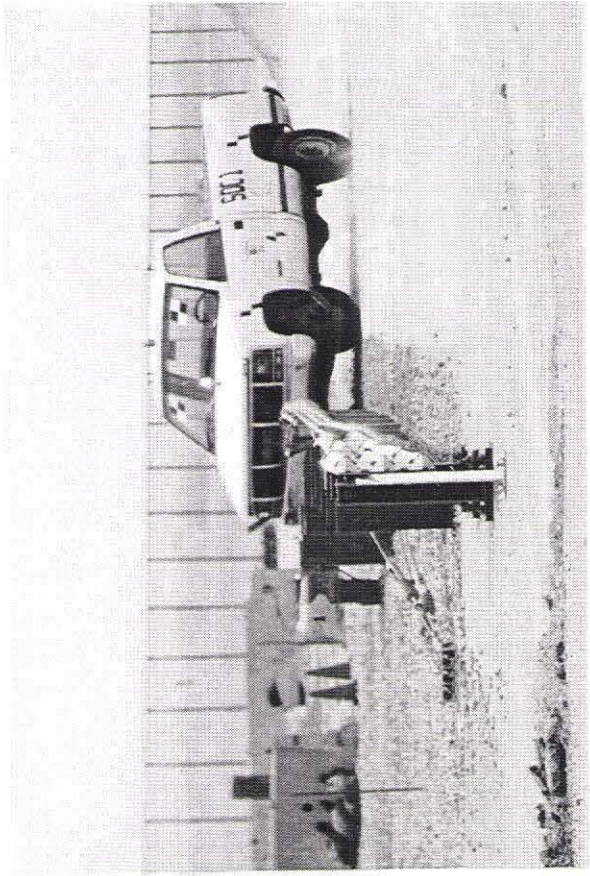
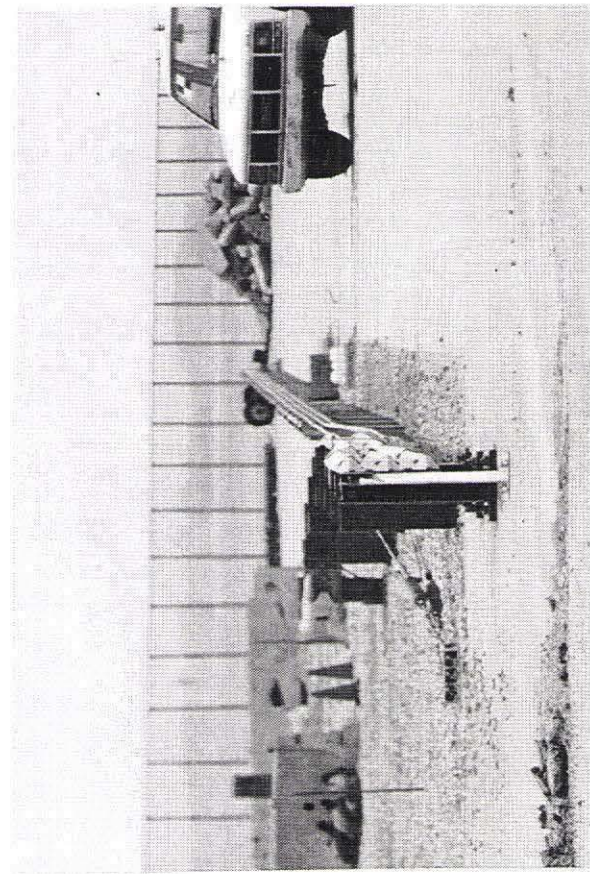


Figure 21. Full-Scale Crash Test, Test SDC-1

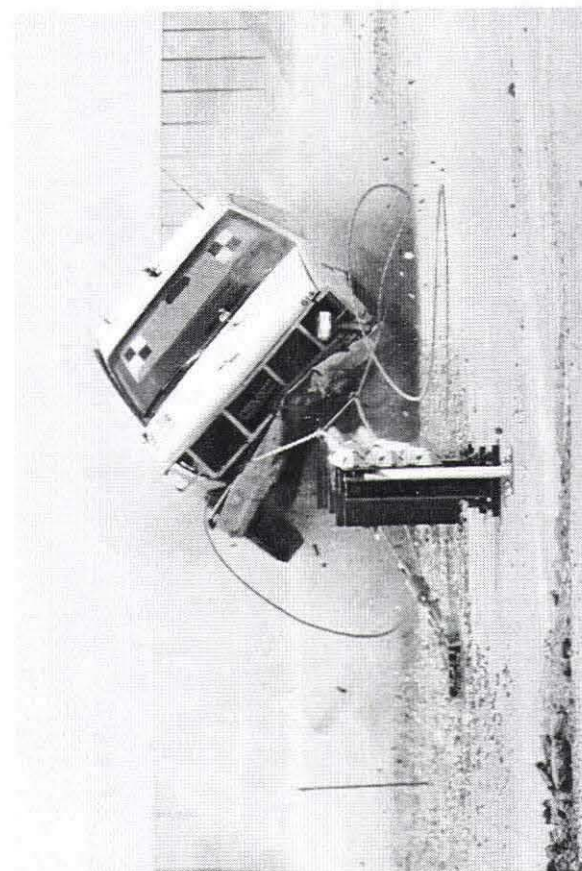


Figure 22. Full-Scale Crash Test, Test SDC-1



Figure 23. Full-Scale Crash Test, Test SDC-1



Figure 24. Impact Location, Test SDC-1

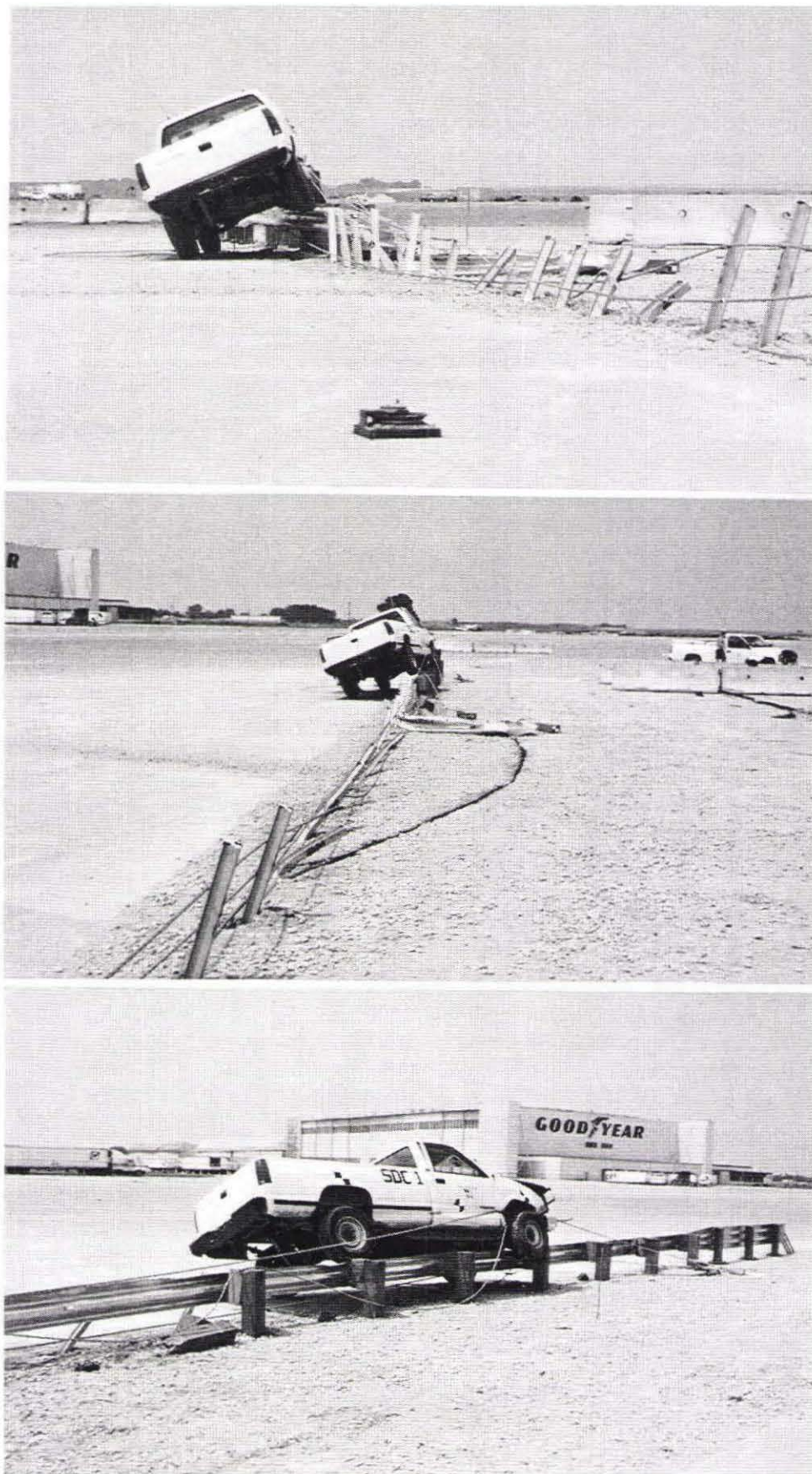


Figure 25. Cable Guardrail to W-Beam Transition Damage, Test SDC-1

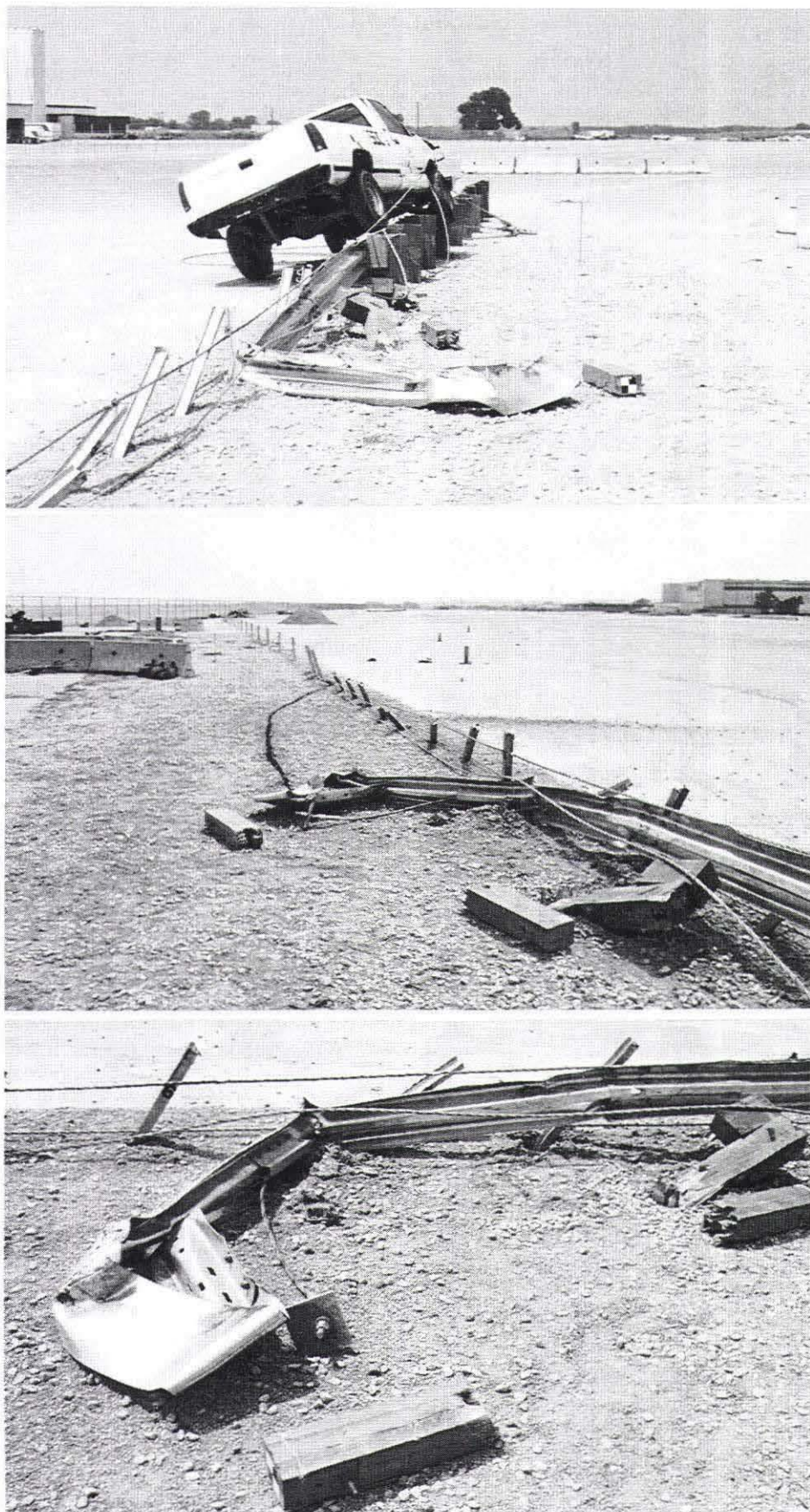


Figure 26. Breakaway Cable Terminal Damage, Test SDC-1

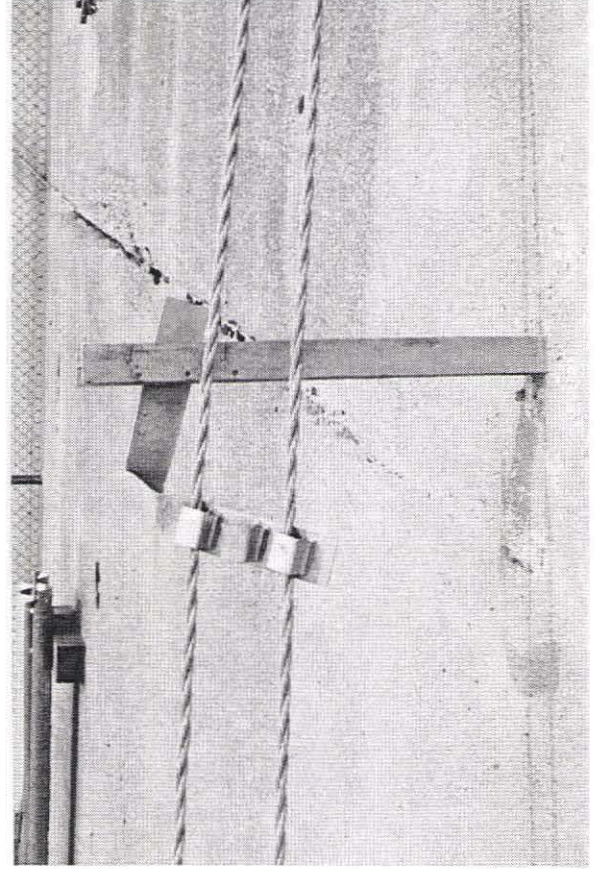
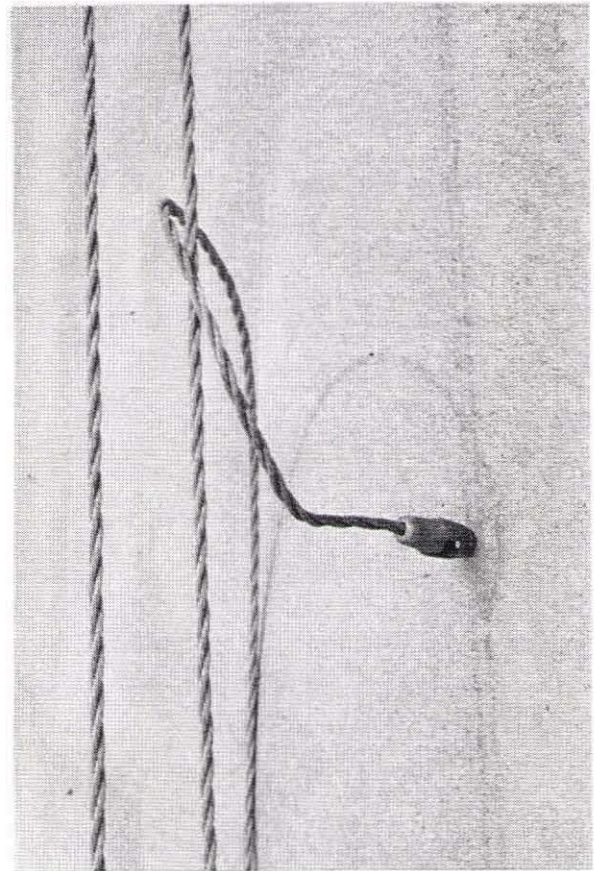
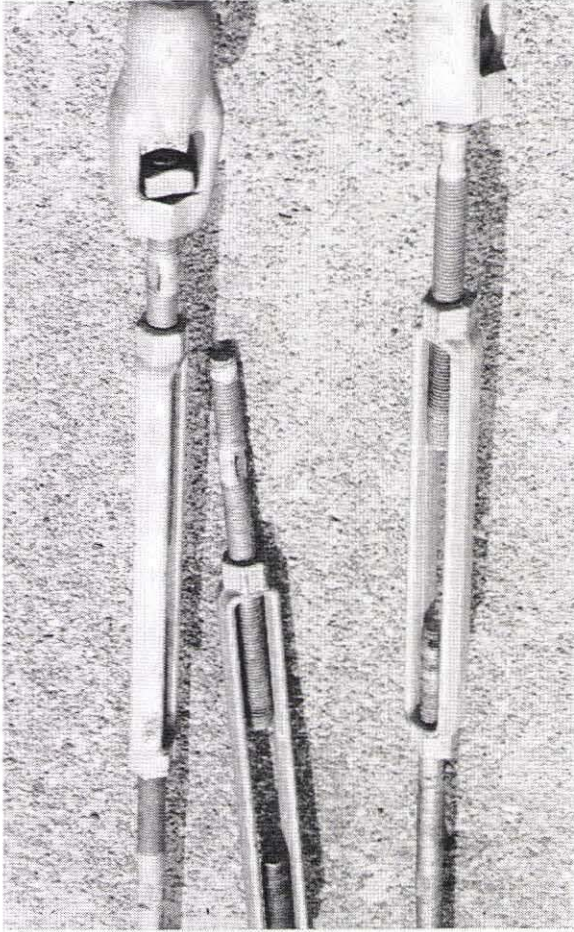
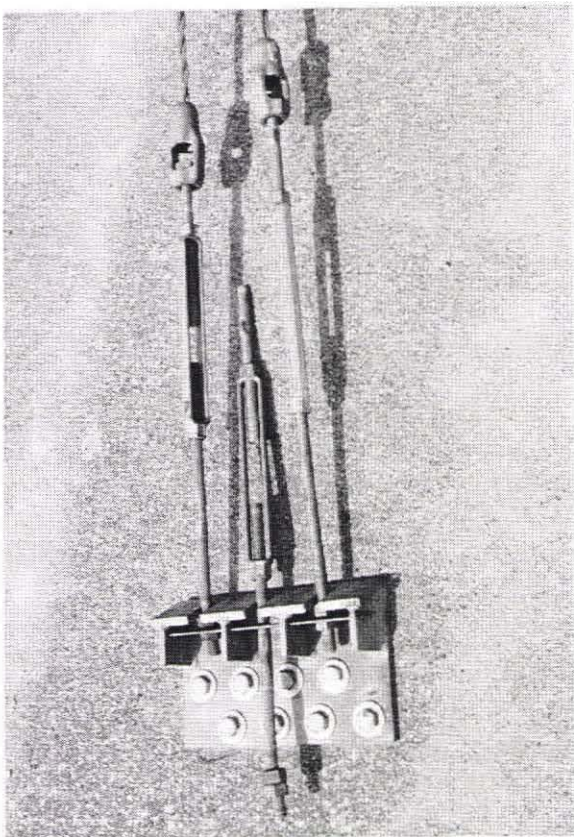


Figure 27. Upstream Cable Anchorage Damage, Test SDC-1

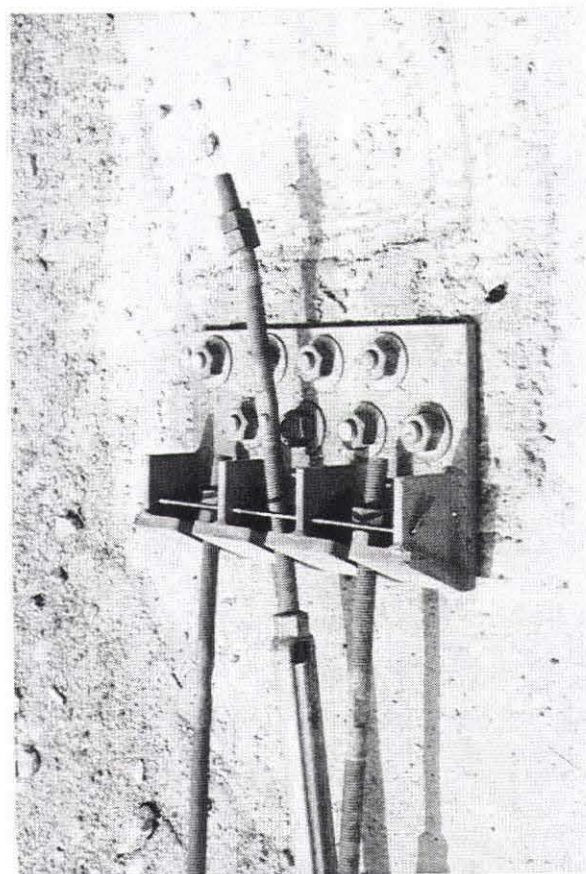
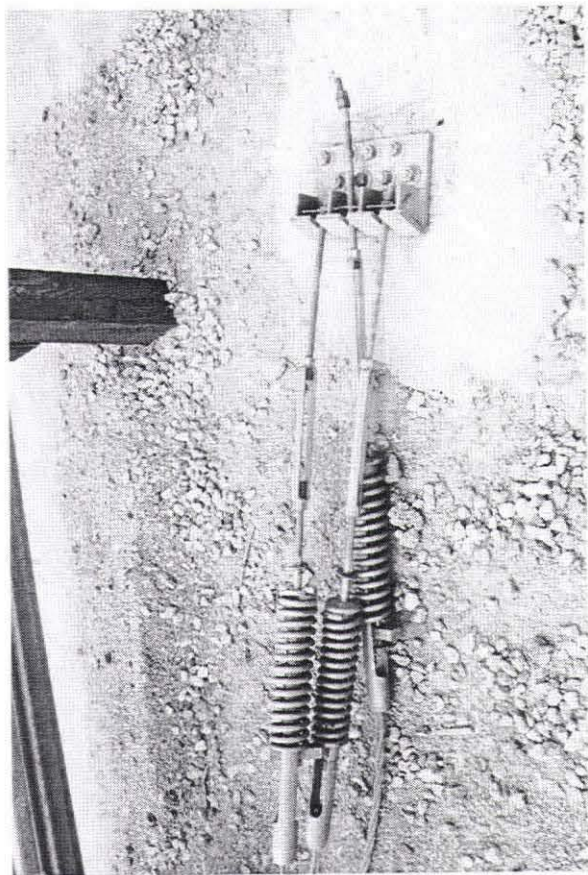


Figure 28. Downstream Cable Anchorage Damage, Test SDC-1



Figure 29. Vehicle Damage, Test SDC-1

8 CRASH TEST NO. 2

8.1 Test SDC-2

The 2,023-kg (4,459-lb) pickup truck impacted the cable guardrail to W-beam transition at a speed of 101.8 km/hr (63.3 mph) and an angle of 25.2 degrees. A summary of the test results and the sequential photographs are shown in Figure 30. Additional sequential photographs are shown in Figure 31. Documentary photographs of the crash test are shown in Figures 32 through 34.

8.2 Test Description

Initial impact occurred at the upstream edge of post no. 4C, as shown in Figure 35. At 0.042 sec after impact, the right-front corner of the vehicle impacted the W-beam rail at the midpoint between post nos. 3W and 4W. The right-front corner of the vehicle reached post no. 4W at 0.089 sec which subsequently fractured. At 0.091, one of the lower cables lost its tensile capacity when it pulled out at the anchorage located on the downstream end. At 0.145 sec after impact, post no. 5W fractured as the remaining lower cable lost its tensile capacity when it also pulled out at the anchorage located at the downstream end. As the vehicle continued to travel along the guardrail and penetrate laterally into the system, tensile loads increased in the W-beam rail located upstream from the original impact location. At 0.184 sec, this tensile loads caused post nos. 3W and 2W to fracture, in that order. In addition, the upper cable slipped over the top of the W-beam rail and was observed to be angled toward the ground at the downstream anchorage system. At 0.230 sec, the rear end of the vehicle contacted the cable, and at 0.246 sec, the left-front tire struck and drove over post no. 1C as the vehicle began to roll clockwise toward the rail. At 0.260 sec, the right-side midpoint of the vehicle contacted post no. 6W as the left-front tire became airborne. Subsequently, post no. 6W fractured about its weak axis at 0.267 sec after impact. At 0.311 sec, the upper cable released from

the right-front corner of the vehicle as the lower two cables continued to flail in the air. The vehicle reached post no. 7W at 0.394 sec which subsequently resulted in the fracture of the post.

At 0.424 sec after impact, the vehicle became parallel to the barrier with a velocity of 44.5 km/hr (27.6 mph). The front of the vehicle reached post no. 8W at 0.552 sec with the vehicle's left side airborne. Subsequently, at 0.607 sec, the right-front tire struck post no. 8, causing the vehicle to slow more rapidly. The vehicle began to move away from the barrier at 0.645 sec with the left side elevated into the air and the right-front tire traveling along the back side of the rail and posts. At 0.868 sec, the vehicle reached its maximum roll angle of 27.4 degrees and clockwise toward the rail. The vehicle's forward motion came to a stop slightly upstream of post no. 9W at 0.878 sec after impact and with the rear end pitched upward. At 1.049 sec, the vehicle rebounded backward slightly while the rear end moved away from the barrier. The left-front tire contacted the concrete surface at 1.272 sec, while the left-rear tire struck the ground at 0.1370 sec and with a vehicle roll angle counter-clockwise away from the rail. The vehicle came to a stop with all four tires on the concrete surface at approximately 2.571 sec.

The vehicle's post-impact trajectory is shown in Figures 30 and 36. The vehicle came to rest on the traffic-side face of the barrier system with the right-front tire located 11.0-m (36-ft 0-in.) downstream from impact and 1.07 m (3 ft - 6 in.) on the traffic-side face of the barrier.

8.3 Barrier Damage

Damage to the barrier was extensive, as shown in Figures 36 through 39. Barrier damage consisted mostly of deformed steel posts and W-beam, fractured wood posts, ruptured or stretched cables, and deformations to the steel anchorage hardware. Steel post nos. 1C through 3C were deformed above the ground line, while post nos. 4C through 5C were rotated in the soil. Wood post

nos. 1W through 7W were fractured, while post no. 8W was displaced, as determined either visually or by measurements taken at the ground line. The initial vehicle contact marks were found on the W-beam rail at a location 330-mm (13-in.) upstream from the midspan between post no. 3W and 4W. In addition, significant flattening of the W-beam rail occurred between post nos. 5W and 7W. The upper cable remained intact while the lower and middle cables were no longer anchored at the downstream end. The steel transition brackets located at post nos. 7W and 9W were deformed.

8.4 Vehicle Damage

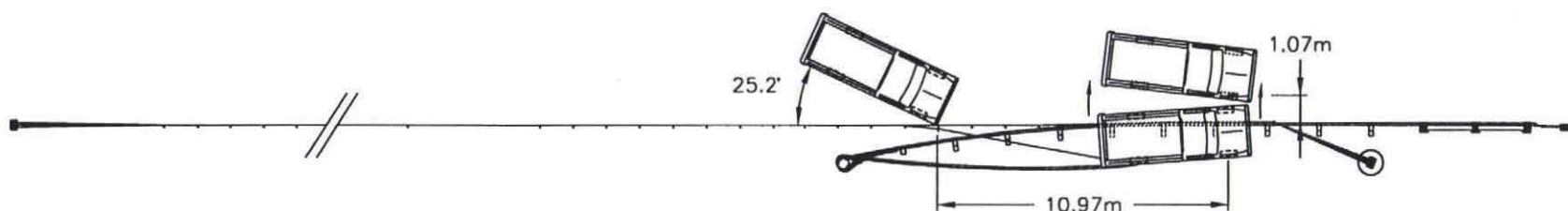
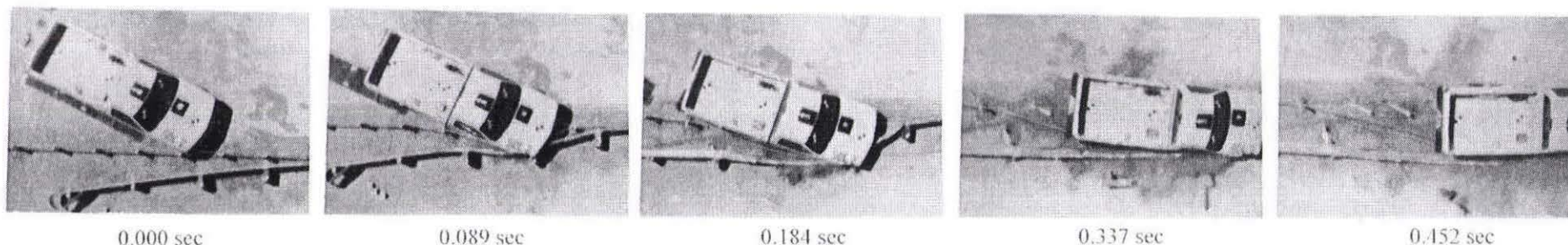
Exterior vehicle damage was moderate and occurred at several body locations, as shown in Figure 40. The vehicle's front end, right-front bumper, and right-front quarter panel were crushed inward toward the engine compartment due to contact with the barrier. Components within the engine compartment and front undercarriage were either deformed or moved backward and upward. Very minor deformations were found on the right-side firewall of the occupant compartment.

8.5 Occupant Risk Values

The normalized longitudinal and lateral occupant impact velocities were determined to be 6.84 m/sec (22.43 ft/sec) and 3.77 m/sec (12.37 ft/sec), respectively. The maximum 0.010-sec average occupant ridedown decelerations in the longitudinal and lateral directions were 9.25 g's and 5.97 g's/-7.44 g's, respectively. It is noted that the occupant impact velocities (QIV) and occupant ridedown decelerations (ORD) were within the suggested limits provided in NCHRP Report 350. The results of the occupant risk, determined from accelerometer data, are summarized in Figure 30. Results are shown graphically in Appendix E. The results from the rate transducer are shown graphically in Appendix F.

8.6 Discussion

The analysis of the test results for test SDC-2 showed that the barrier adequately contained and redirected the vehicle with controlled lateral displacement of the barrier. Detached elements, fragments, or other debris from the test article did not penetrate or show potential for penetrating the occupant compartment, or present undue hazard to other traffic. Minor deformations to the occupant compartment were evident but not considered excessive enough to cause serious injuries to the occupants. The vehicle remained upright both during and after the collision. Vehicle roll, pitch, and yaw angular displacements were noted, but they were deemed acceptable because they did not adversely influence occupant safety criteria or cause rollover. After collision, the vehicle's trajectory did not intrude into adjacent traffic lanes. In addition, the vehicle's exit angle was less than 60 percent of the impact angle as the vehicle was contained along the system. Therefore, test SDC-2 conducted on the cable guardrail to W-beam transition system was determined to be acceptable according to the NCHRP Report 350 criteria.



- Test Number SDC-2
- Date 8/18/98
- Appurtenance Cable Guardrail to W-Beam Transition
- Three-Strand Cable Guardrail
 - Diameter 19.0 mm
 - Specification 3 x 7 Wire Rope
 - Top Mounting Height 686 mm (center of upper cable)
- Steel Posts
 - Post Nos. 1C - 32C W76x8.5
- W-Beam Guardrail
 - Thickness 2.66 mm
 - Top Mounting Height 686 mm
- Wood Posts
 - Spacing 1,905 mm
 - Post Nos. 1W - 2W 140 mm x 190 mm x 1,080 mm
 - Post Nos. 3W - 11W 152 mm x 203 mm x 1,829 mm
- Wood Spacer Blocks
 - Post Nos. 3W - 11W 152 mm x 203 mm x 356 mm
- Soil Type Grading B - AASHTO M 147-65 (1990)
- Vehicle Model 1994 GMC 2500 (¾-ton) 2WD
 - Curb 2,045 kg
 - Test Inertial 2,023 kg
 - Gross Static 2,023 kg

- Vehicle Speed
 - Impact 101.8 km/hr
 - Exit NA
- Vehicle Angle
 - Impact 25.2 deg
 - Exit NA
- Vehicle Snagging Minor tire snagging on posts
- Vehicle Pocketing None
- Vehicle Stability Moderate roll angle but stable
- Occupant Ridedown Deceleration (10 msec avg.)
 - Longitudinal 9.25 G's < 20 G's
 - Lateral (not required) 5.97 G's/-7.44 G's
- Occupant Impact Velocity (Normalized)
 - Longitudinal 6.84 m/s < 12 m/s
 - Lateral (not required) 3.77 m/s
- Vehicle Damage Moderate
 - TAD¹³ 1-RFQ-4
 - SAE¹⁴ 01RFEW3
- Vehicle Stopping Distance 11.0 m downstream
 - 1.07 m on traffic-side face
- Barrier Damage Extensive
- Maximum Dynamic Deflection Not visible

Figure 30. Summary of Test Results and Sequential Photographs, Test SDC-2



0.000 sec



0.092 sec



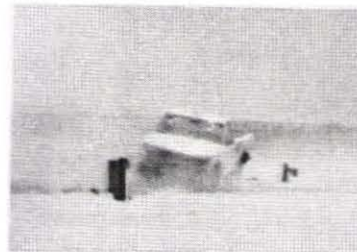
0.153 sec



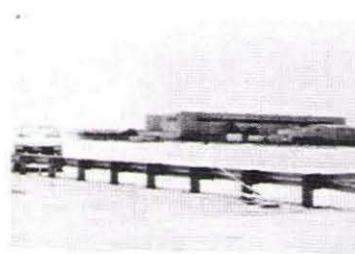
0.250 sec



0.645 sec



1.407 sec



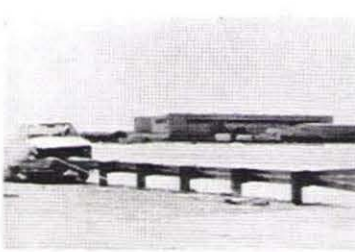
0.000 sec



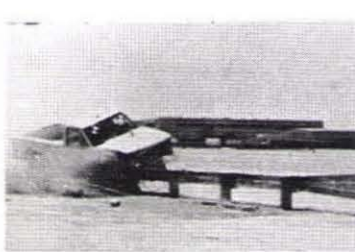
0.091 sec



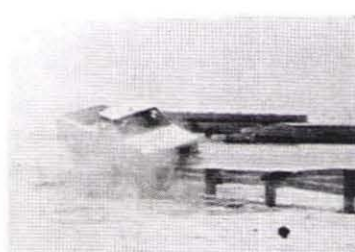
0.149 sec



0.260 sec



0.607 sec



1.152 sec

Figure 31. Additional Sequential Photographs, Test SDC-2

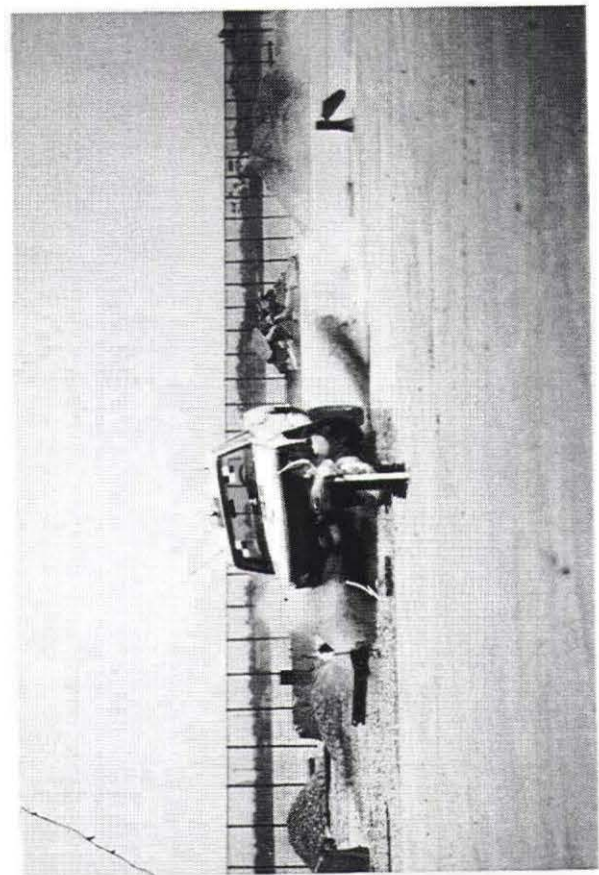
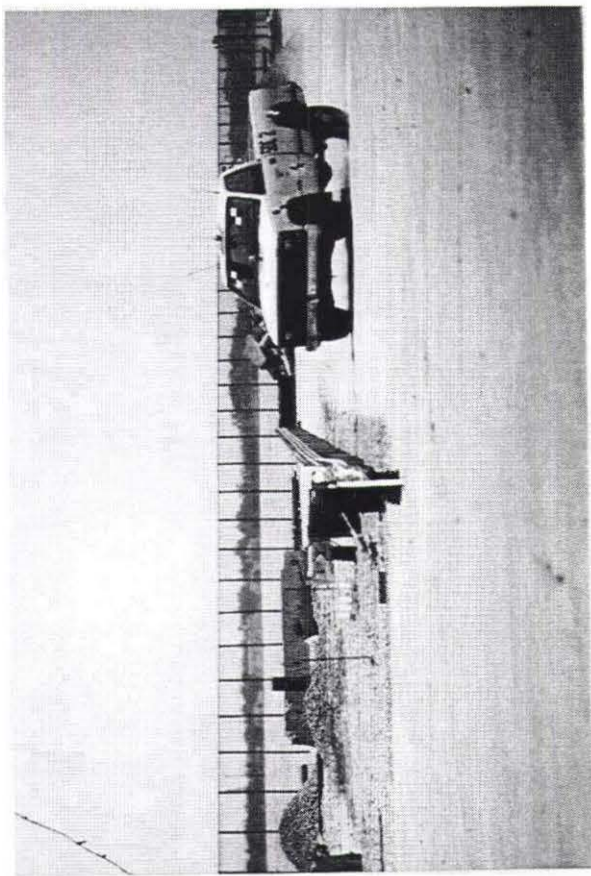
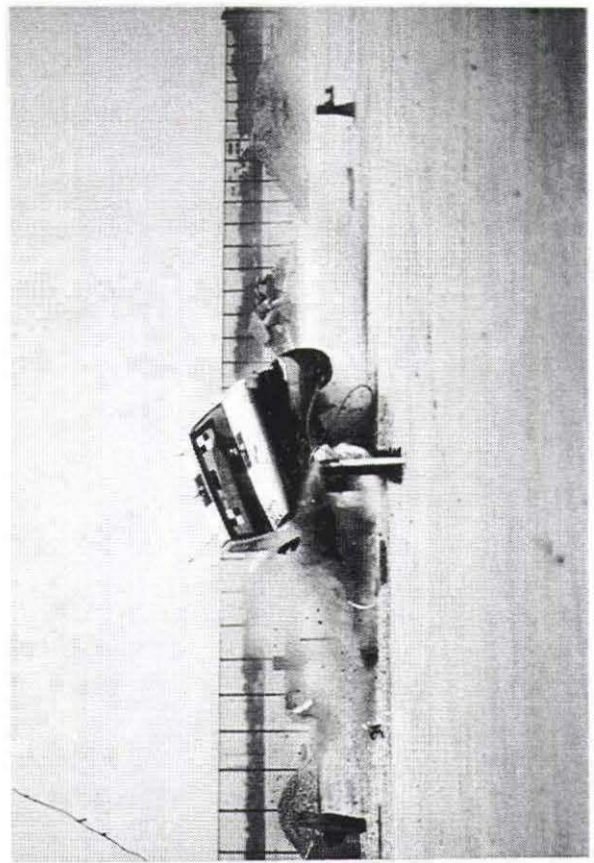
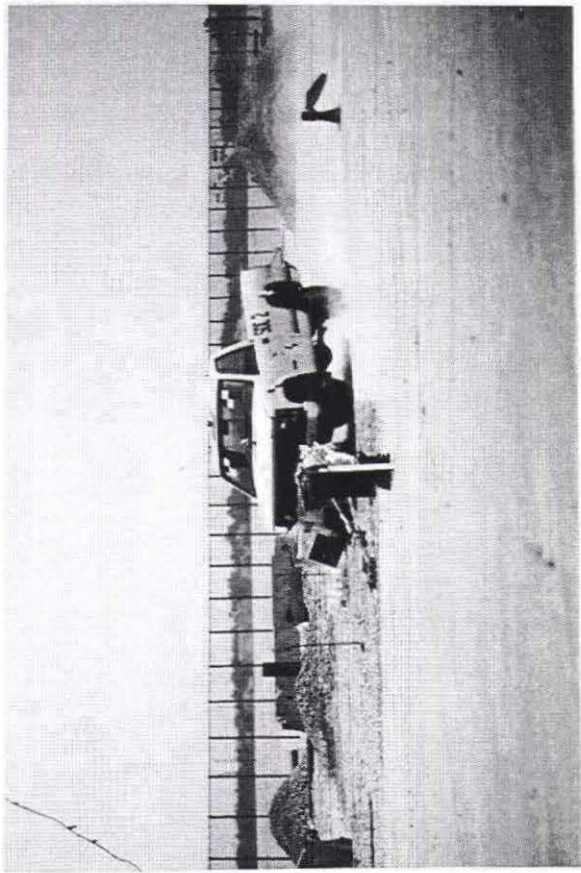
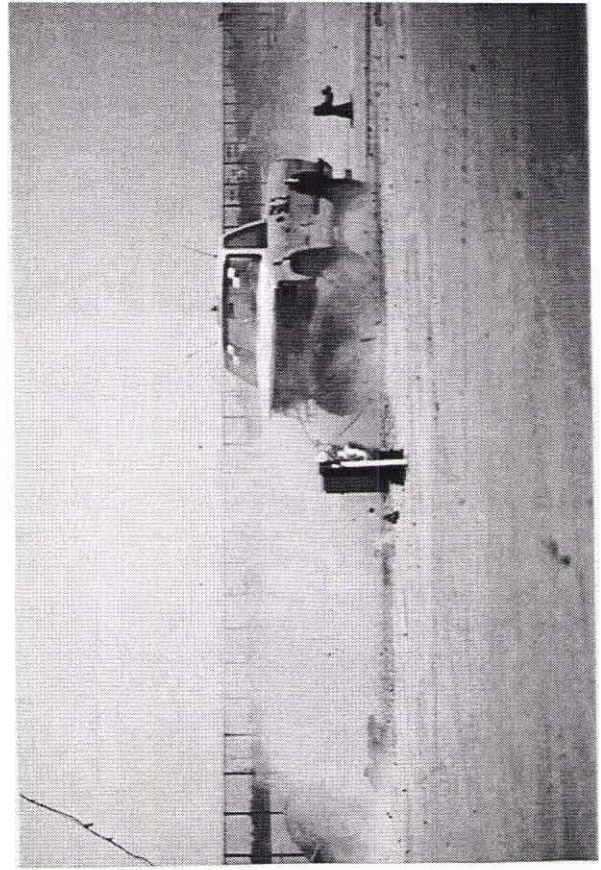
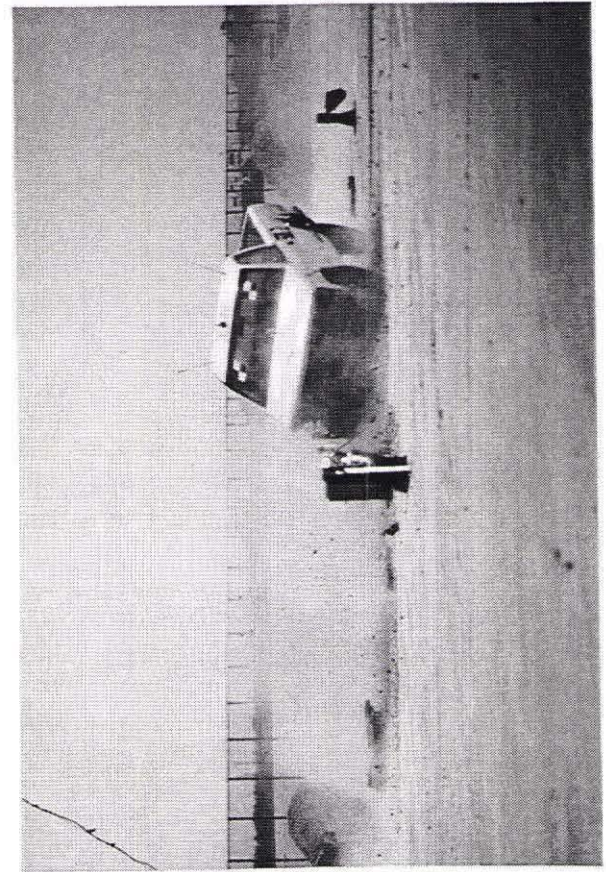
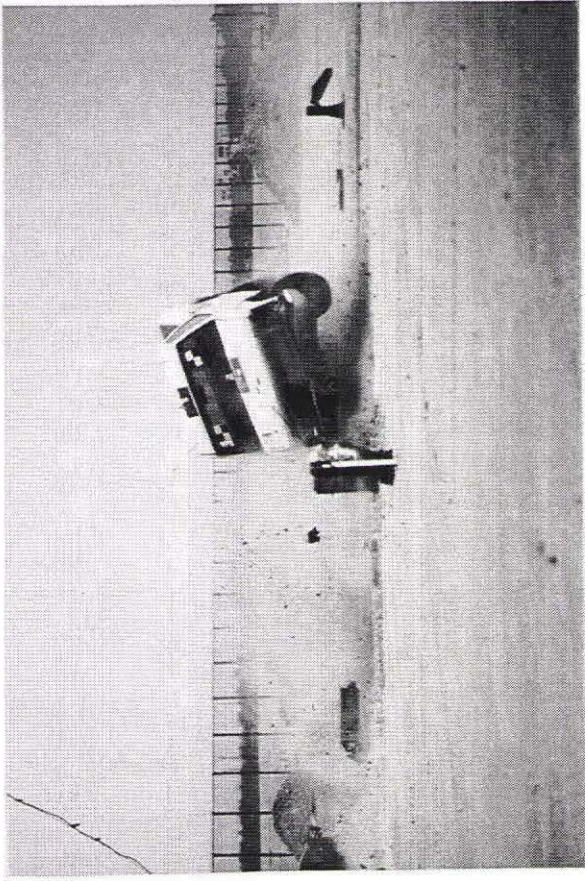
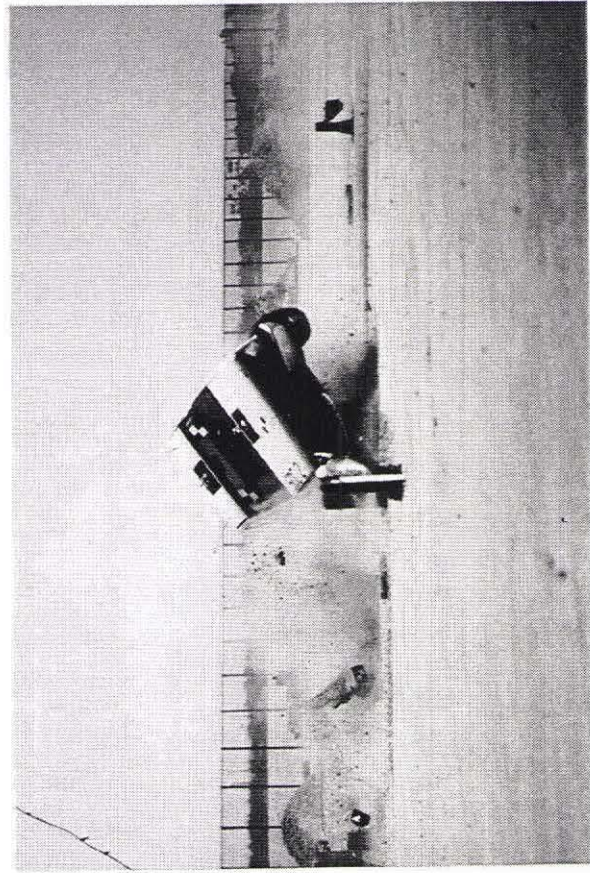


Figure 32. Full-Scale Crash Test, Test SDC-2



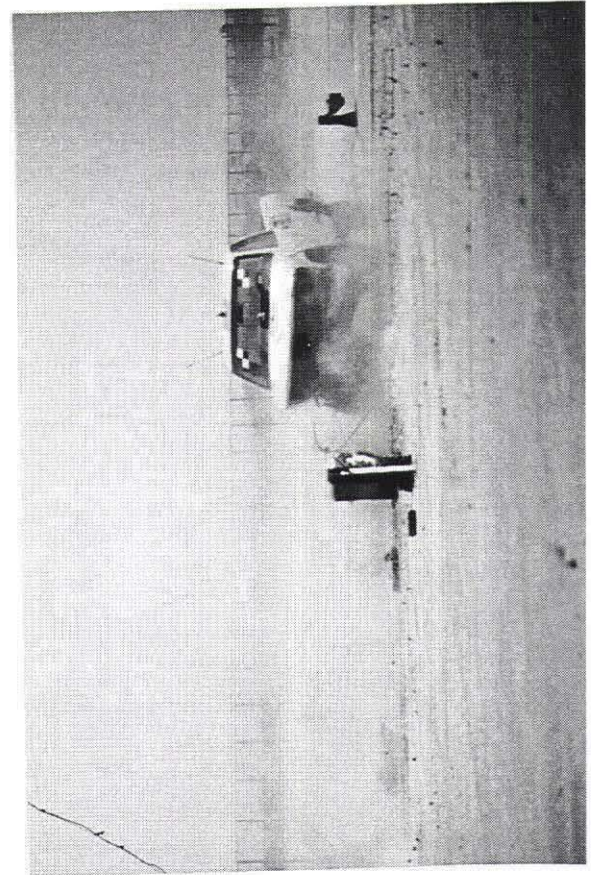
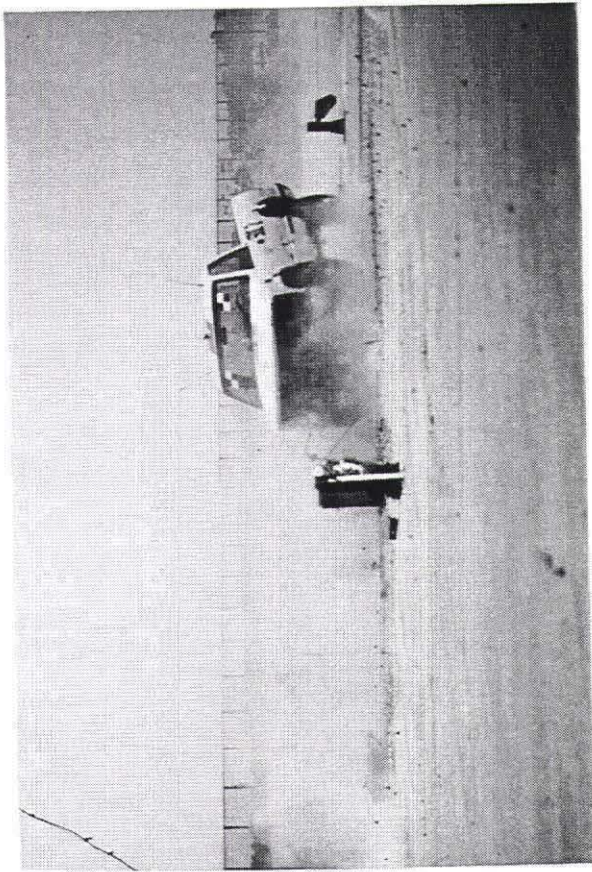
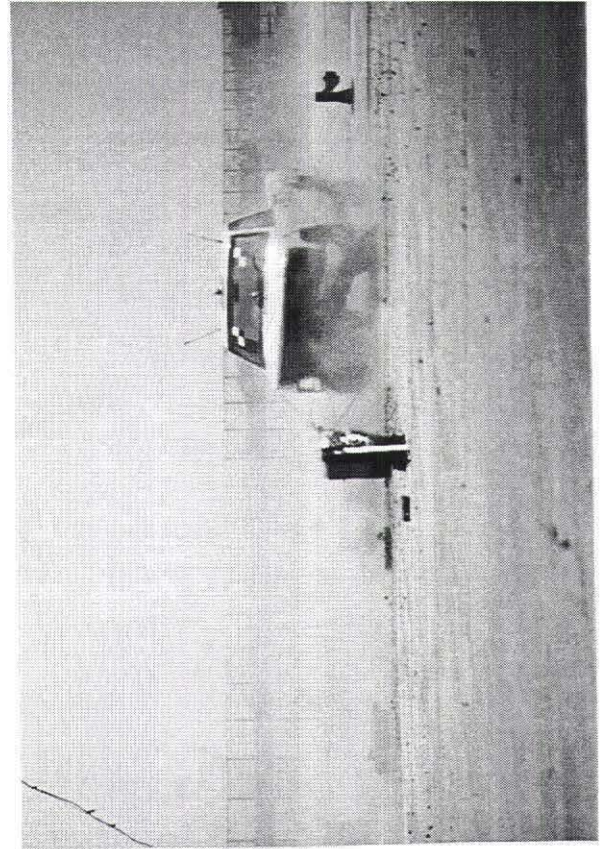
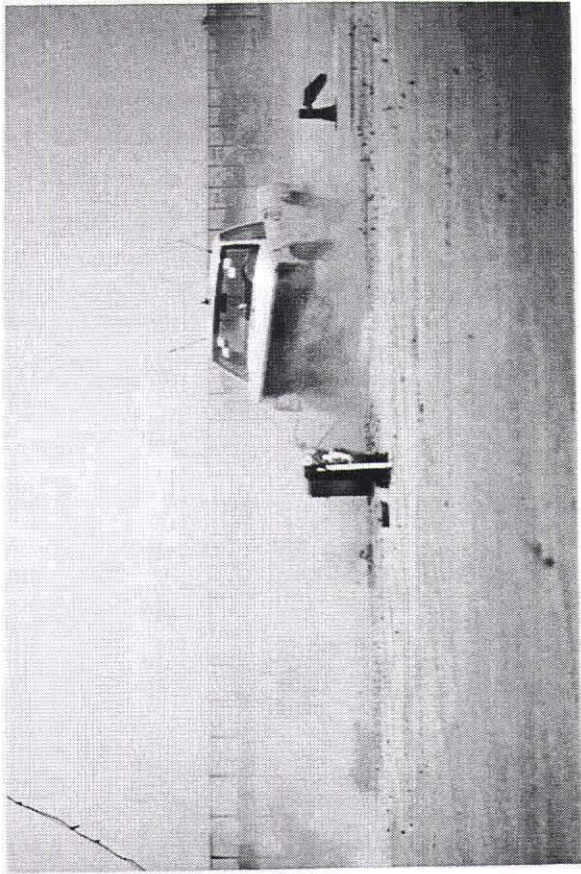


Figure 34. Full-Scale Crash Test, Test SDC-2



Figure 35. Impact Location, Test SDC-2



Figure 36. Cable Guardrail to W-Beam Transition Damage, Test SDC-2

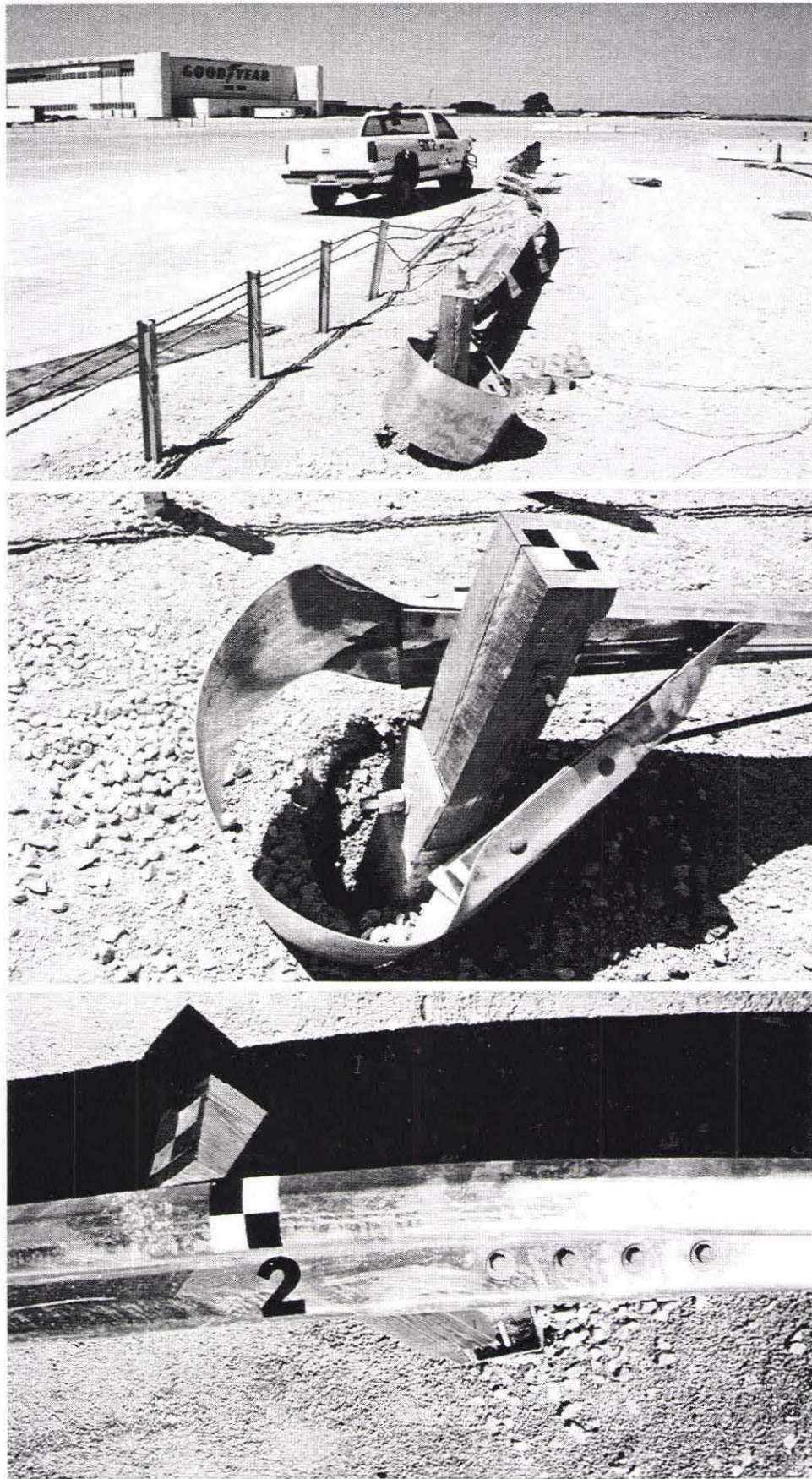


Figure 37. Breakaway Cable Terminal Damage, Test SDC-2

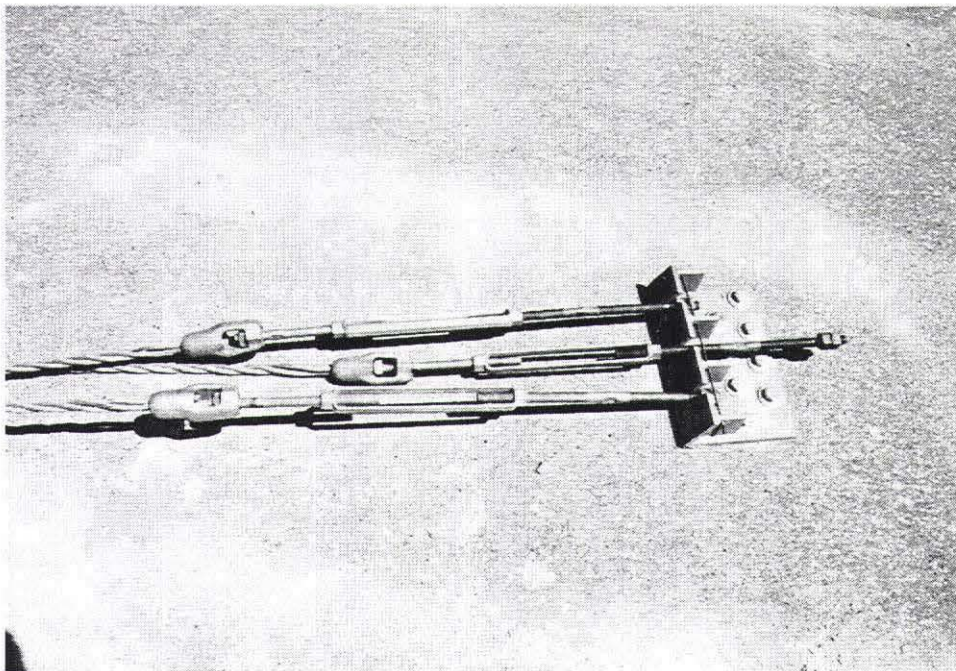
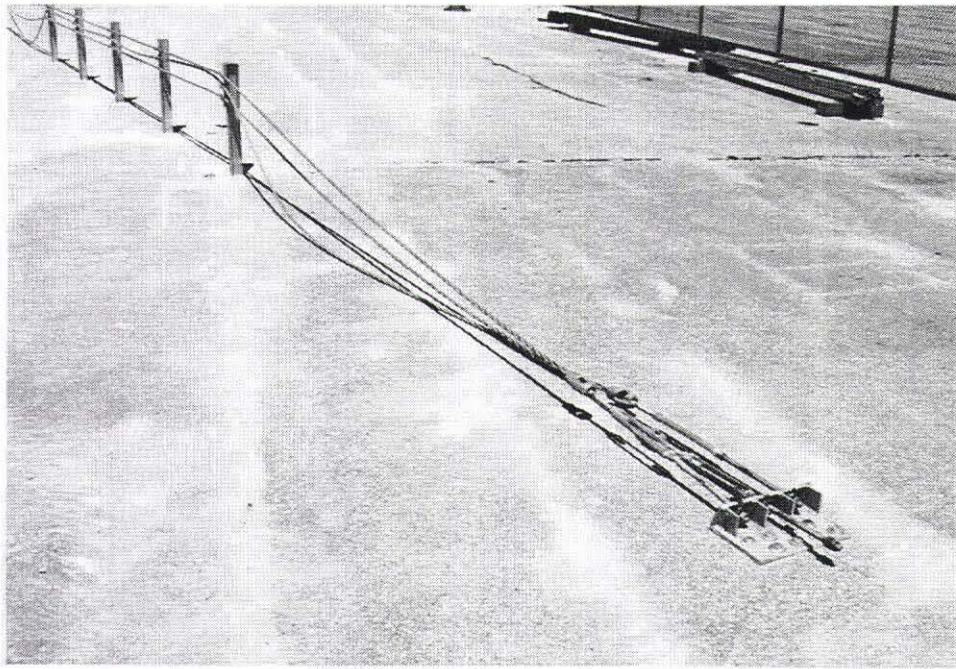


Figure 38. Upstream Cable Anchorage Damage, Test SDC-2

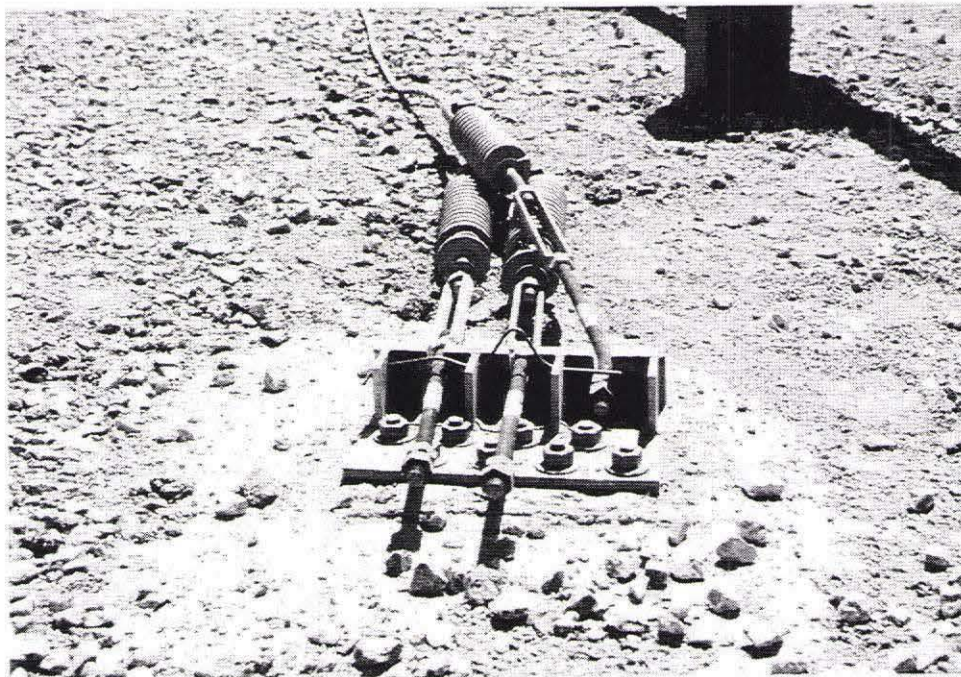


Figure 39. Downstream Cable Anchorage Damage, Test SDC-2



Figure 40. Vehicle Damage, Test SDC-2

9 CRASH TEST NO. 3

9.1 Test SDC-3

The 878-kg (1,935-lb) small car impacted the cable guardrail to W-beam transition at a speed of 99.6 km/hr (61.9 mph) and an angle of 20.2 degrees. A summary of the test results and the sequential photographs are shown in Figure 41. Additional sequential photographs are shown in Figure 42. Documentary photographs of the crash test are shown in Figures 43 and 44.

9.2 Test Description

Initial impact occurred at 305-mm (12-in.) downstream of post no. 1C, as shown in Figure 45. At 0.048 sec, the right-front corner of the vehicle reached the midspan between post nos. 5W and 6W and with the top cable extending over the hood. Later, at 0.053 sec, it was evident that post nos. 5W and 6W had begun to deflect. The upper cable contacted the A-pillar of the vehicle at 0.078 sec, while the right-front corner of the vehicle was near post no. 6W at 0.082 sec after impact. Shortly thereafter, the upper cable reached the lower corner of the windshield as post no. 7W began to deflect. At 0.100 sec, the right-front tire protruded under the W-beam rail and snagged on post no. 6W, and at 0.110 sec, this vehicle contact caused the blockout to rotate and subsequently split. The right-front corner of the vehicle reached the midspan between post nos. 6W and 7W at 0.120 sec and with noticeable counter-clockwise vehicle roll away from the rail. At 0.141 sec, the maximum lateral dynamic post and W-beam rail deflection was observed to be 0.50 m (1.64 ft). At 0.155 sec, the right-front corner of the vehicle reached the transition cable bracket on the downstream side of post no. 7W, thus causing the cable on the hood to pull up on the bracket.

At 0.164 sec after impact, the vehicle became parallel to the barrier with a velocity of 82.0 km/hr (50.9 mph) as the cable was nearly off the hood. The right-front tire extended under the W-

beam rail and snagged on post no. 7W at 0.178 sec after impact, resulting in the transition cable bracket being pulled downward and becoming twisted. At 0.180 sec, the vehicle reached its maximum roll angle of 5.1 degrees and counter-clockwise roll away from the rail. At 0.193 sec, the right-front corner of the vehicle was at the midspan location between post no. 7W and 8W as the front of the vehicle was moving away from the rail, while the right-front corner was at post no. 8W at 0.237 sec. At 0.352 sec after impact, the vehicle exited the barrier at an angle of 7.4 degrees and a speed of 78.8 km/hr (49.0 mph).

The vehicle's post-impact trajectory is shown in Figures 41 and 46. The vehicle came to rest on behind the traffic-side face of the barrier system with the right-front tire located 45.7-m (150-ft) downstream from impact and 13.7 m (45 ft) on the traffic-side face of the barrier.

9.3 Barrier Damage

Damage to the barrier was moderate, as shown in Figures 46 through 47. Barrier damage consisted mostly of deformed W-beam, displaced steel and wood posts, and stretched cables. Steel post no. 1C and wood post nos. 3W through 9W were rotated in the soil, as determined either visually or by measurements taken at the ground line. Tire contact marks were found on the front face of post no. 6W and the front and upstream side faces of post no. 7W. Vehicle contact marks were found on the W-beam rail between the post no. 5W through 152-mm (6-in.) downstream from post no. 7W. All three cables remained intact and no damage was found at either cable anchorage device. The steel transition bracket located at post no. 7W was deformed with all three cables pulled out. The maximum lateral dynamic post and W-beam rail deflection was 0.50 m (1.64 ft), as determined from the high-speed film analysis.

9.4 Vehicle Damage

Exterior vehicle damage was moderate and occurred at several body locations, as shown in Figure 48. The vehicle's front end and hood, right-front bumper, and right-front quarter panel were crushed inward toward the engine compartment due to contact with the barrier. The right-front tire was deflated while the steel rim was deformed. Evidence of vehicle-rail interlock was also found from the front end to the midpoint of the rear quarter panel. Minor deformations were found on the right-side floorboard and firewall of the occupant compartment.

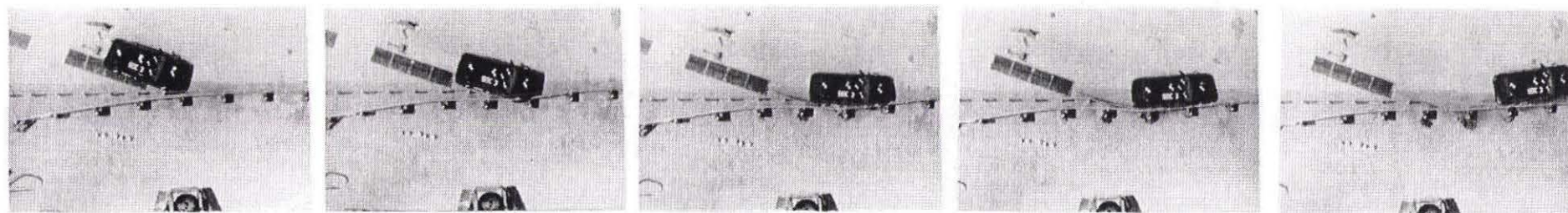
9.5 Occupant Risk Values

The normalized longitudinal and lateral occupant impact velocities were determined to be 5.72 m/sec (18.78 ft/sec) and 5.94 m/sec (19.47 ft/sec), respectively. The maximum 0.010-sec average occupant ridedown decelerations in the longitudinal and lateral directions were 2.83 g's/-3.24 g's and 16.64 g's, respectively. It is noted that the occupant impact velocities (OIV) and occupant ridedown decelerations (ORD) were within the suggested limits provided in NCHRP Report 350. The results of the occupant risk, determined from accelerometer data, are summarized in Figure 41. Results are shown graphically in Appendix G. The results from the rate transducer are shown graphically in Appendix H.

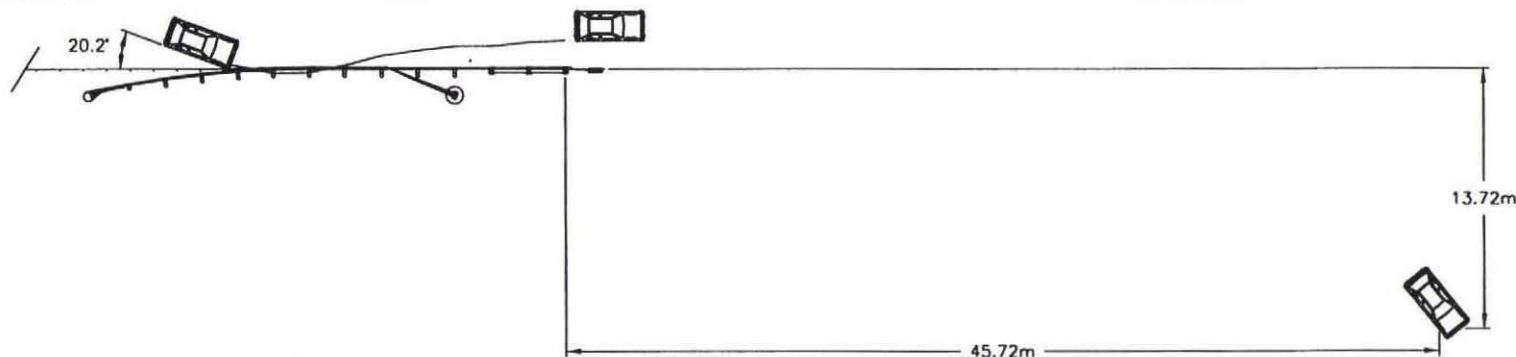
9.6 Discussion

The analysis of the test results for test SDC-3 showed that the barrier adequately contained and redirected the vehicle with controlled lateral displacement of the barrier. Detached elements, fragments, or other debris from the test article did not penetrate or show potential for penetrating the occupant compartment, or present undue hazard to other traffic. Minor deformations to the occupant compartment were evident but not considered excessive enough to cause serious injuries to the

occupants. The vehicle remained upright both during and after the collision. Vehicle roll, pitch, and yaw angular displacements were noted, but they were deemed acceptable because they did not adversely influence occupant safety criteria or cause rollover. After collision, the vehicle's trajectory did not intrude into adjacent traffic lanes. In addition, the vehicle's exit angle was less than 60 percent of the impact angle. Therefore, test SDC-3 conducted on the cable guardrail to W-beam transition system was determined to be acceptable according to the NCHRP Report 350 criteria.



0.000 sec 0.082 sec 0.155 sec 0.193 sec 0.287 sec



- Test Number SDC-3
- Date 8/31/98
- Appurtenance Cable Guardrail to W-Beam Transition
- Three-Strand Cable Guardrail
 - Diameter 19.0 mm
 - Specification 3 x 7 Wire Rope
 - Top Mounting Height 686 mm (center of upper cable)
- Steel Posts
 - Post Nos. 1C - 32C W76x8.5
- W-Beam Guardrail
 - Thickness 2.66 mm
 - Top Mounting Height 686 mm
- Wood Posts
 - Spacing 1,905 mm
 - Post Nos. 1W - 2W 140 mm x 190 mm x 1,080 mm
 - Post Nos. 3W - 11W 152 mm x 203 mm x 1,829 mm
- Wood Spacer Blocks
 - Post Nos. 3W - 11W 152 mm x 203 mm x 356 mm
- Soil Type Grading B - AASHTO M 147-65 (1990)
- Vehicle Model 1991 Geo Metro
 - Curb 753 kg
 - Test Inertial 802 kg
 - Gross Static 878 kg

- Vehicle Speed
 - Impact 99.6 km/hr
 - Exit 78.8 km/hr
- Vehicle Angle
 - Impact 20.2 deg
 - Exit 7.4 deg
- Vehicle Snagging Minor tire snagging on posts
- Vehicle Pocketing None
- Vehicle Stability Very Stable
- Occupant Ridedown Deceleration (10 msec avg.)
 - Longitudinal 2.83 G's/-3.24 G's < 20 G's
 - Lateral 16.64 G's < 20 G's
- Occupant Impact Velocity (Normalized)
 - Longitudinal 5.72 m/s < 12 m/s
 - Lateral 5.94 m/s < 12 m/s
- Vehicle Damage Moderate
 - TAD¹³ 1-RFQ-3
 - SAE¹⁴ 01RDAW2
- Vehicle Stopping Distance 45.7 m downstream
13.7 m behind traffic-side face
- Barrier Damage Moderate
- Maximum Dynamic Deflection 0.50 m

Figure 41. Summary of Test Results and Sequential Photographs, Test SDC-3



0.000 sec



0.000 sec



0.078 sec



0.087 sec



0.112 sec



0.110 sec



0.165 sec



0.172 sec



0.271 sec



0.252 sec

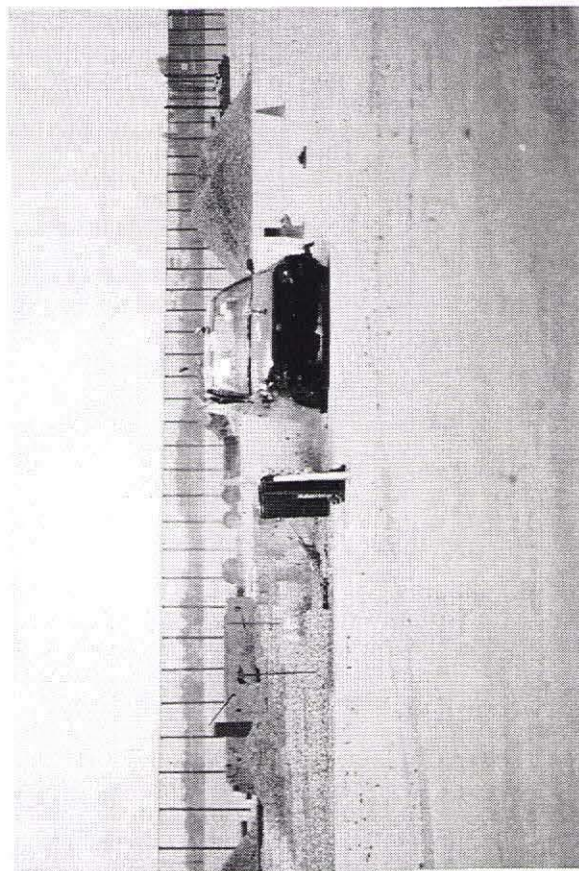
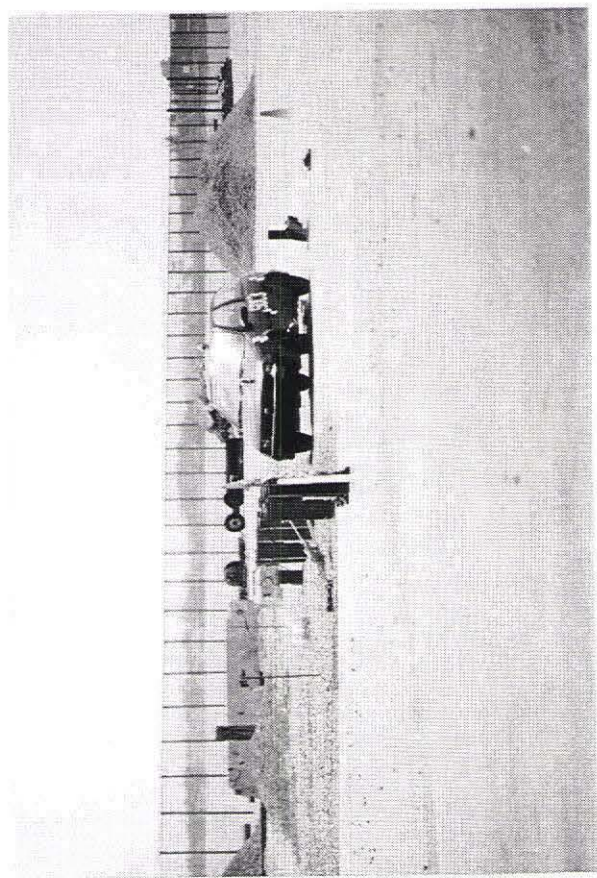
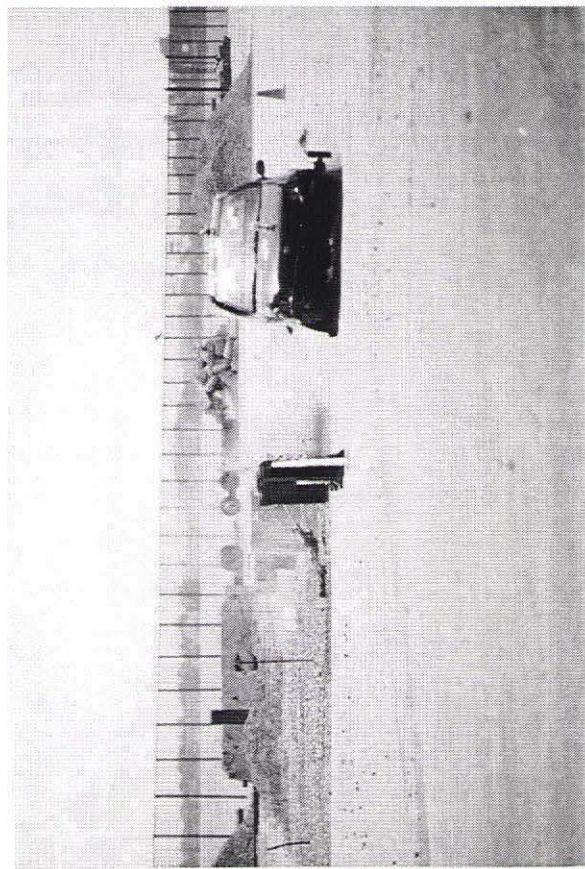
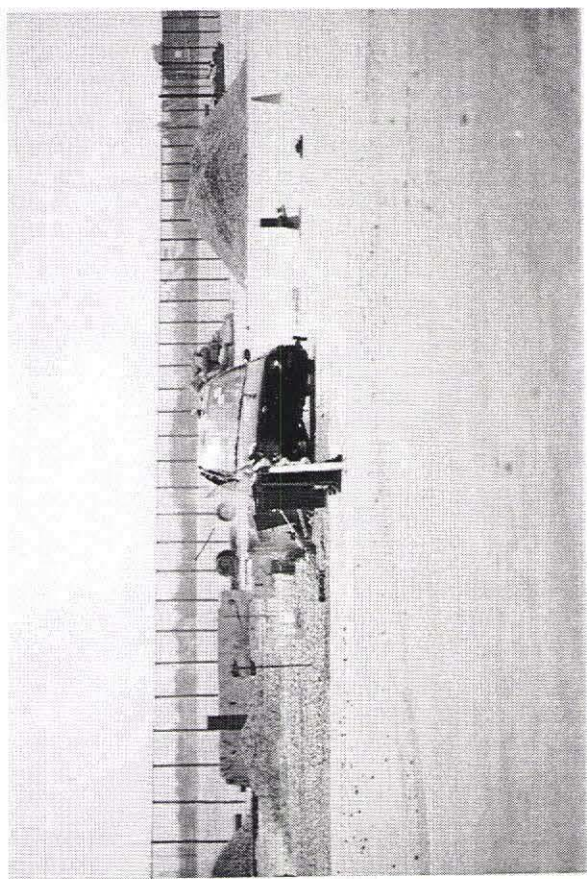


0.589 sec



0.339 sec

Figure 42. Additional Sequential Photographs, Test SDC-3



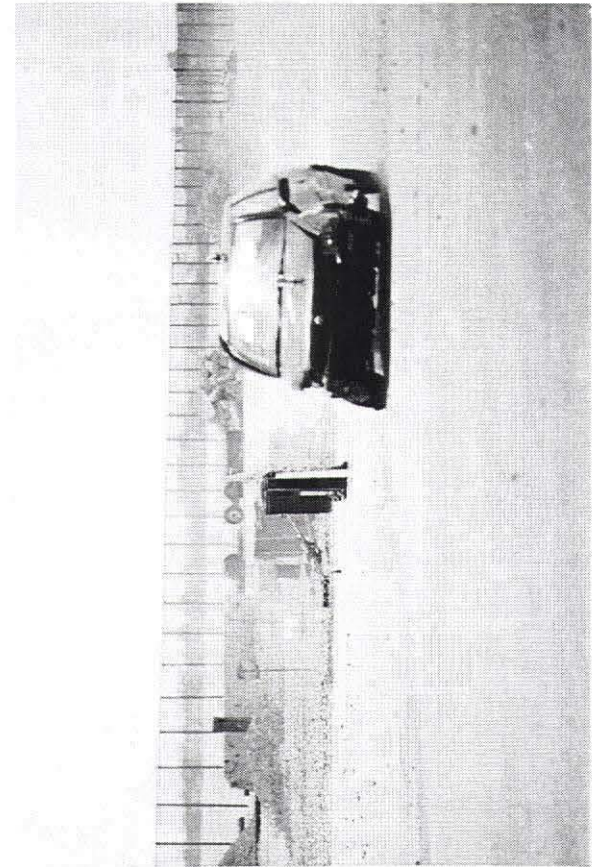
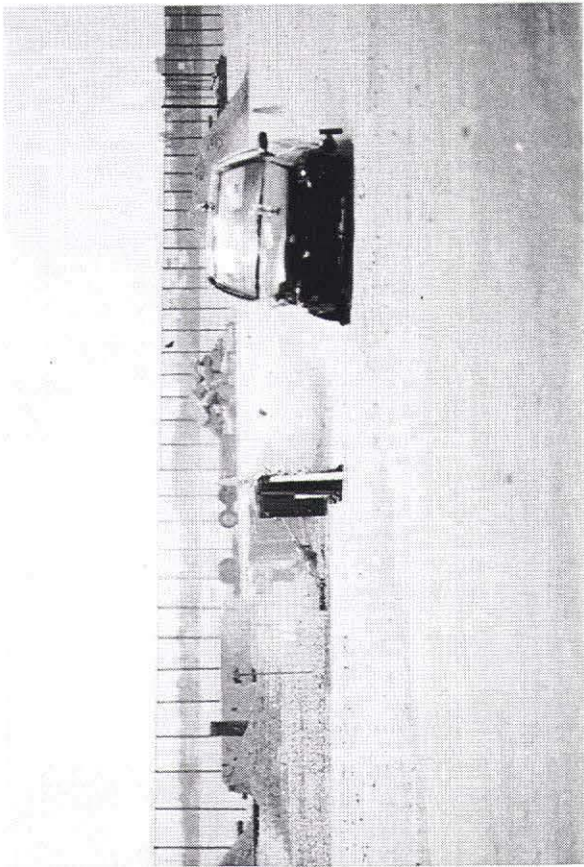
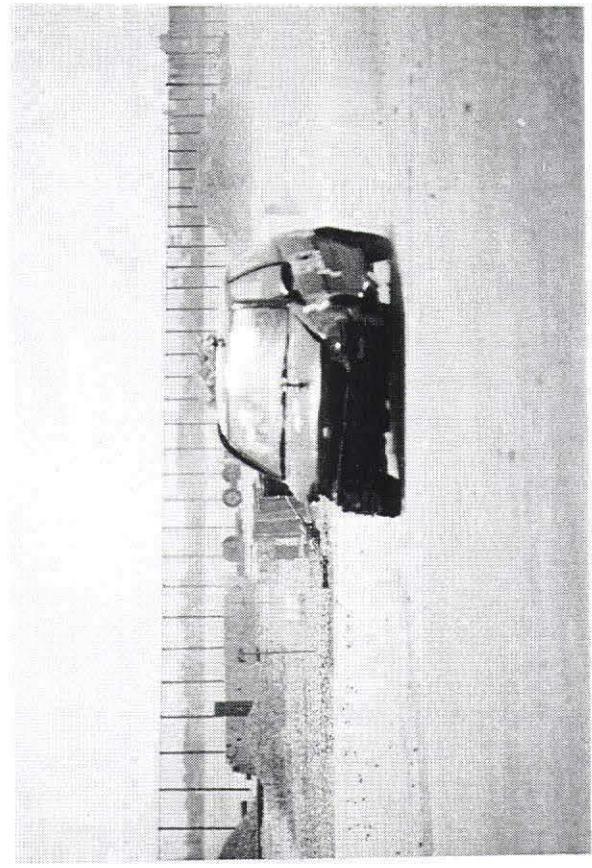
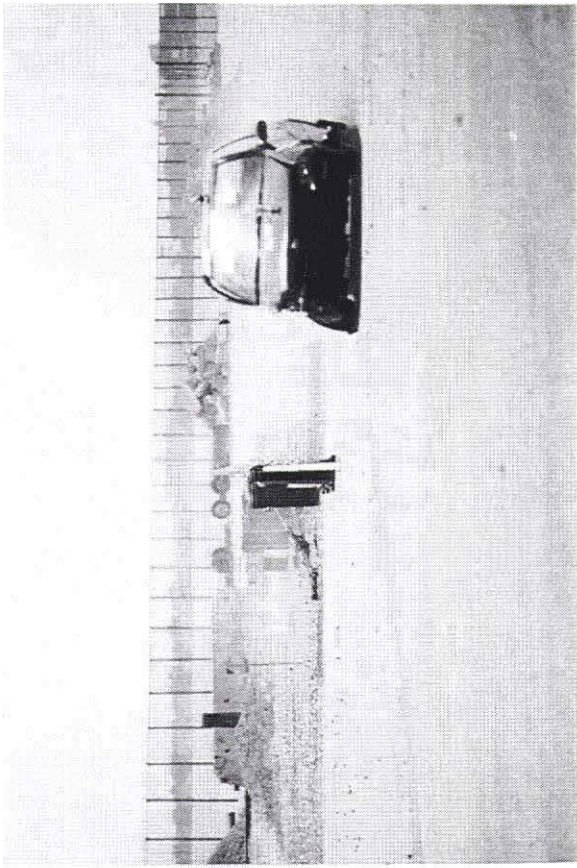


Figure 44. Full-Scale Crash Test, Test SDC-3



Figure 45. Impact Location, Test SDC-3

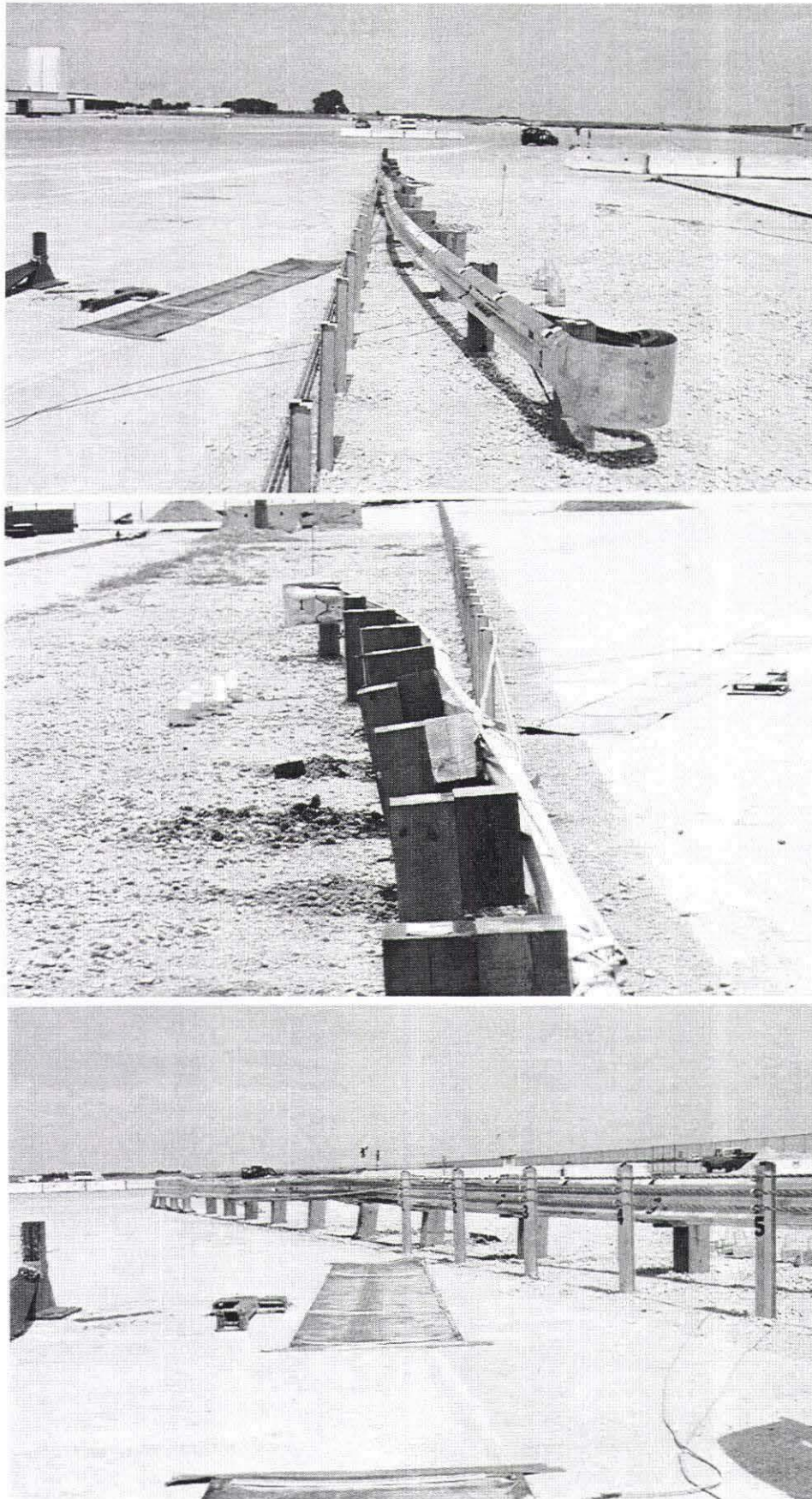


Figure 46. Cable Guardrail to W-Beam Transition Damage, Test SDC-3

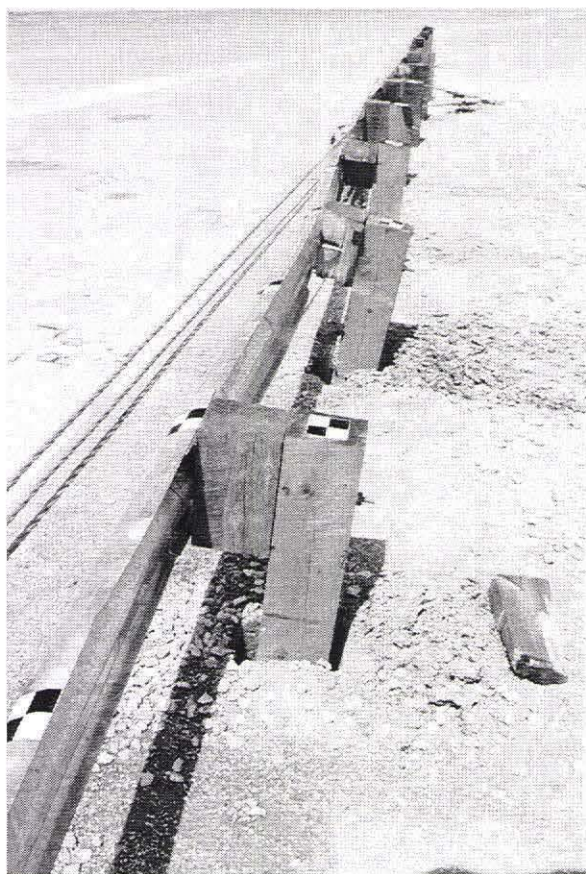


Figure 47. Cable Guardrail to W-Beam Transition Damage, Test SDC-3



Figure 48. Vehicle Damage, Test SDC-3

10 SUMMARY AND CONCLUSIONS

A cable guardrail to W-beam transition was crash tested according to the safety performance criteria presented in NCHRP Report No. 350. Three full-scale vehicle crash tests were performed to determine whether the system meets current TL-3 impact safety standards specified in NCHRP Report 350. Two tests - one using a small car and one with a pickup truck - were used to evaluate the potential for vehicle snagging in the region where the cable guardrail transitions into the W-beam guardrail. One additional pickup truck crash test was performed to evaluate the potential for snagging and pocketing when the pickup impacts the cable guardrail upstream of the BCT terminal and deflects the cable guardrail such that the pickup contacts the BCT terminal in a critical manner.

The first crash test, test SDC-1, was successfully performed with a 2,013-kg (4,438-lb) pickup truck impacting 438-mm (17¼-in.) upstream from post no. 14C at a speed of 101.9 km/hr (63.3 mph) and an angle of 27.6 degrees. The second crash test, test SDC-2, was successfully performed with a 2,023-kg (4,459-lb) pickup truck impacting at the upstream edge of post no. 4C at a speed of 101.8 km/hr (63.3 mph) and an angle of 25.2 degrees. The third crash test, test SDC-3, was successfully performed with a 878-kg (1,935-lb) small car impacting 305-mm (12-in.) downstream from post no. 1C at a speed of 99.6 km/hr (61.9 mph) and an angle of 20.2 degrees. Thus, the South Dakota cable guardrail to W-beam transition has successfully met current safety standards. A summary of the safety performance evaluation for the three tests is provided in Table 2.

Table 2. Summary of Safety Performance Evaluation Results

Evaluation Factors	Evaluation Criteria	Test SDC-1	Test SDC-2	Test SDC-3
Structural Adequacy	A. Test article should contain and redirect the vehicle; the vehicle should not penetrate, underride, or override the installation although controlled lateral deflection of the test article is acceptable.	S	S	S
Occupant Risk	D. Detached elements, fragments or other debris from the test article should not penetrate or show potential for penetrating the occupant compartment, or present an undue hazard to other traffic, pedestrians, or personnel in a work zone. Deformations of, or intrusions into, the occupant compartment that could cause serious injuries should not be permitted.	S	S	S
	F. The vehicle should remain upright during and after collision although moderate roll, pitching and yawing are acceptable.	S	S	S
	H. Longitudinal and lateral occupant impact velocities (m/s) should satisfy the following: <u>Preferred</u> <u>Maximum</u> 9 12	S	S	S
	I. Longitudinal and lateral occupant ridedown accelerations (G's) should satisfy the following: <u>Preferred</u> <u>Maximum</u> 15 20	S	S	S
Vehicle Trajectory	K. After collision it is preferable that the vehicle's trajectory not intrude into adjacent traffic lanes.	S	S	S
	L. The occupant impact velocity in the longitudinal direction should not exceed 12 m/sec and the occupant ridedown acceleration in the longitudinal direction should not exceed 20 G's.	S	S	S
	M. The exit angle from the test article preferably should be less than 60 percent of test impact angle, measured at time of vehicle loss of contact with test device.	S	S	S

S - (Satisfactory)

M - (Marginal)

U - (Unsatisfactory)

11 RECOMMENDATIONS

Based upon the successful completion of the three compliance tests conducted according to the NCHRP Report No. 350 safety standards, it is recommended that the Federal Highway Administration accept this longitudinal barrier system for use on federal-aid highways located on the National Highway System.

12 REFERENCES

1. Ross, H.E., Sicking, D.L., Zimmer, R.A. and Michie, J.D., *Recommended Procedures for the Safety Performance Evaluation of Highway Features*, National Cooperative Research Program (NCHRP) Report No. 350, Transportation Research Board, Washington, D.C., 1993.
2. Michie, J.D., *Recommended Procedures for the Safety Performance Evaluation of Highway Appurtenances*, National Cooperative Highway Research Program (NCHRP) Report No. 230, Transportation Research Board, Washington, D.C., March 1981.
3. *Test No. MSD-2*, SwRI Project No. 06-8299-001, Report to the South Dakota Department of Transportation and the Federal Highway Administration, Prepared by Southwest Research Institute, San Antonio, Texas, January 1989.
4. *Test No. MSD-2A*, SwRI Project No. 06-8299-001, Report to the South Dakota Department of Transportation and the Federal Highway Administration, Prepared by Southwest Research Institute, San Antonio, Texas, January 1989.
5. *Test No. MSD-4*, SwRI Project No. 06-8299-001, Report to the South Dakota Department of Transportation and the Federal Highway Administration, Prepared by Southwest Research Institute, San Antonio, Texas, January 1989.
6. *Crash-Test Evaluation of a Franklin Post and Cable Guardrail System - Test No. SD-1*, SwRI Project No. 06-2696-001, Report to the South Dakota Department of Transportation, Prepared by Southwest Research Institute, San Antonio, Texas, August 1989.
7. *Crash-Test Evaluation of a Franklin Post and Cable Guardrail System - Test No. SD-2*, SwRI Project No. 06-2696-001, Report to the South Dakota Department of Transportation, Prepared by Southwest Research Institute, San Antonio, Texas, August 1989.
8. *Crash-Test Evaluation of a Franklin Post and Cable Guardrail System - Test No. SD-3*, SwRI Project No. 06-2696-001, Report to the South Dakota Department of Transportation, Prepared by Southwest Research Institute, San Antonio, Texas, August 1989.
9. Mak, K.K., and Menges, W.C., *Crash Testing and Evaluation of G1 Wire Rope Guardrail System*, Research Study No. RF 471470, Contract No. DTFH61-89-C-00089, Draft Report to the Federal Highway Administration, Prepared by Texas Transportation Institute, Texas A&M University, College Station, Texas, December 1994.
10. Hinch, J., Yang, T-L, and Owings, R., *Guidance Systems for Vehicle Testing*, ENSCO, Inc., Springfield, VA 1986.

11. *Center of Gravity Test Code - SAE J874 March 1981*, SAE Handbook Vol. 4, Society of Automotive Engineers, Inc., Warrendale, Pennsylvania, 1986.
12. Powell, G.H., *BARRIER VII: A Computer Program For Evaluation of Automobile Barrier Systems*, Prepared for: Federal Highway Administration, Report No. FHWA RD-73-51, April 1973.
13. *Vehicle Damage Scale for Traffic Investigators*, Second Edition, Technical Bulletin No. 1, Traffic Accident Data (TAD) Project, National Safety Council, Chicago, Illinois, 1971.
14. *Collision Deformation Classification - Recommended Practice J224 March 1980*, Handbook Volume 4, Society of Automotive Engineers (SAE), Warrendale, Pennsylvania, 1985.

13 APPENDICES

APPENDIX A

DESIGN DETAILS FOR CABLE GUARDRAIL TO W-BEAM TRANSITION

Figure A-1. Cable Guardrail to W-Beam Transition Design Details

Figure A-2. Cable Guardrail to W-Beam Transition Design Details (Continued)

Figure A-3. Cable Guardrail to W-Beam Transition Design Details (Continued)

Figure A-4. Cable Guardrail to W-Beam Transition Design Details (Continued)

Figure A-5. Cable Guardrail to W-Beam Transition Design Details (Continued)

Figure A-6. Cable Guardrail to W-Beam Transition Design Details (Continued)

Figure A-7. Cable Guardrail to W-Beam Transition Design Details (Continued)

Figure A-8. Cable Guardrail to W-Beam Transition Design Details (Continued)

Figure A-9. Cable Guardrail to W-Beam Transition Design Details (Continued)

Figure A-10. Cable Guardrail to W-Beam Transition Design Details (Continued)

Figure A-11. Cable Guardrail to W-Beam Transition Design Details (Continued)

Figure A-12. Cable Guardrail to W-Beam Transition Design Details (Continued)

Figure A-13. Cable Guardrail to W-Beam Transition Design Details (Continued)

Figure A-14. Cable Guardrail to W-Beam Transition Design Details (Continued)

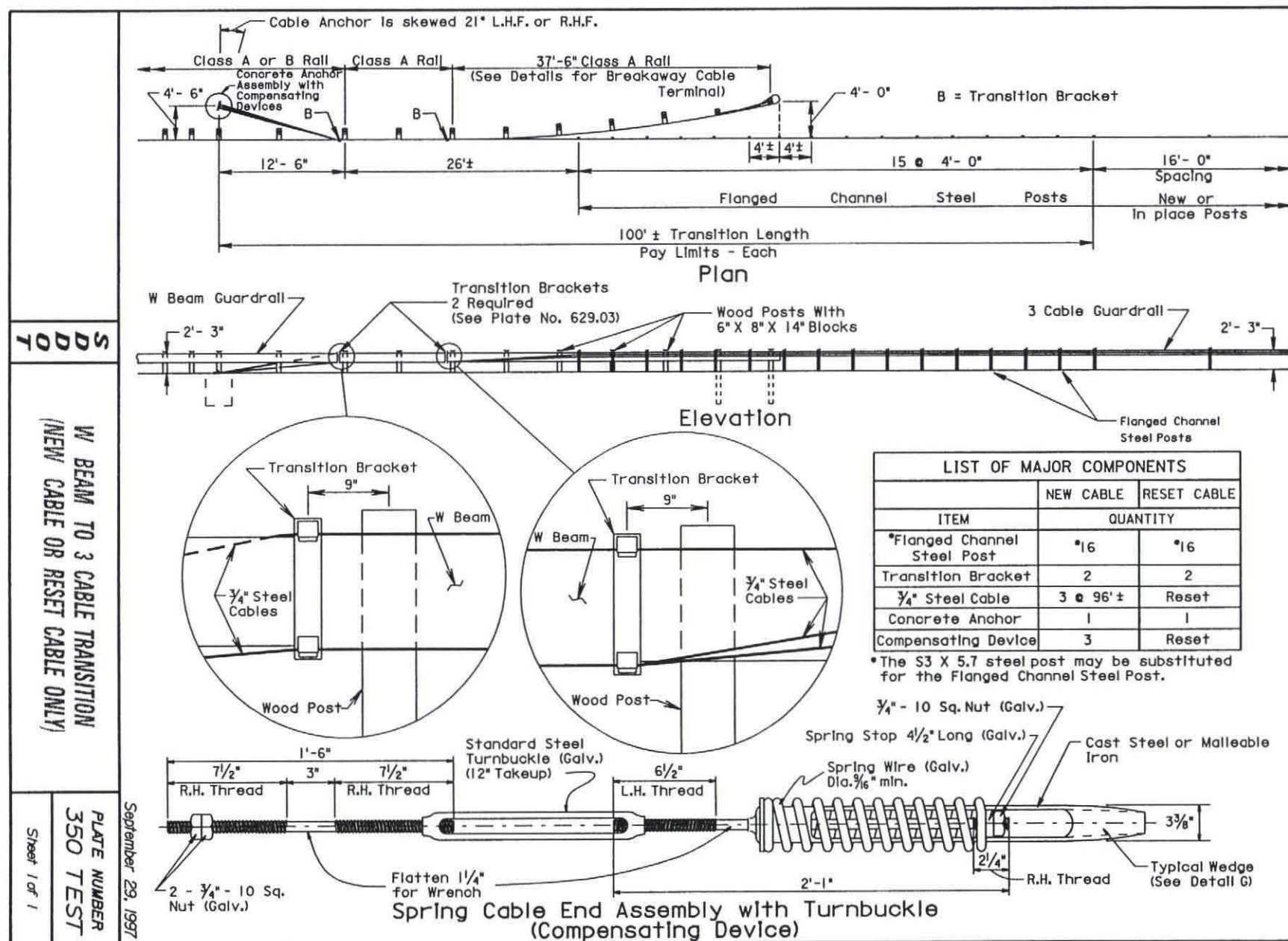


Figure A-1. Cable Guardrail to W-Beam Transition Design Details

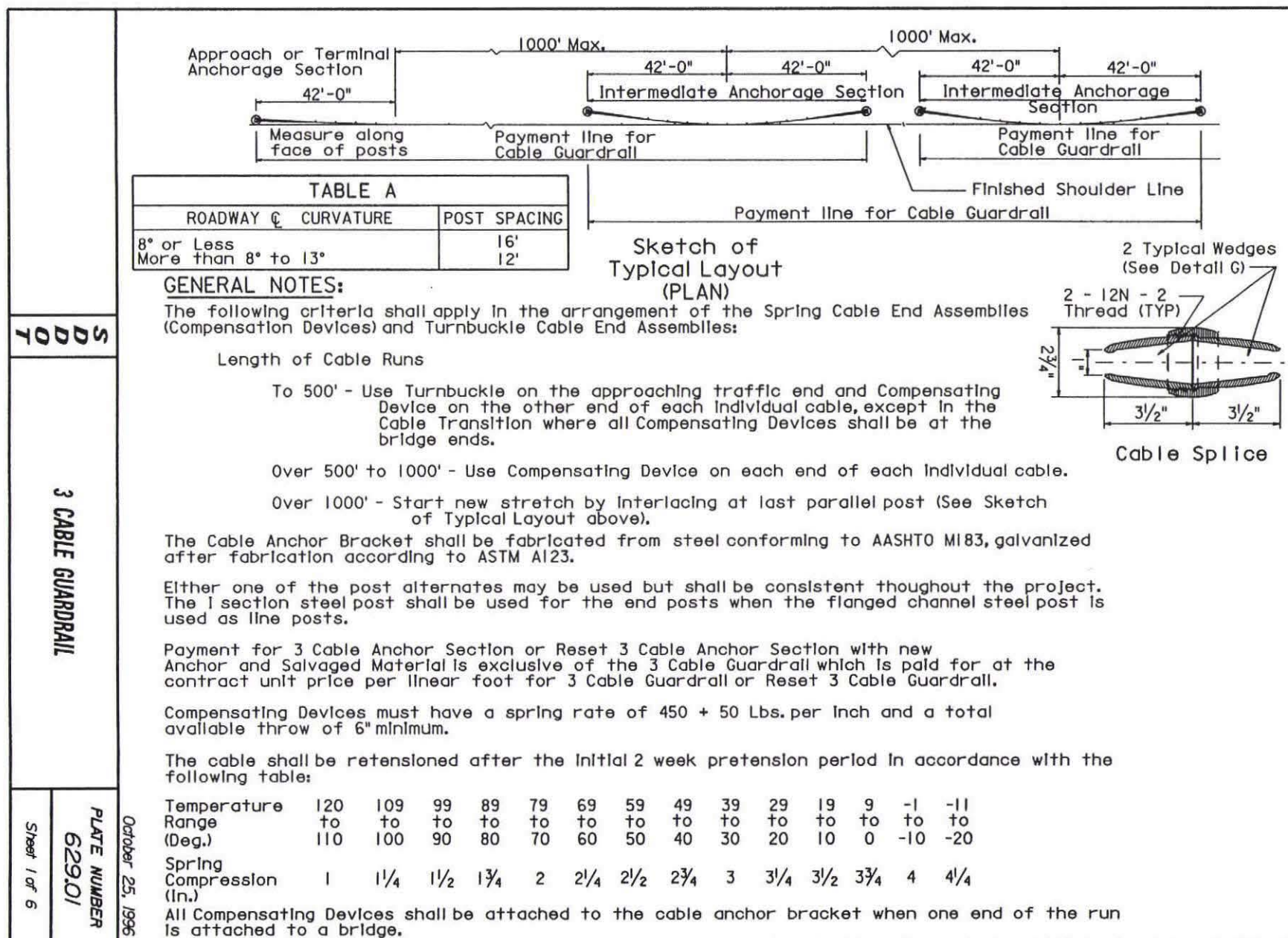


Figure A-2. Cable Guardrail to W-Beam Transition Design Details (Continued)

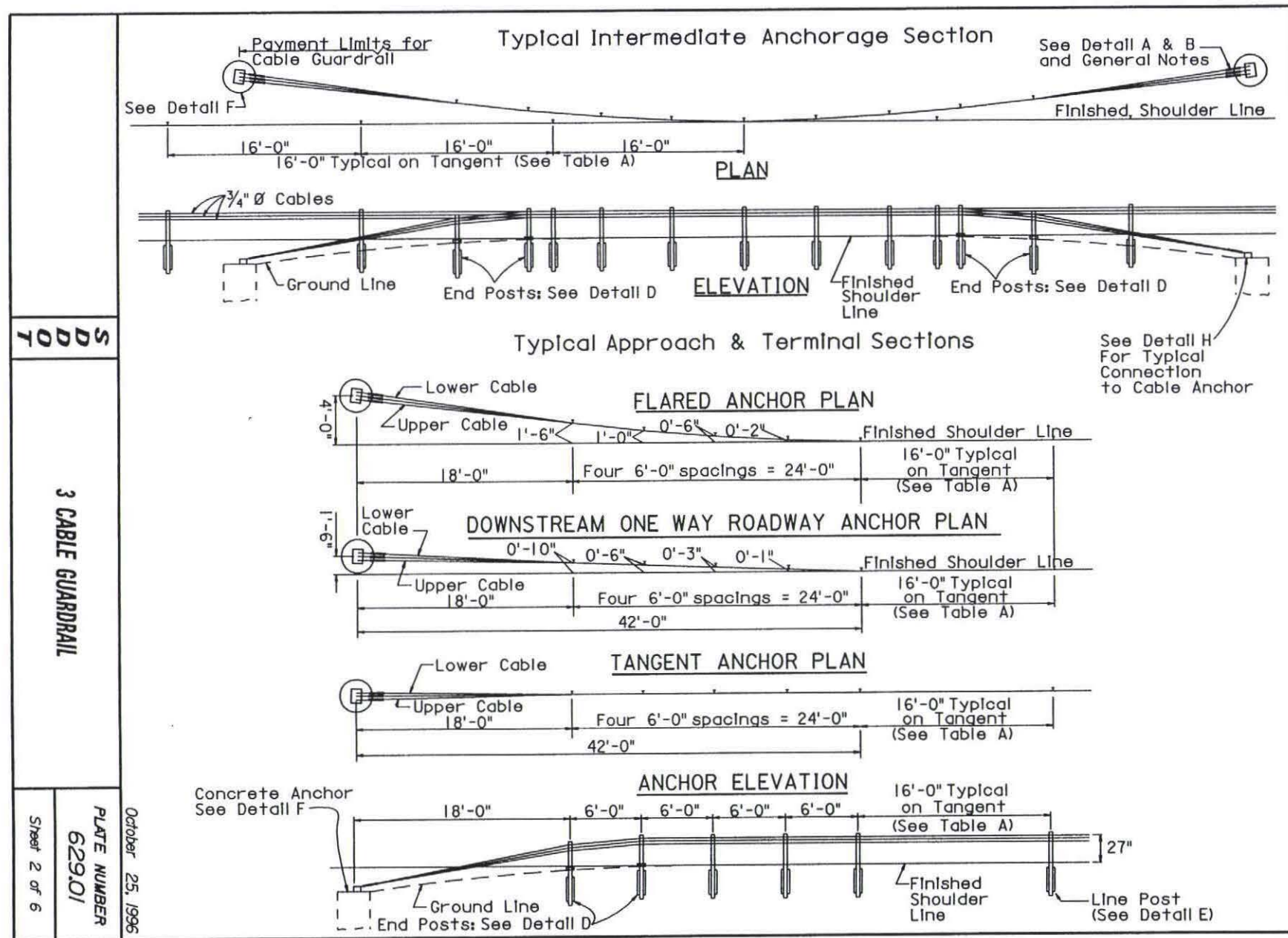


Figure A-3. Cable Guardrail to W-Beam Transition Design Details (Continued)

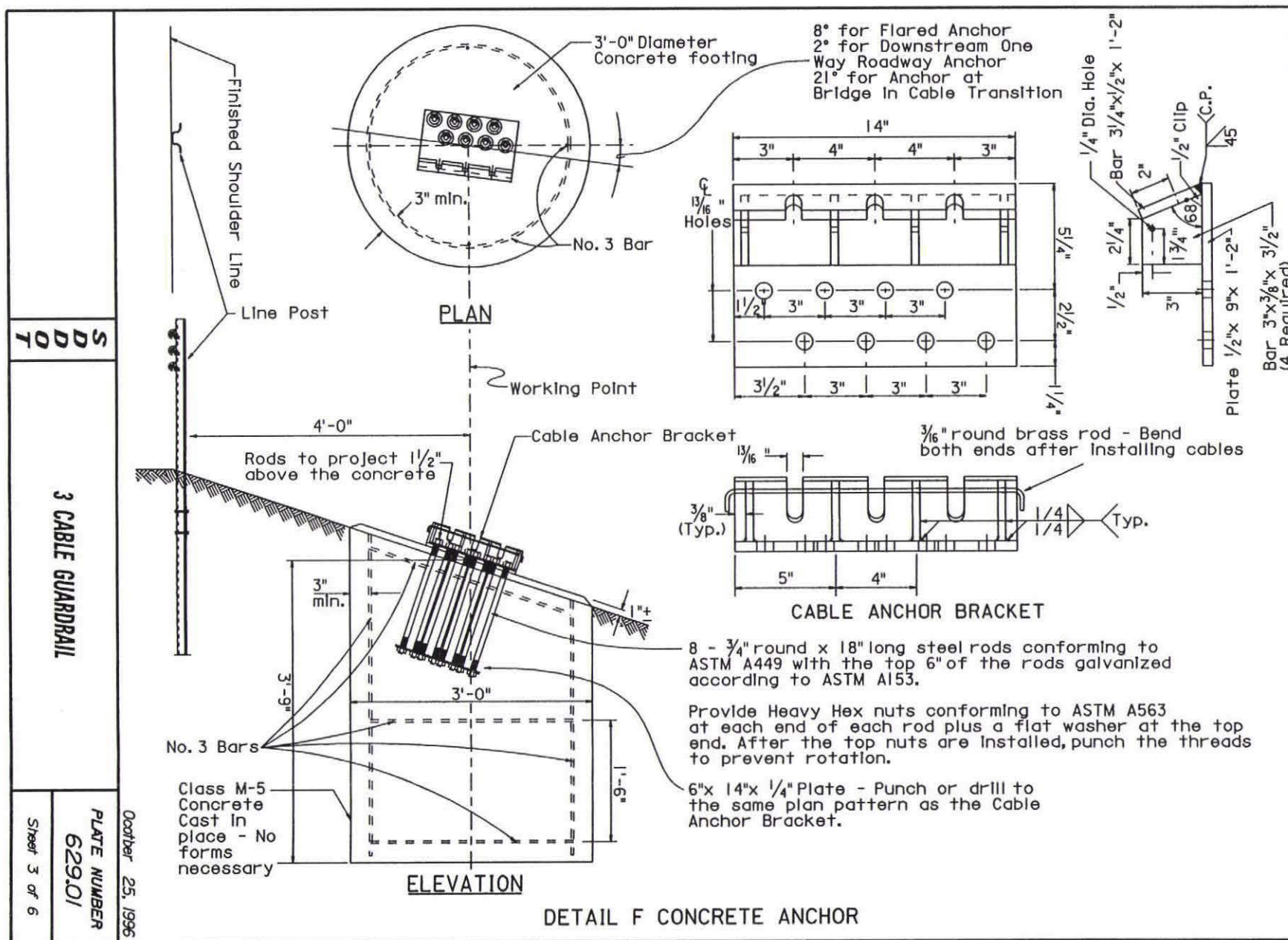


Figure A-4. Cable Guardrail to W-Beam Transition Design Details (Continued)

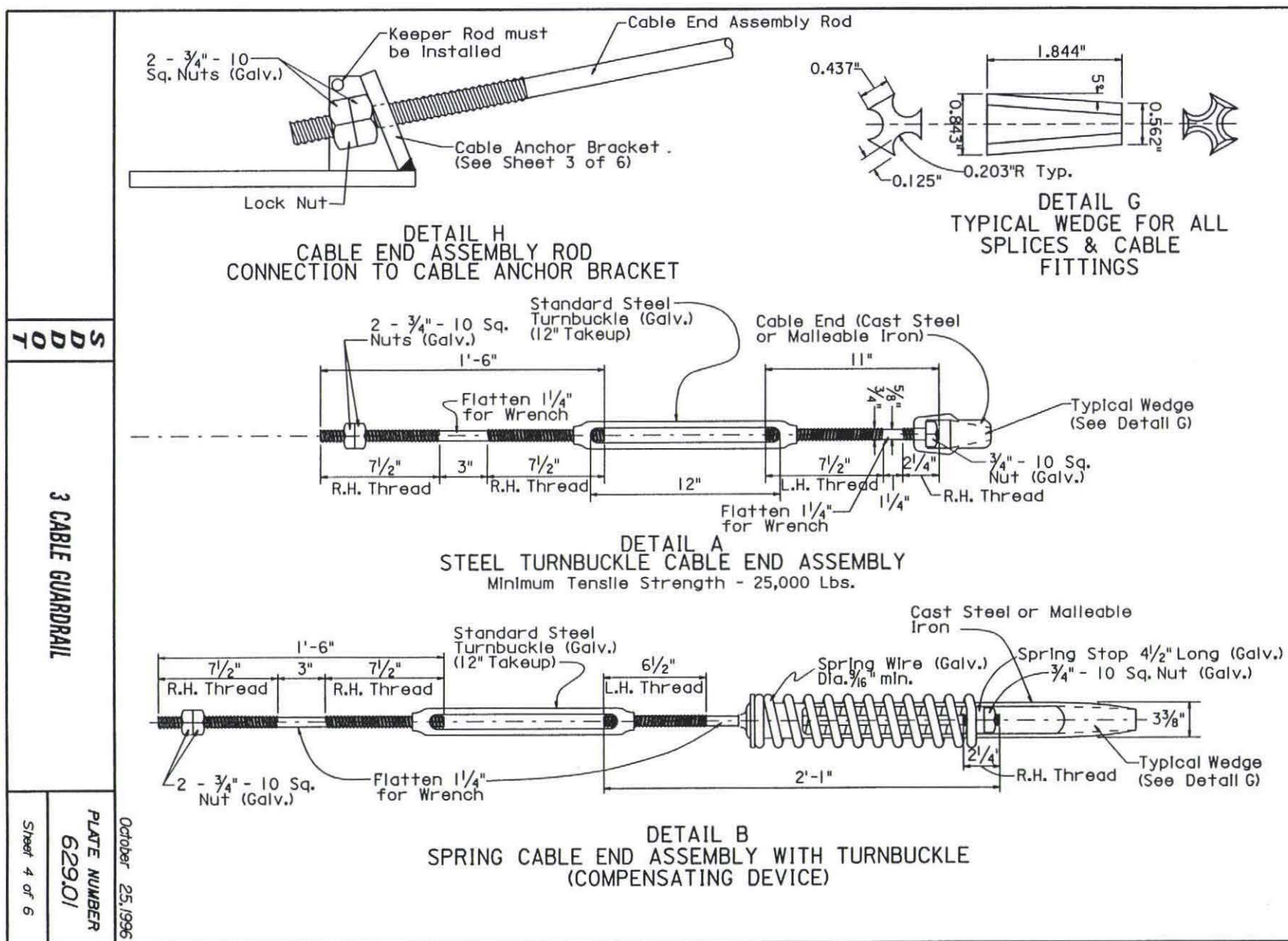


Figure A-5. Cable Guardrail to W-Beam Transition Design Details (Continued)

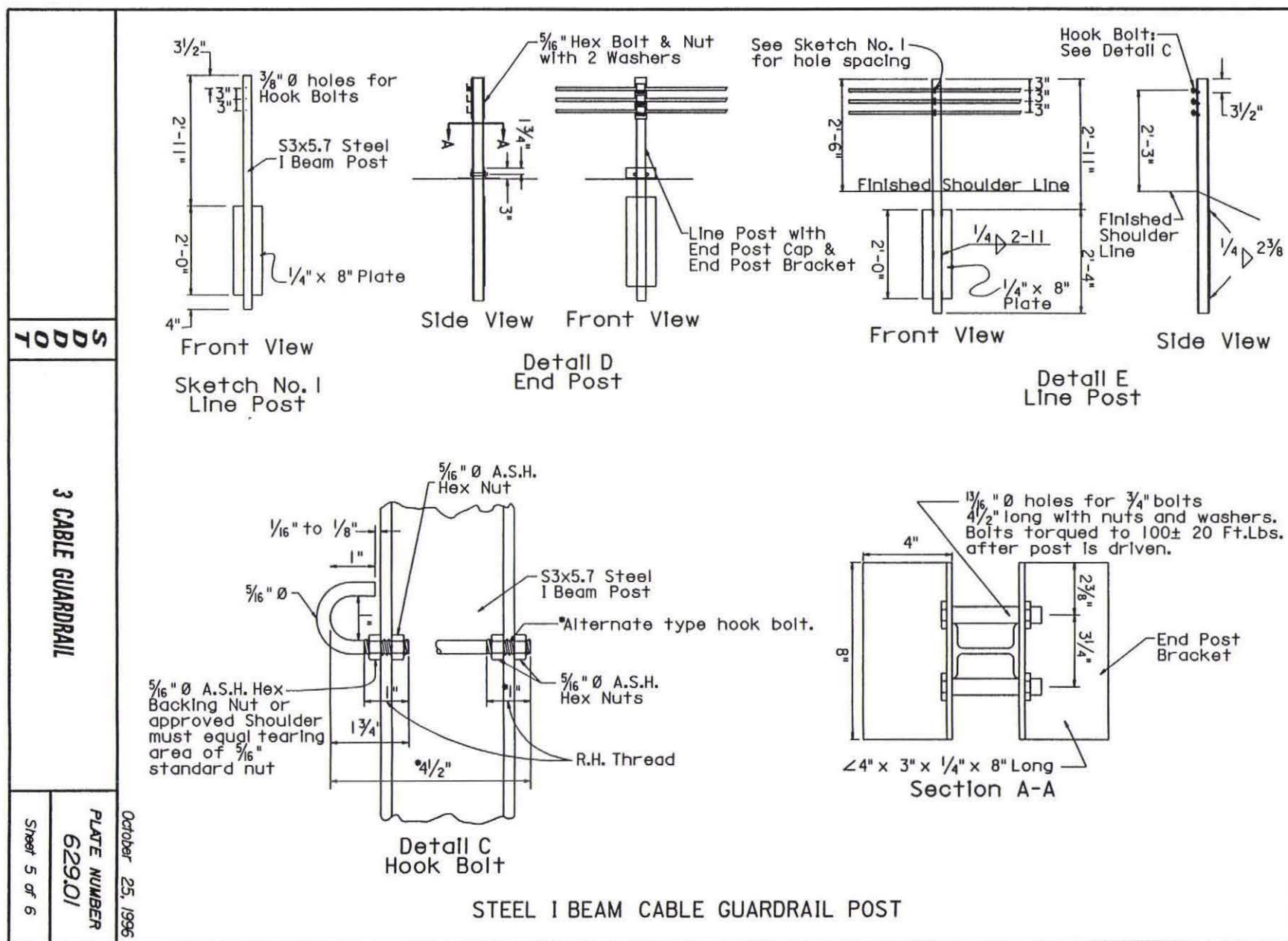


Figure A-6. Cable Guardrail to W-Beam Transition Design Details (Continued)

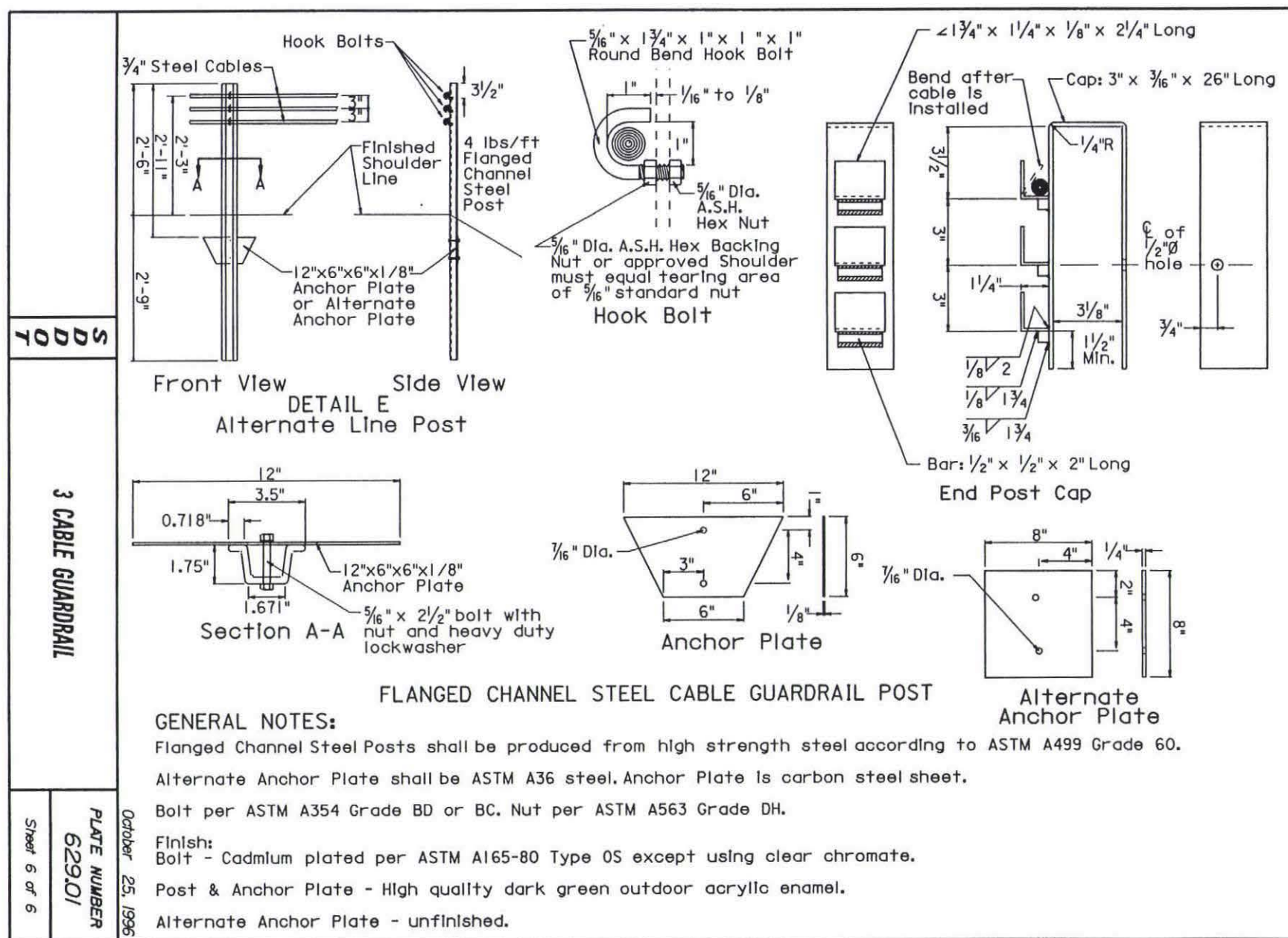
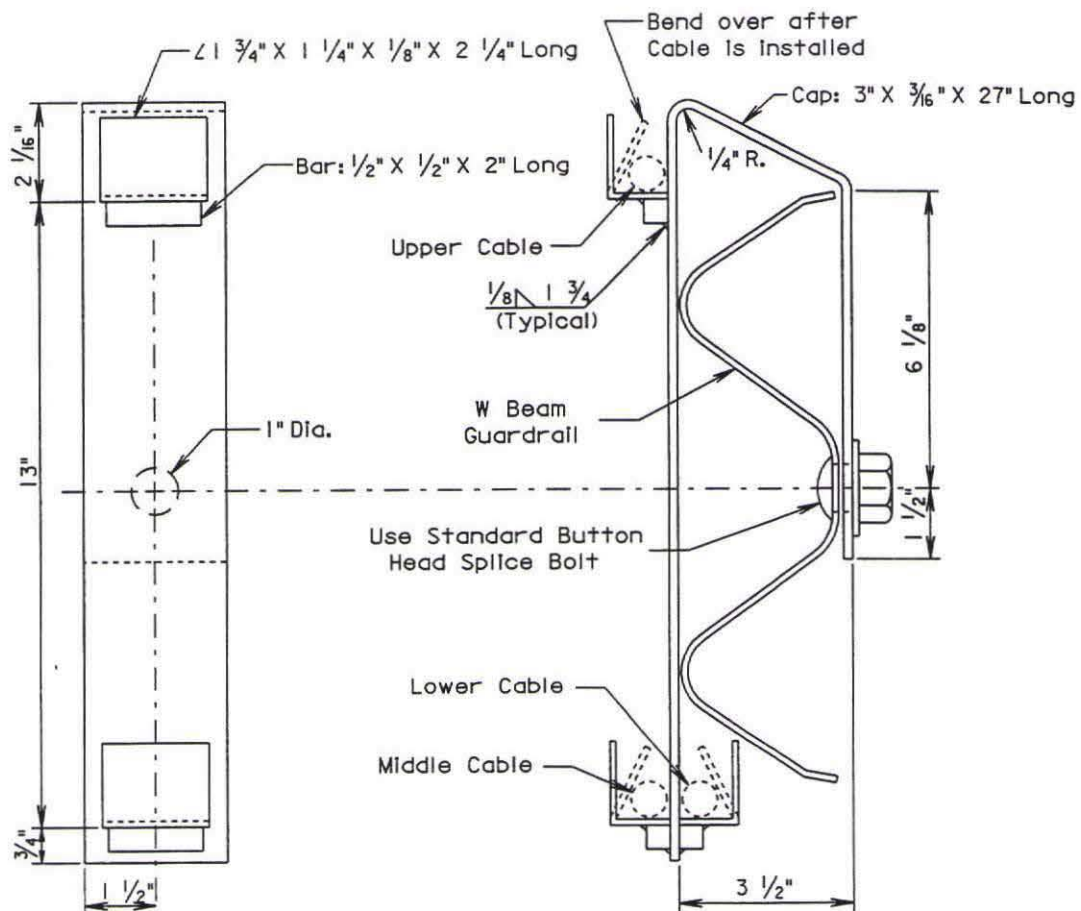


Figure A-7. Cable Guardrail to W-Beam Transition Design Details (Continued)



GENERAL NOTES:

Steel used in the fabrication of the bracket shall conform to ASTM A36.
The bracket shall be galvanized after fabrication according to ASTM A123.

August 16, 1995

**S
D
D
T**

W BEAM TO 3 CABLE TRANSITION BRACKET

**PLATE NUMBER
629.03**

Sheet 1 of 1

Figure A-8. Cable Guardrail to W-Beam Transition Design Details (Continued)

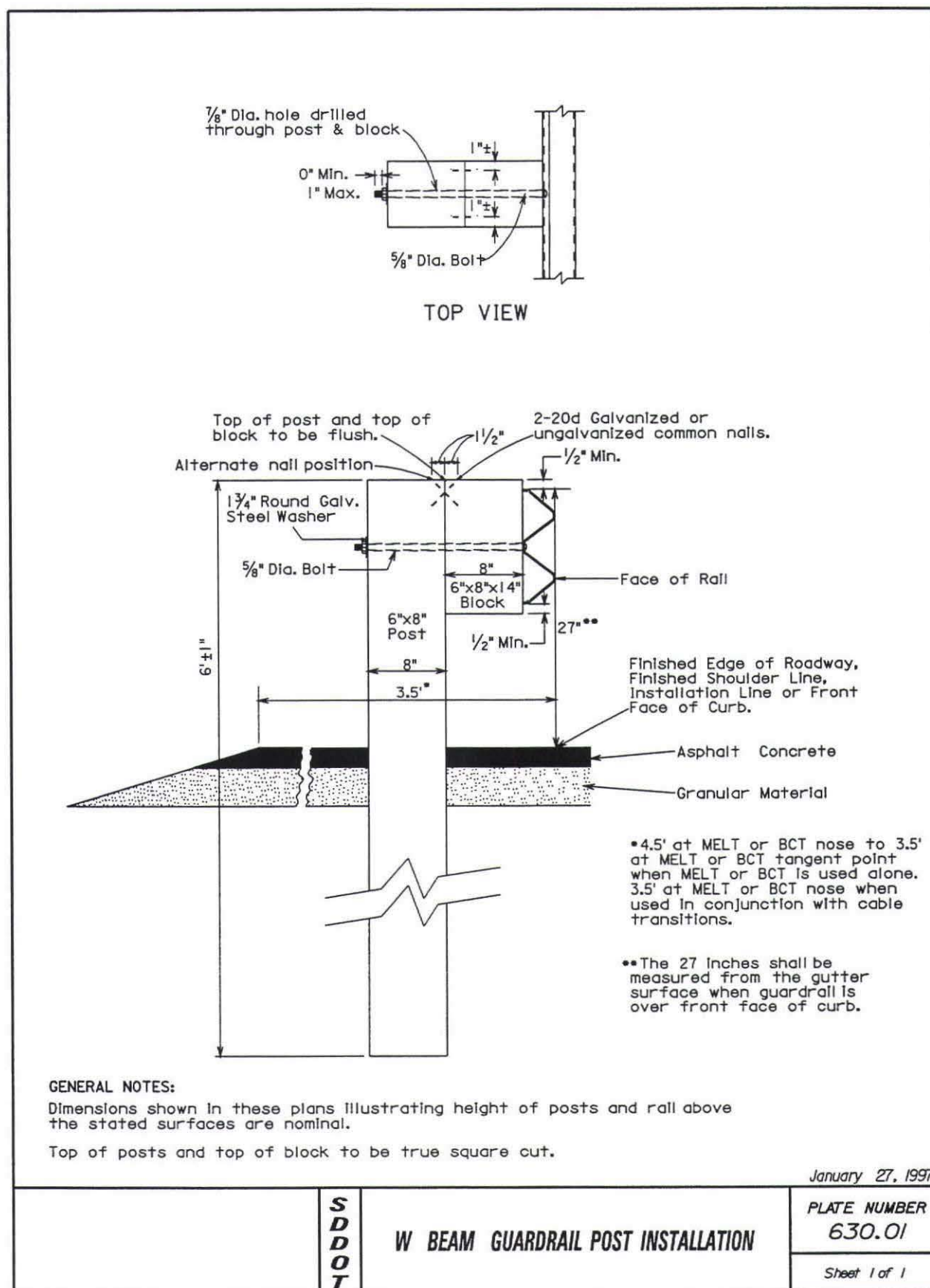
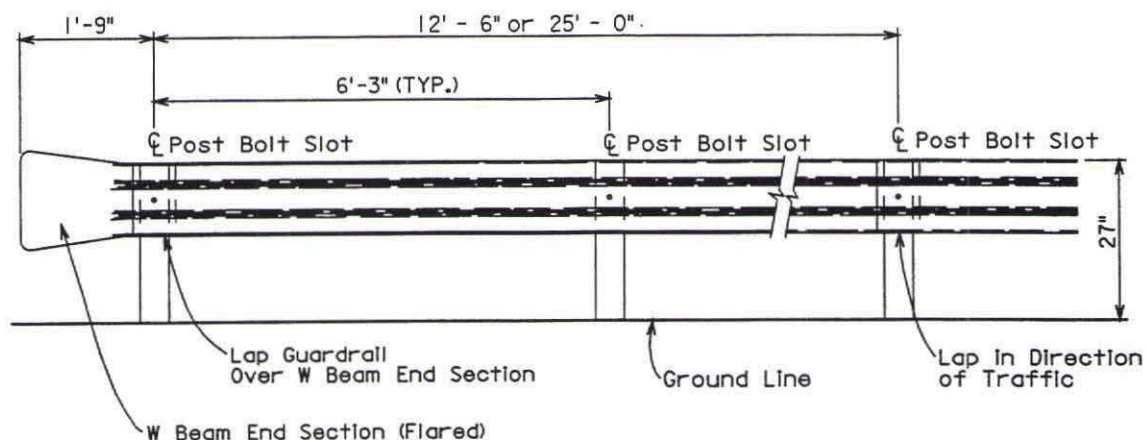


Figure A-9. Cable Guardrail to W-Beam Transition Design Details (Continued)



GENERAL NOTES:

All beam type guardrail shall be Type I.

There will be no separate payment for furnishing and installing W Beam End Sections (Flared) or W Beam Terminal Connectors. All costs for same to be included in the contract unit price per linear foot for the guardrail involved.

Beam section lengths may be 12'-6" and / or 25'-0". The combination of section lengths used shall be compatible with the run of the rail called for in the plans.

W Beam End Sections (Flared) shall only be used in a one way traffic situation in the Trailing End Terminal shown on Plate Number 630.25.

April 9, 1998

	S D D O T	INSTALLATION OF W BEAM GUARDRAIL	PLATE NUMBER 630.04
			Sheet 1 of 1

Figure A-10. Cable Guardrail to W-Beam Transition Design Details (Continued)

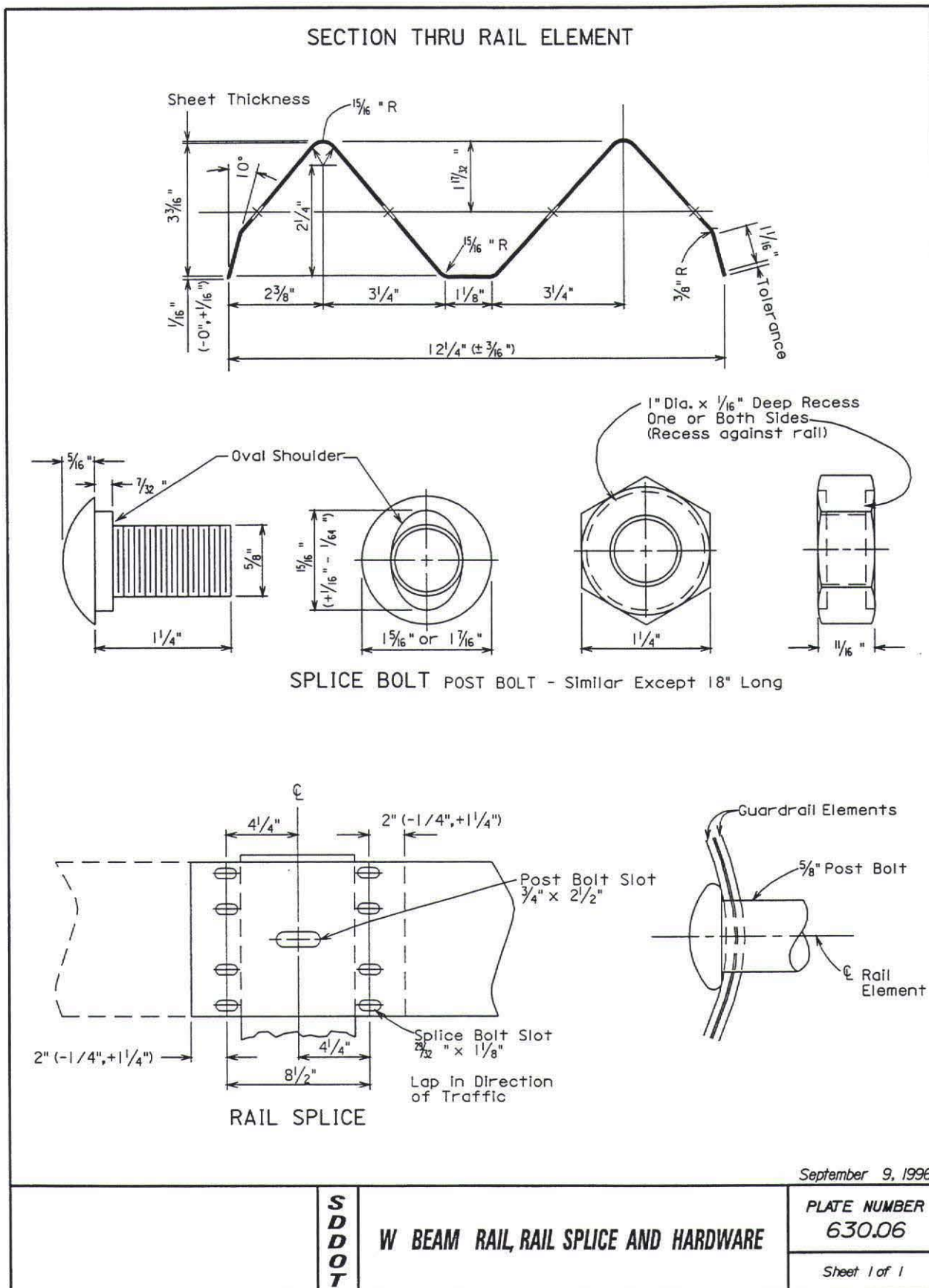


Figure A-11. Cable Guardrail to W-Beam Transition Design Details (Continued)

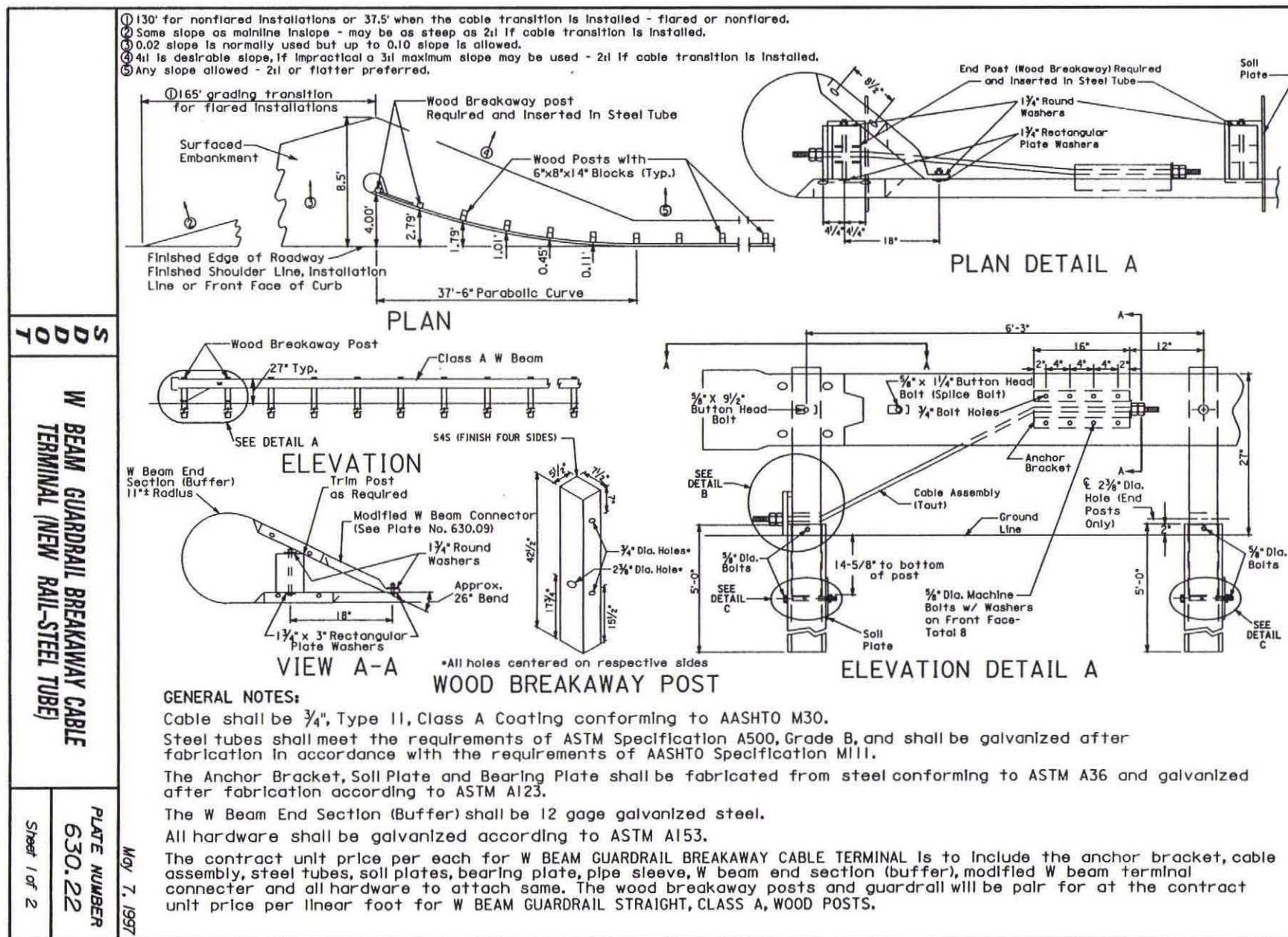


Figure A-12. Cable Guardrail to W-Beam Transition Design Details (Continued)

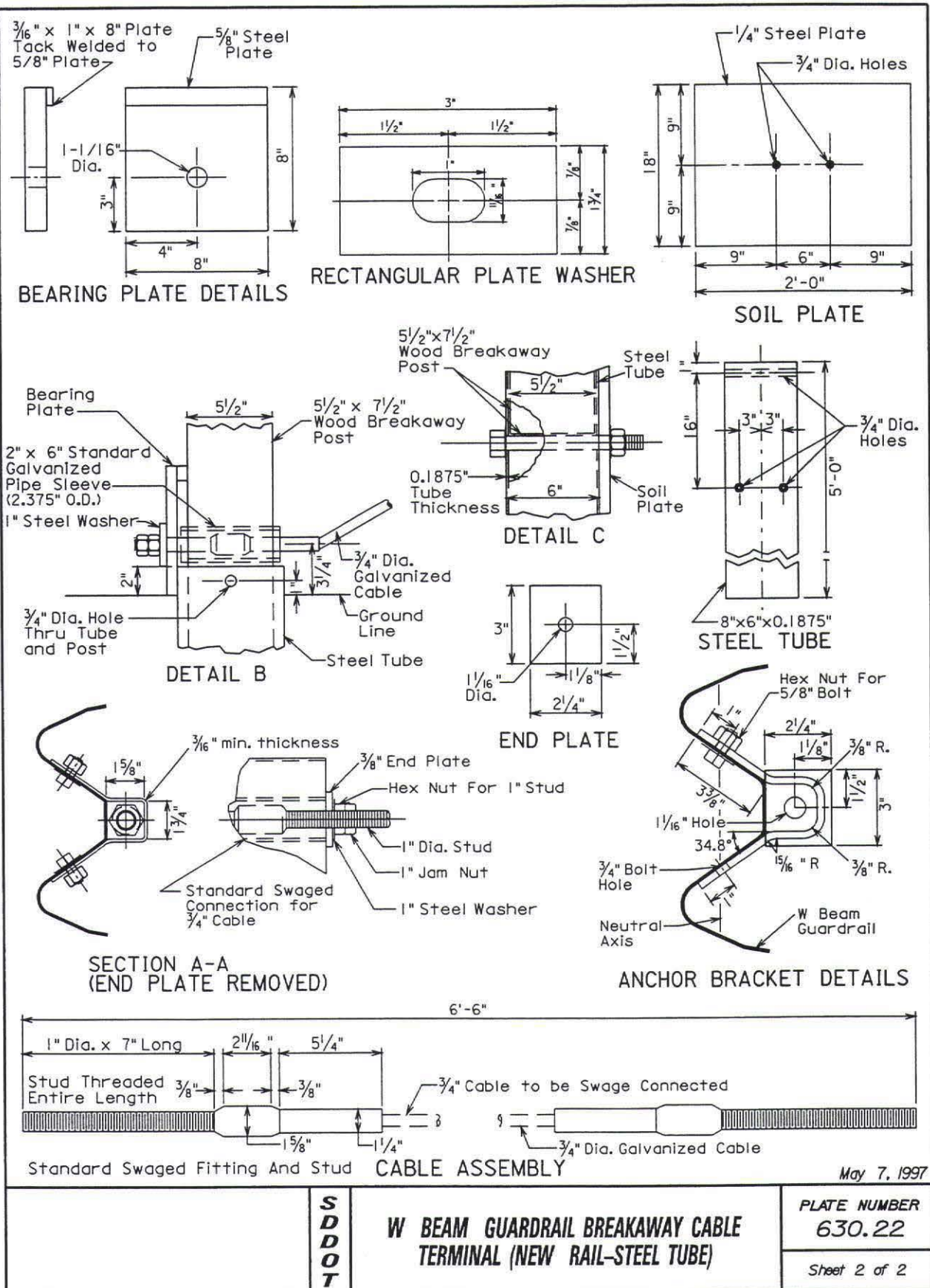


Figure A-13. Cable Guardrail to W-Beam Transition Design Details (Continued)

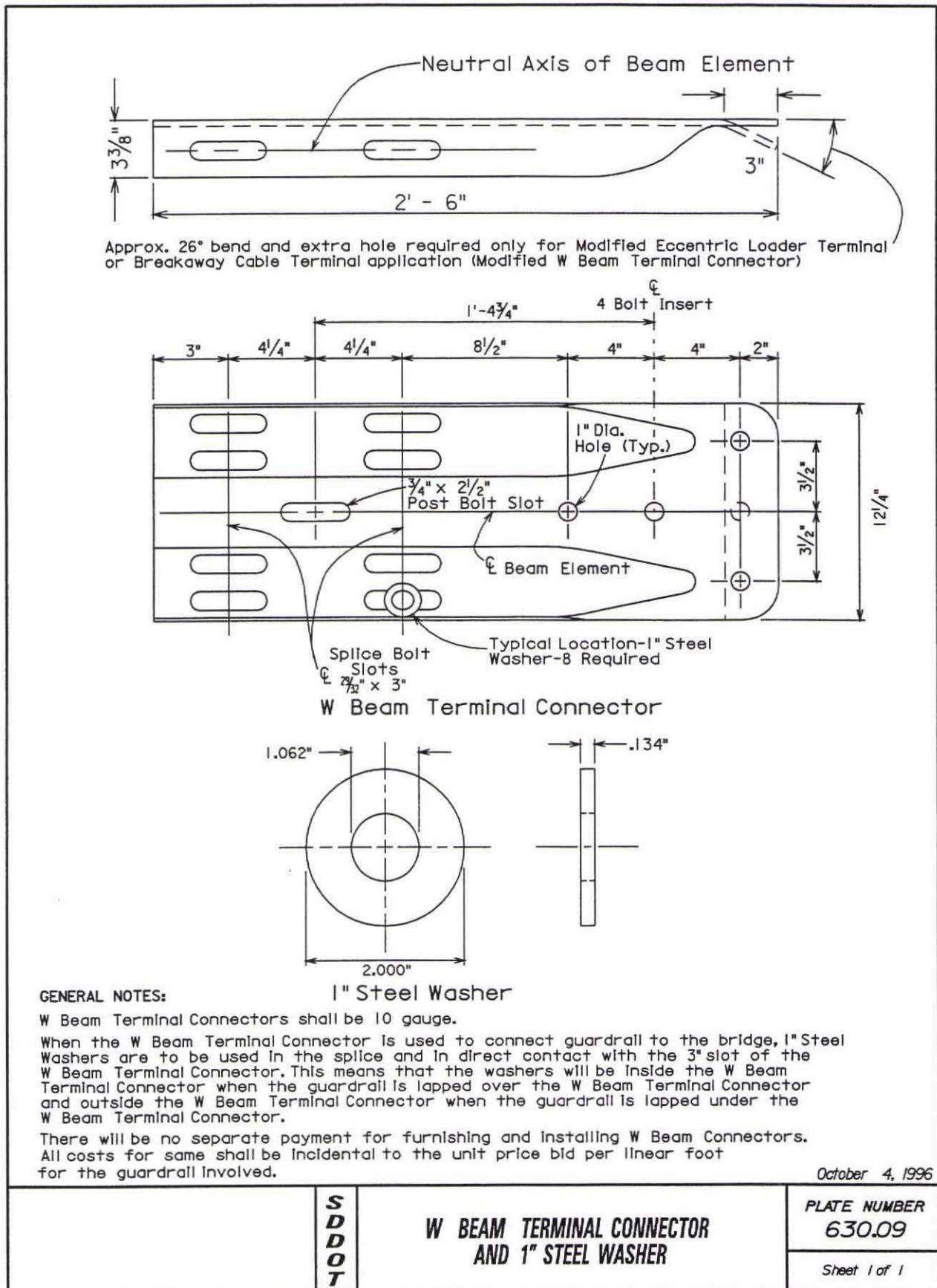


Figure A-14. Cable Guardrail to W-Beam Transition Design Details (Continued)

APPENDIX B

ACCELEROMETER DATA ANALYSIS, SDC-1

Figure B-1. Graph of Longitudinal Deceleration, Test SDC-1

Figure B-2. Graph of Longitudinal Occupant Impact Velocity, Test SDC-1

Figure B-3. Graph of Longitudinal Occupant Displacement, Test SDC-1

Figure B-4. Graph of Lateral Deceleration, Test SDC-1

Figure B-5. Graph of Lateral Occupant Impact Velocity, Test SDC-1

Figure B-6. Graph of Lateral Occupant Displacement, Test SDC-1

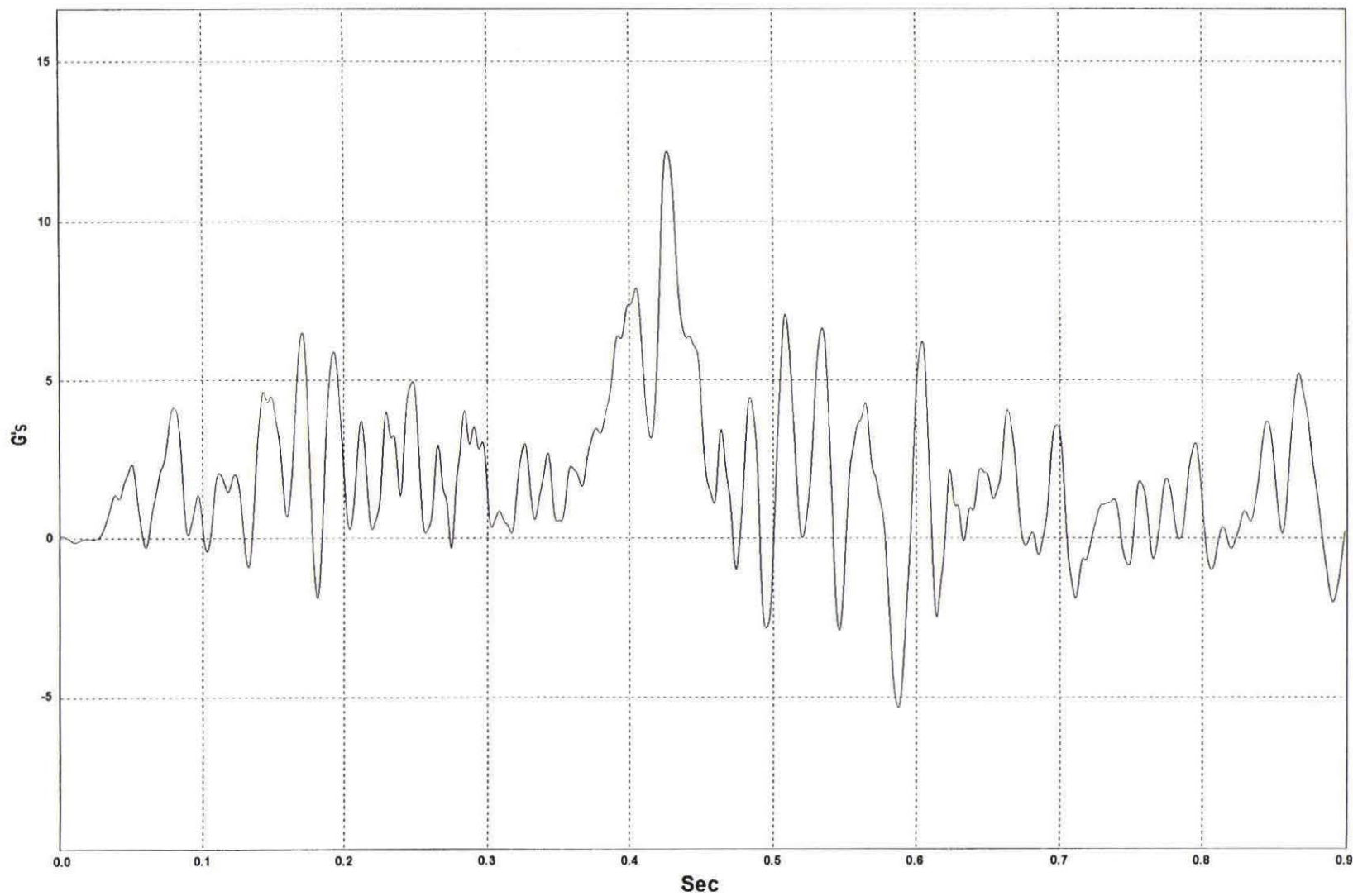
W5: Longitudinal Deceleration - Test SDC-1 (EDR-4)

Figure B-1. Graph of Longitudinal Deceleration, Test SDC-1

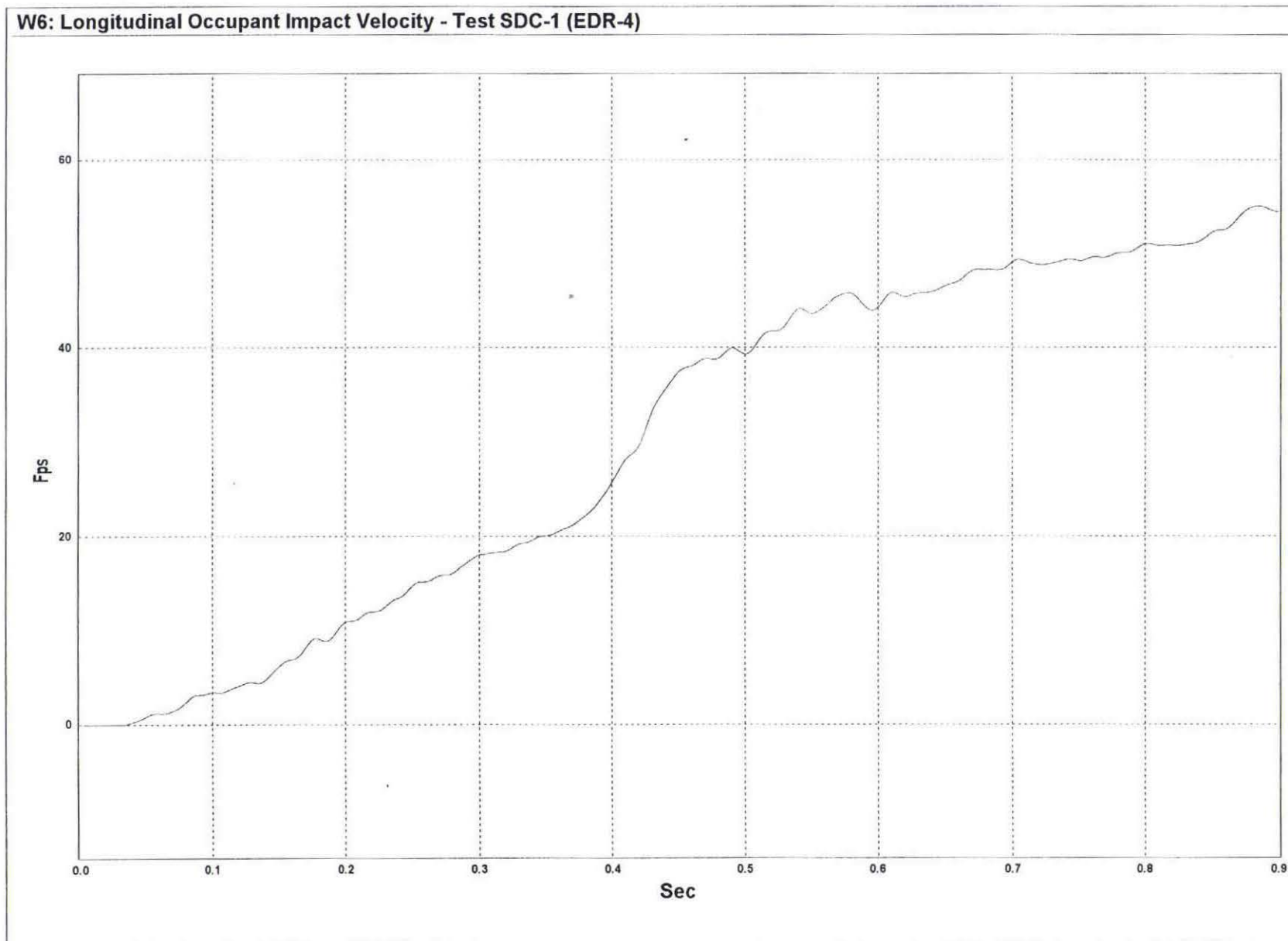


Figure B-2. Graph of Longitudinal Occupant Impact Velocity, Test SDC-1

W12: Longitudinal Occupant Displacement - Test SDC-1 (EDR-4)

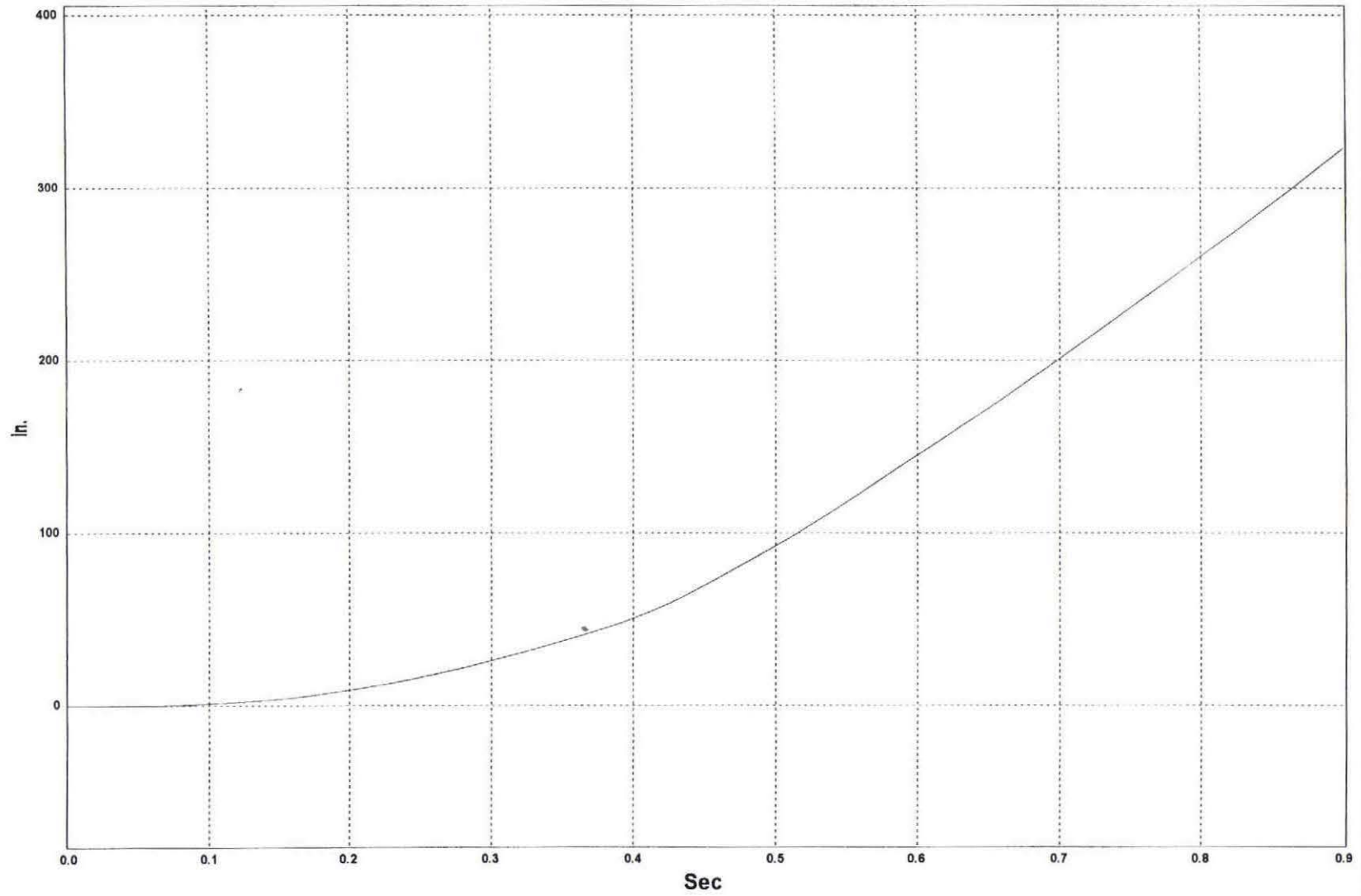


Figure B-3. Graph of Longitudinal Occupant Displacement, Test SDC-1

W5: Lateral Deceleration - Test SDC-1 (EDR-4)

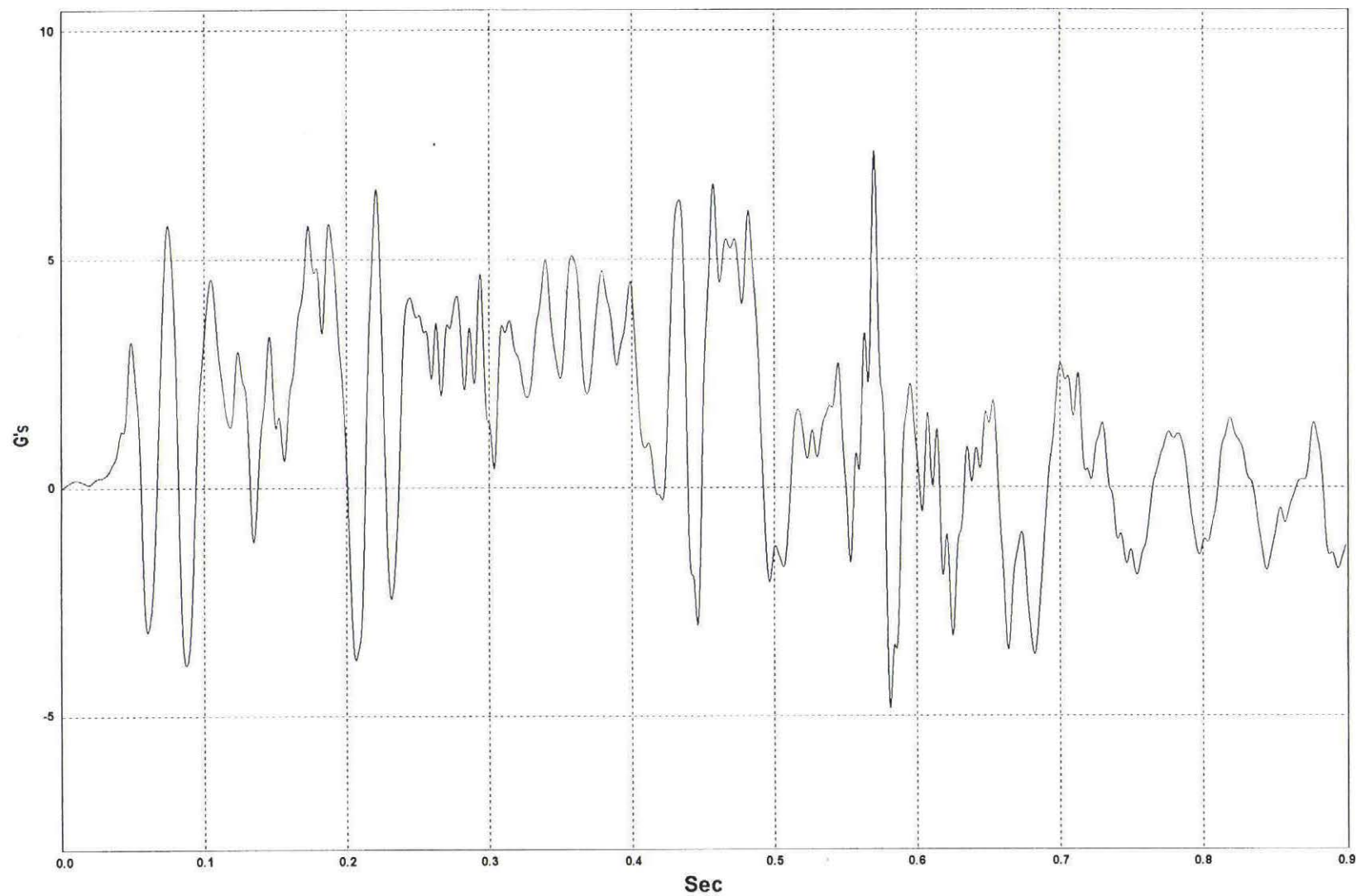


Figure B-4. Graph of Lateral Deceleration, Test SDC-1

W6: Lateral Occupant Impact Velocity - Test SDC-1 (EDR-4)

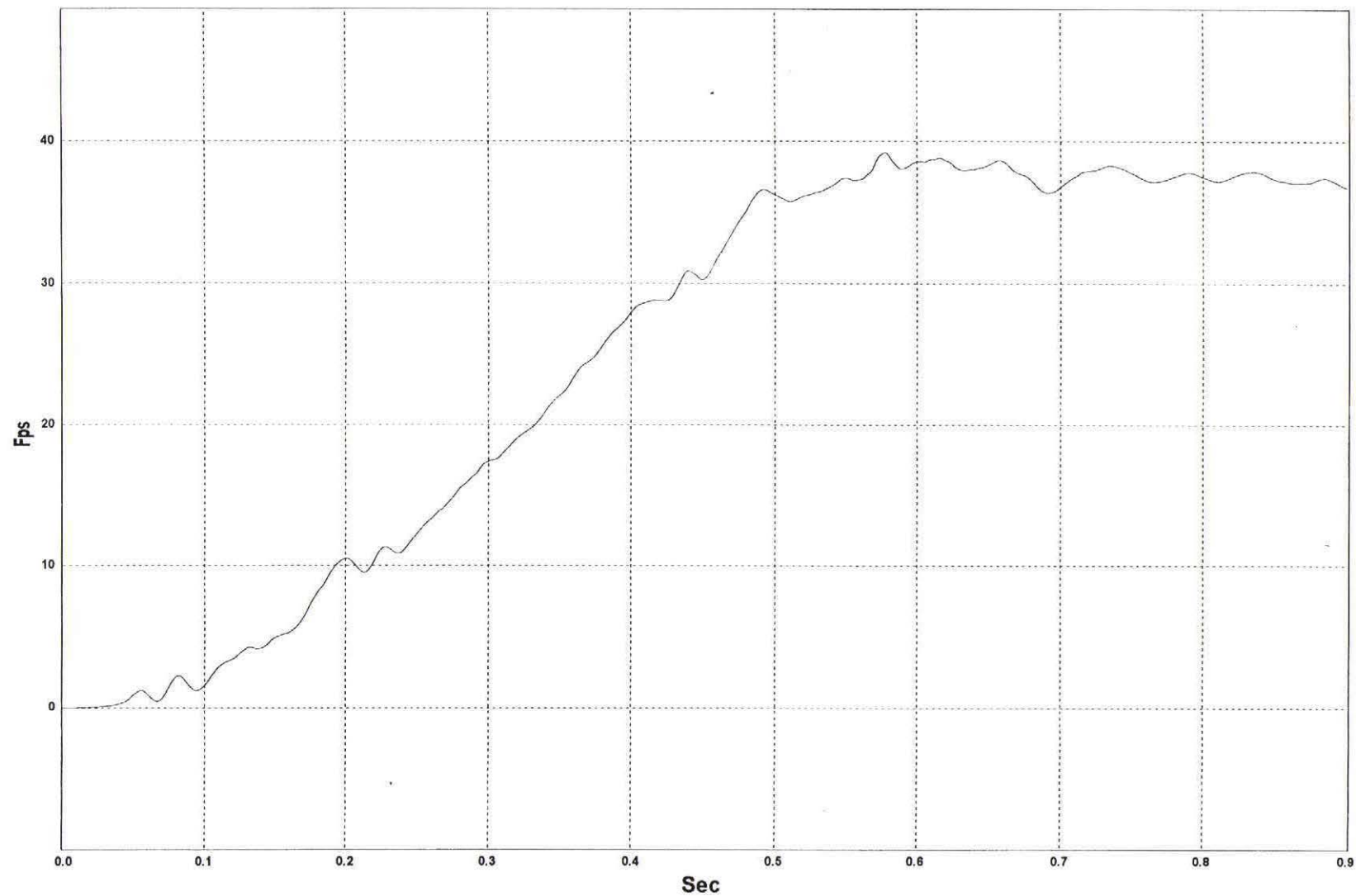


Figure B-5. Graph of Lateral Occupant Impact Velocity, Test SDC-1

W7: Lateral Occupant Displacement - Test SDC-1 (EDR-4)

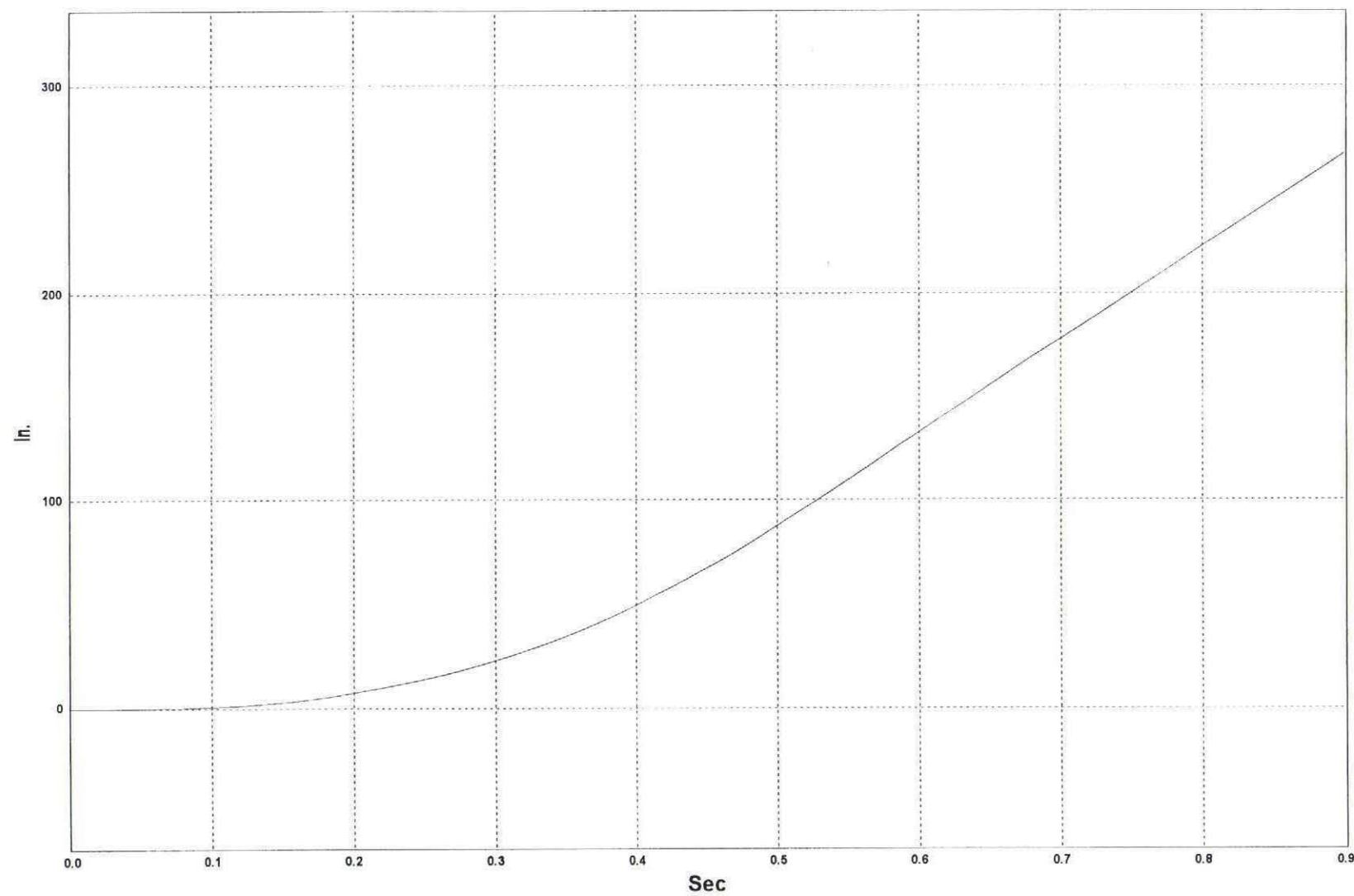


Figure B-6. Graph of Lateral Occupant Displacement, Test SDC-1

APPENDIX C

RATE TRANSDUCER DATA ANALYSIS, SDC-1

Figure C-1. Graph of Roll, Pitch, and Yaw Angular Displacements, Test SDC-1

W19: TEST SDC-1 UNCOUPLED ANGULAR DISPLACEMENTS

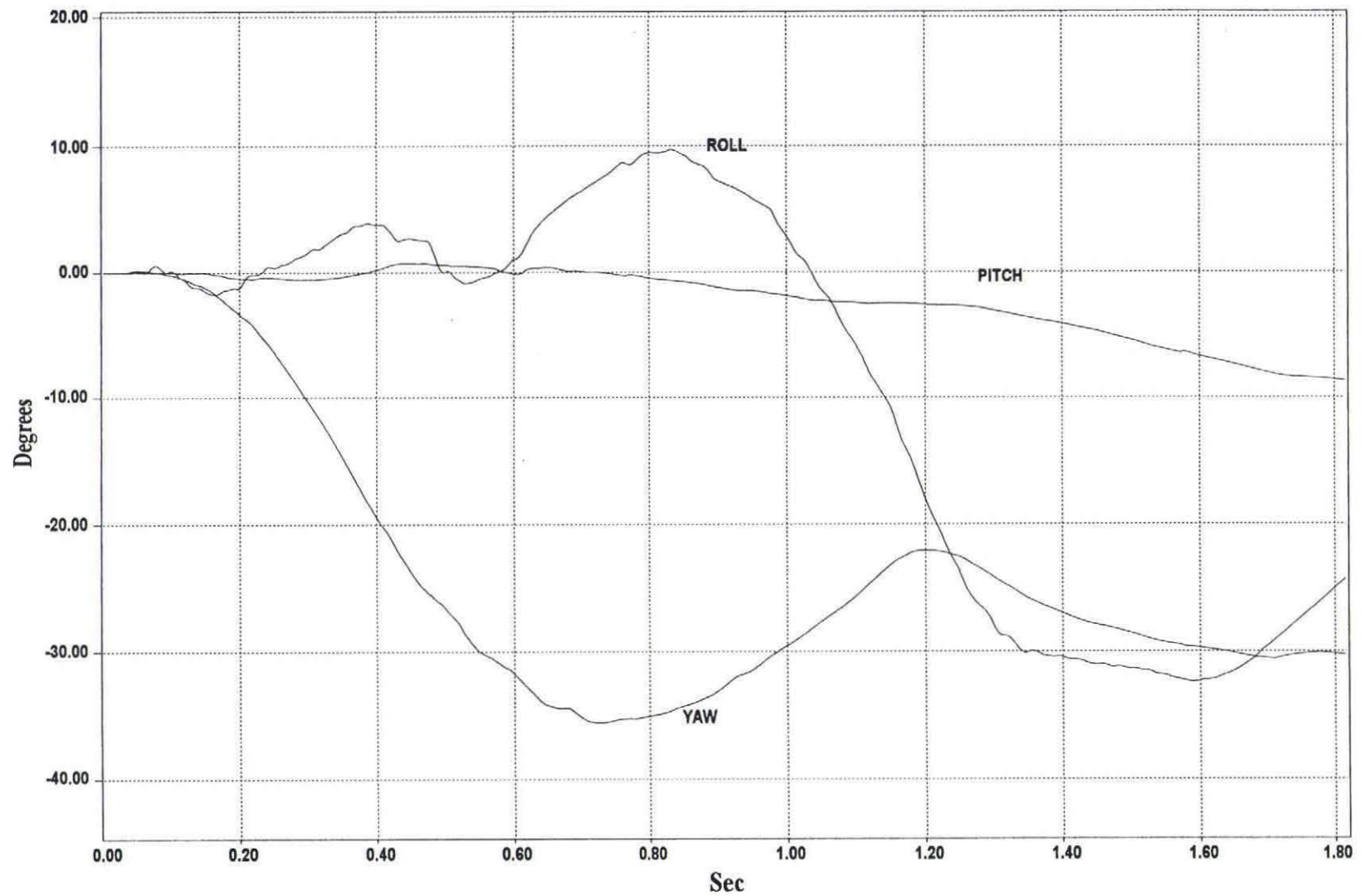


Figure C-1. Graph of Roll, Pitch, and Yaw Angular Displacements, Test SDC-1

APPENDIX D

ACCELEROMETER DATA ANALYSIS, SDC-2

Figure D-1. Graph of Longitudinal Deceleration, Test SDC-2

Figure D-2. Graph of Longitudinal Occupant Impact Velocity, Test SDC-2

Figure D-3. Graph of Longitudinal Occupant Displacement, Test SDC-2

Figure D-4. Graph of Lateral Deceleration, Test SDC-2

Figure D-5. Graph of Lateral Occupant Impact Velocity, Test SDC-2

Figure D-6. Graph of Lateral Occupant Displacement, Test SDC-2

W5: Longitudinal Deceleration - Test SDC-2 (EDR-4)

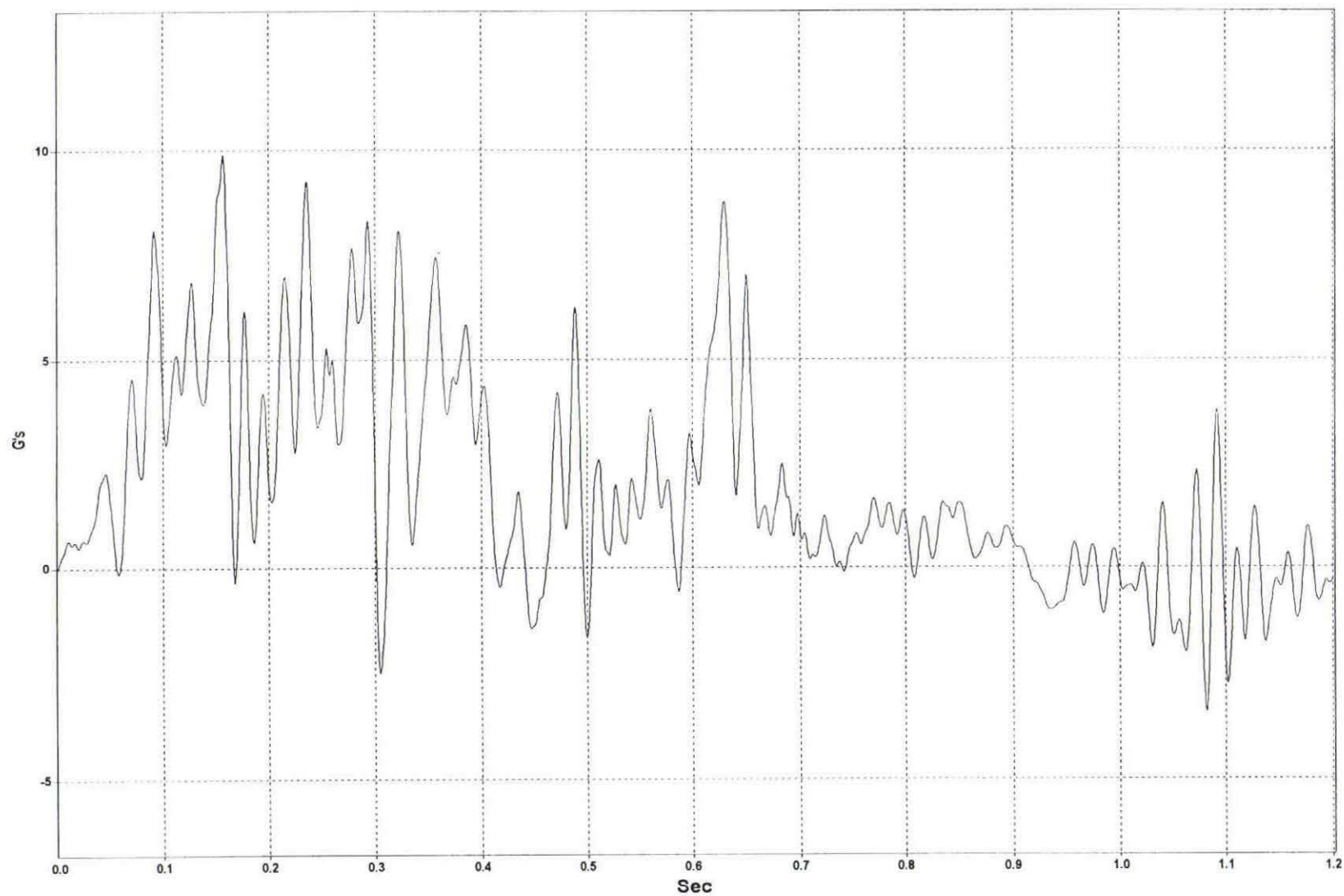


Figure D-1. Graph of Longitudinal Deceleration, Test SDC-2

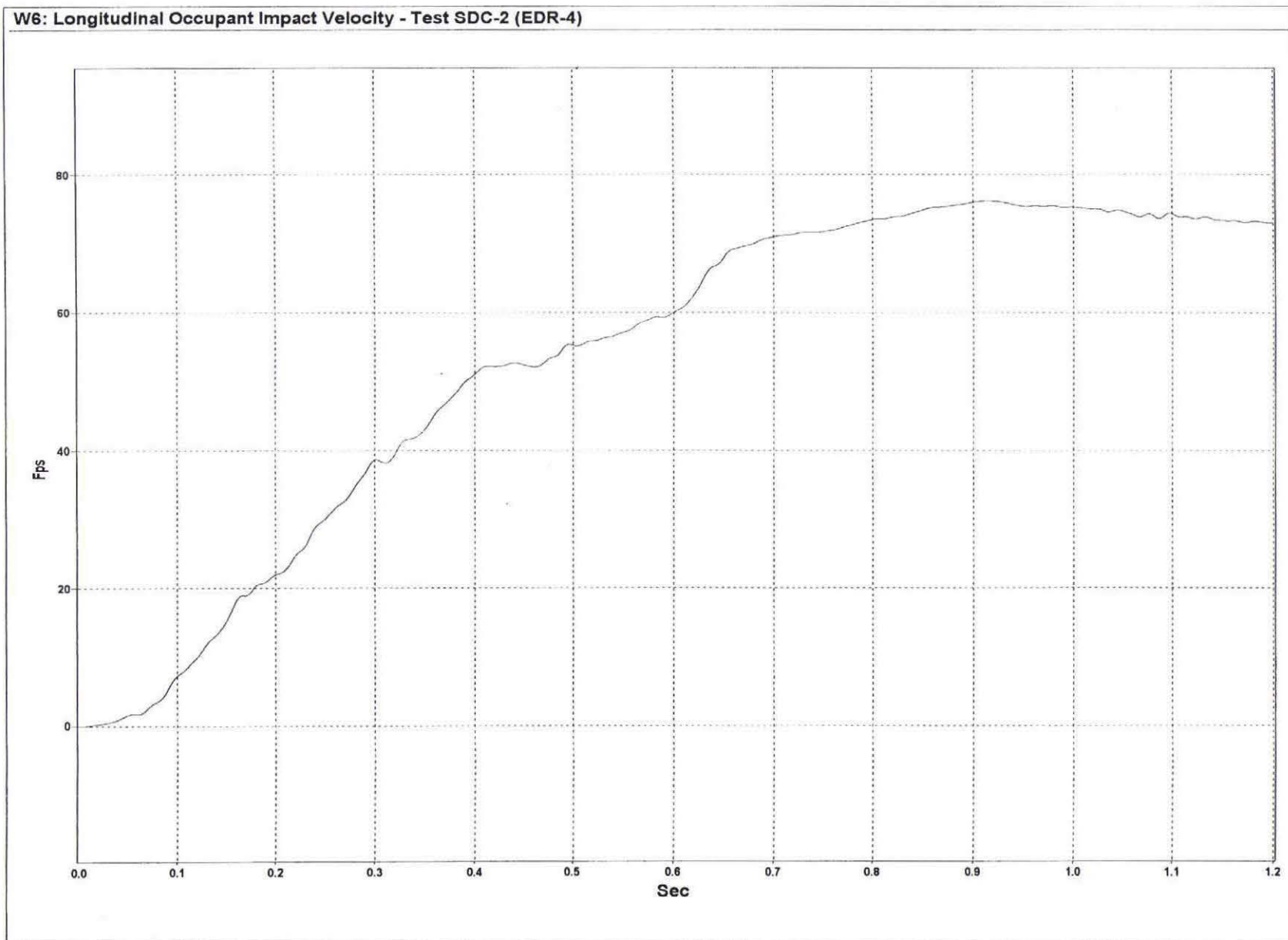


Figure D-2. Graph of Longitudinal Occupant Impact Velocity, Test SDC-2

W12: Longitudinal Occupant Displacement - Test SDC-2 (EDR-4)

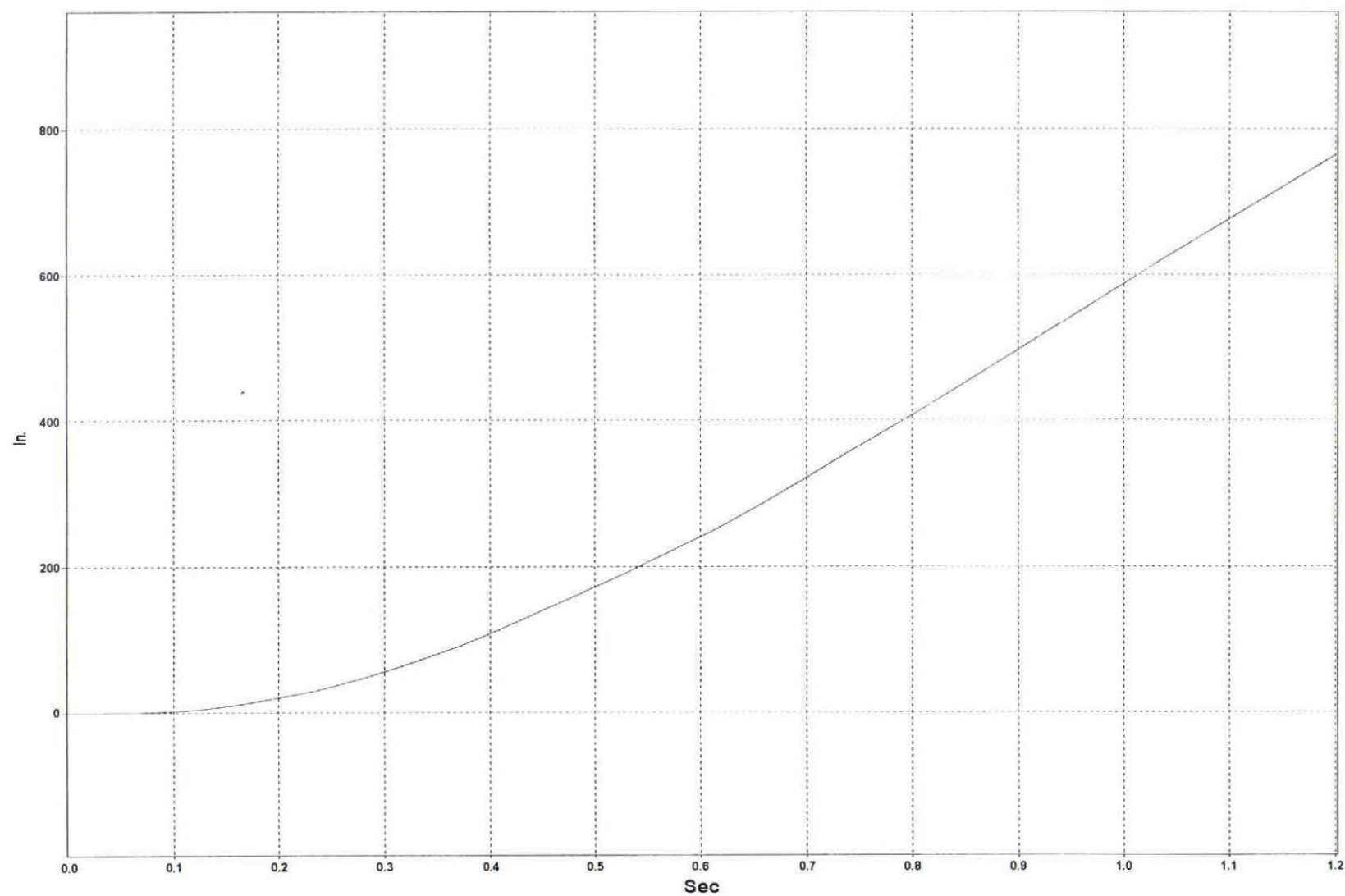


Figure D-3. Graph of Longitudinal Occupant Displacement, Test SDC-2

W6: Lateral Deceleration - Test SDC-2 (EDR-4)

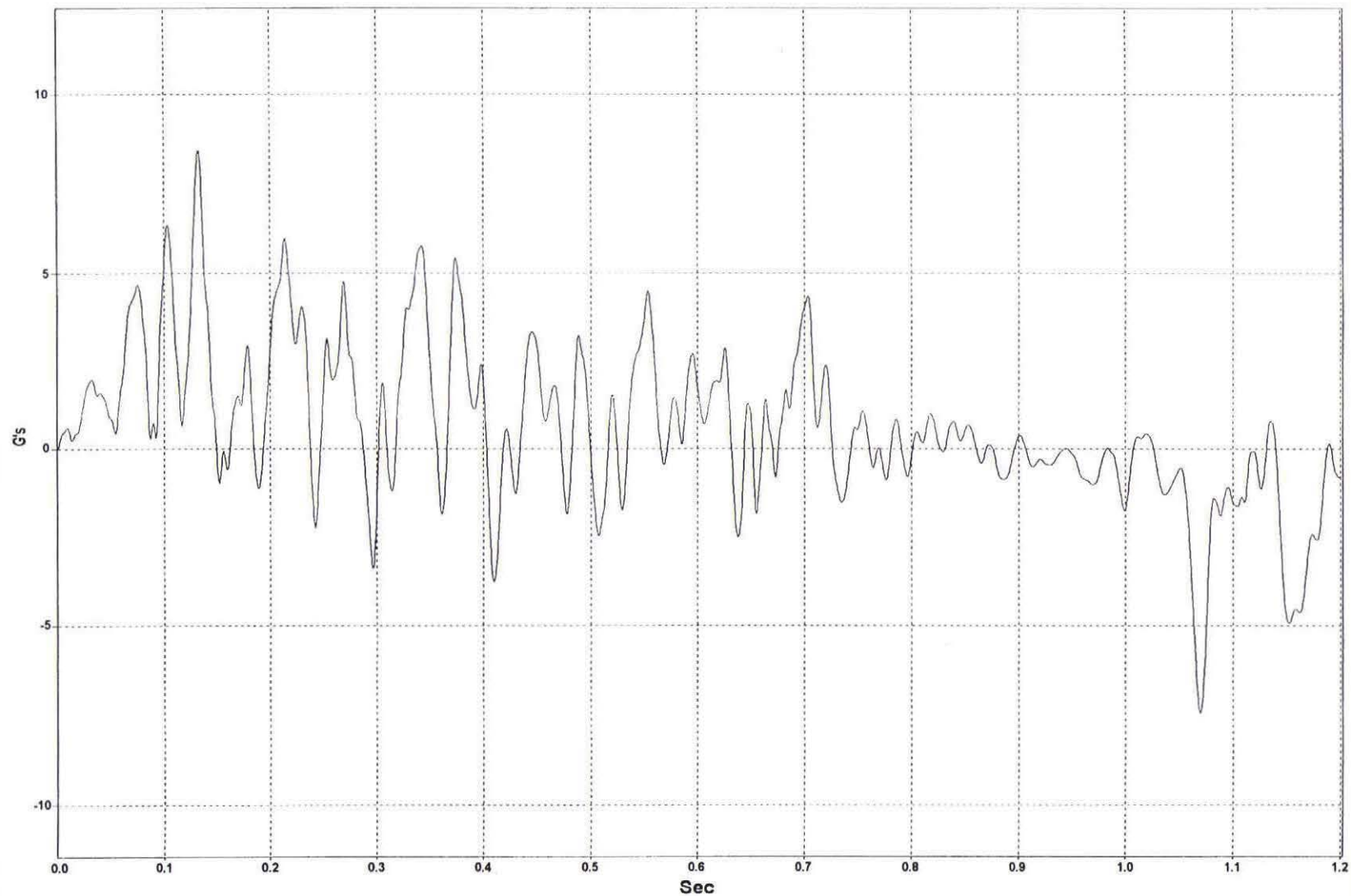


Figure D-4. Graph of Lateral Deceleration, Test SDC-2

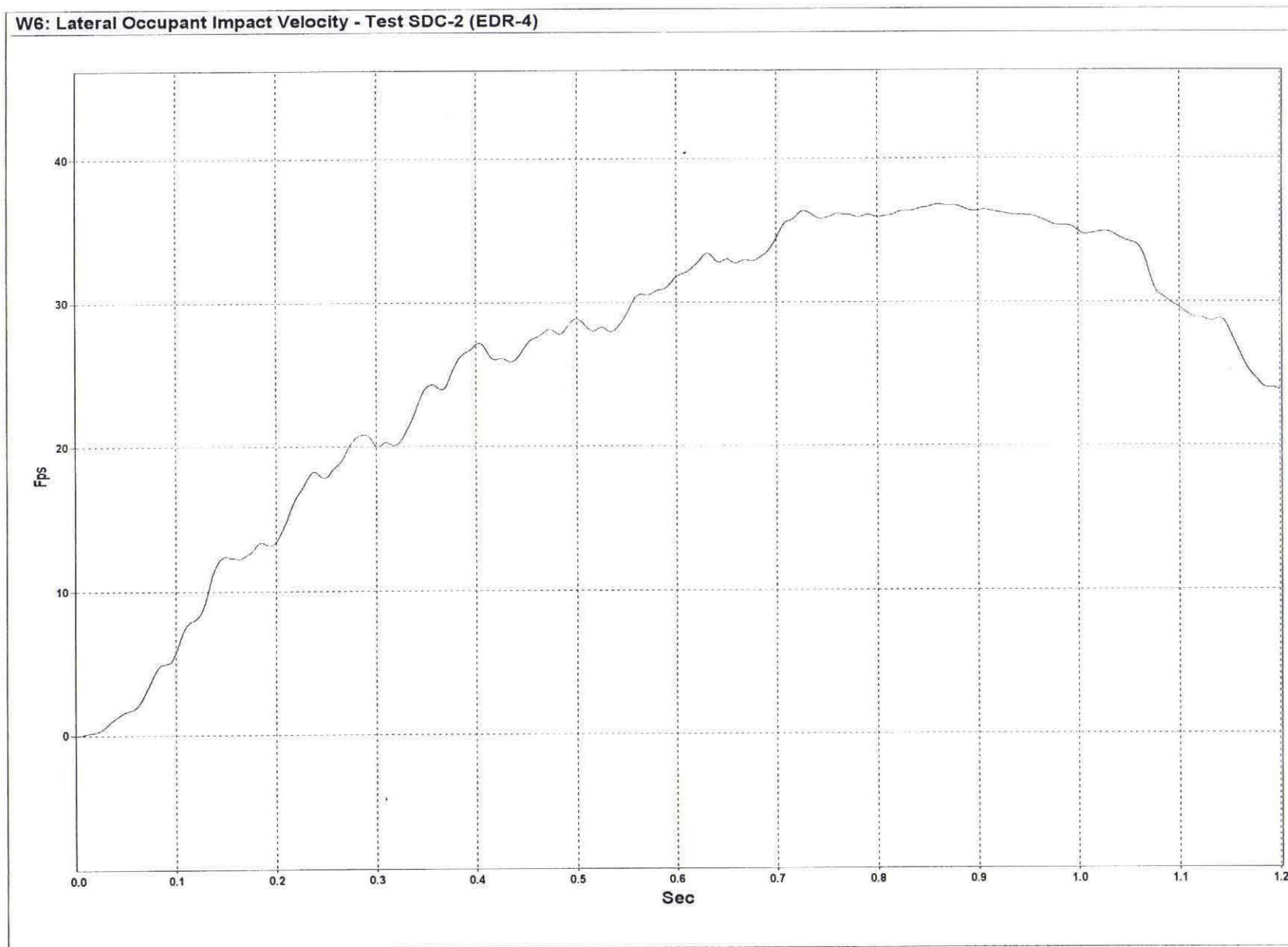


Figure D-5. Graph of Lateral Occupant Impact Velocity, Test SDC-2

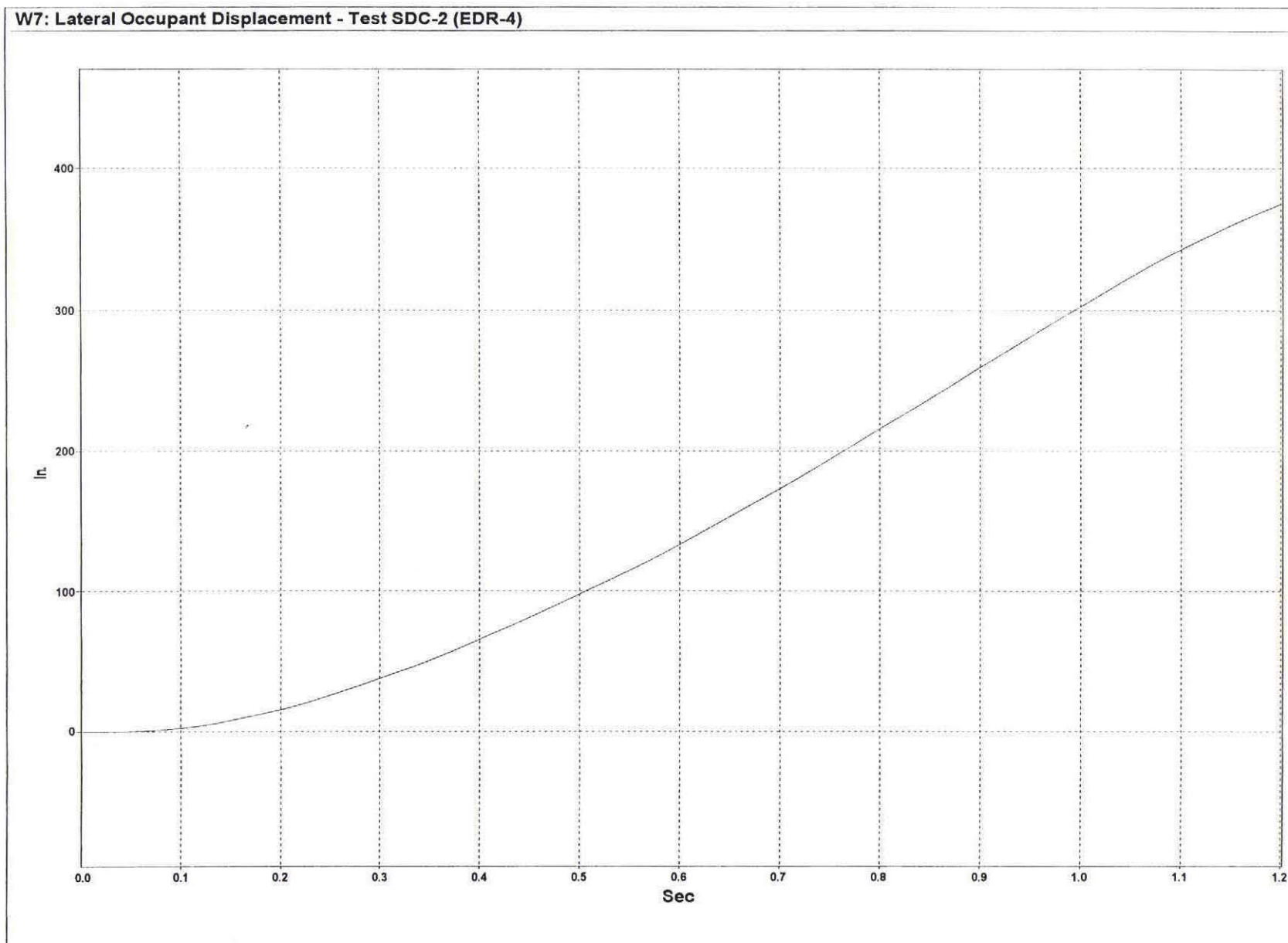


Figure D-6. Graph of Lateral Occupant Displacement, Test SDC-2

APPENDIX E

RATE TRANSDUCER DATA ANALYSIS, SDC-2

Figure E-1. Graph of Roll, Pitch, and Yaw Angular Displacements, Test SDC-2

W19: TEST SDC-2 UNCOUPLED ANGULAR DISPLACEMENTS

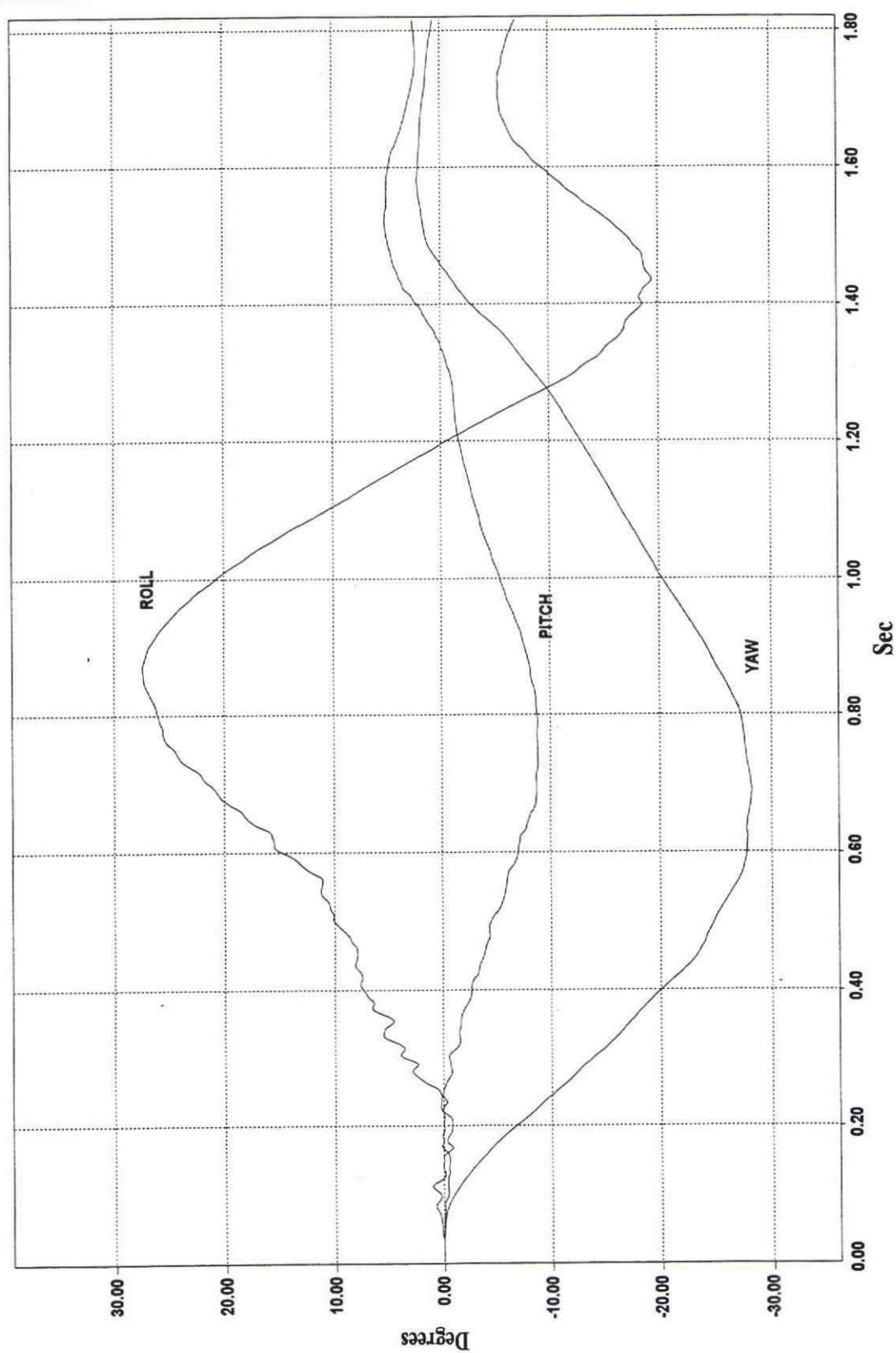


Figure E-1. Graph of Roll, Pitch, and Yaw Angular Displacements, Test SDC-2

APPENDIX F

ACCELEROMETER DATA ANALYSIS, SDC-3

Figure F-1. Graph of Longitudinal Deceleration, Test SDC-3

Figure F-2. Graph of Longitudinal Occupant Impact Velocity, Test SDC-3

Figure F-3. Graph of Longitudinal Occupant Displacement, Test SDC-3

Figure F-4. Graph of Lateral Deceleration, Test SDC-3

Figure F-5. Graph of Lateral Occupant Impact Velocity, Test SDC-3

Figure F-6. Graph of Lateral Occupant Displacement, Test SDC-3

W5: Longitudinal Deceleration - Test SDC-3 (EDR-4)

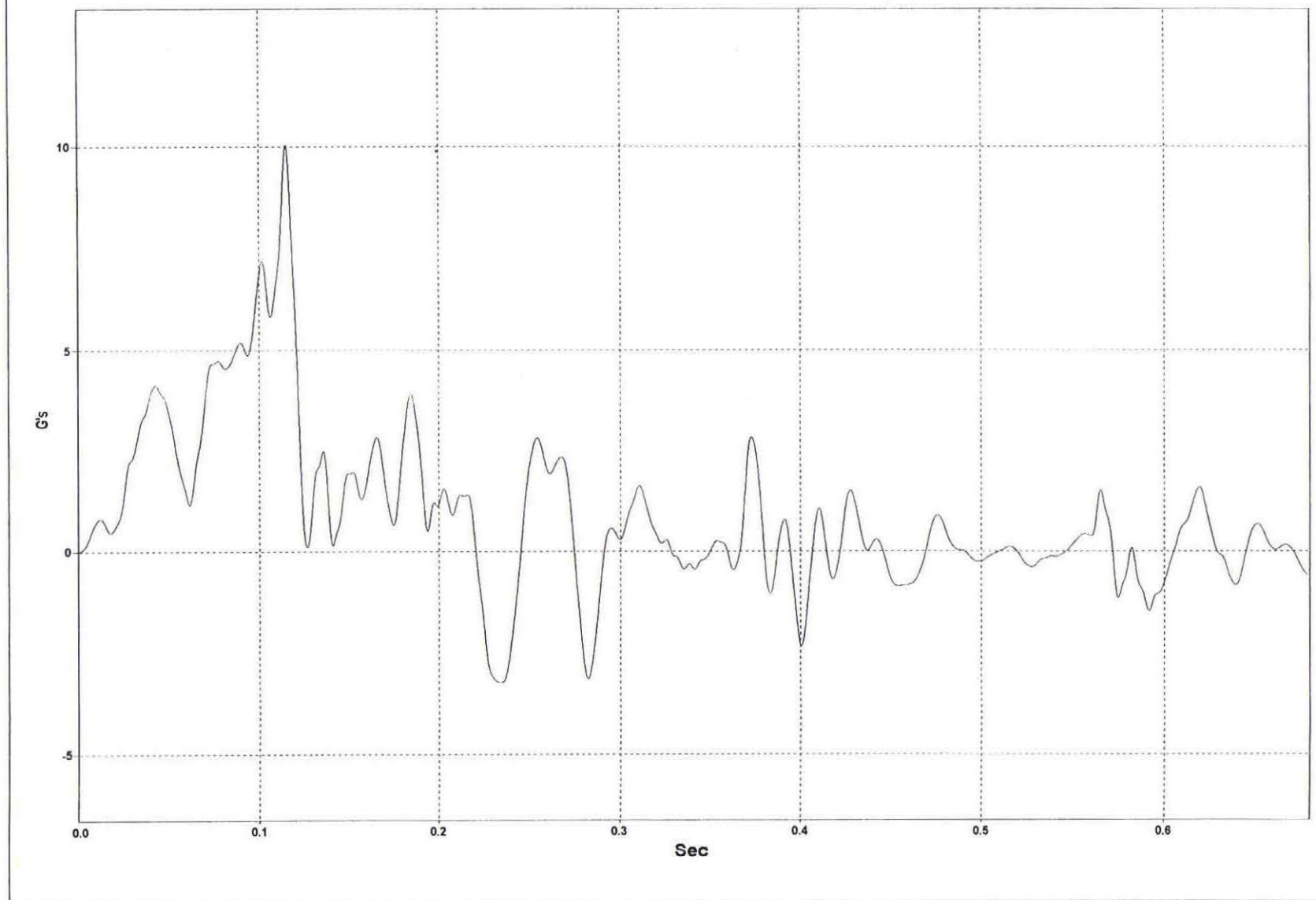


Figure F-1. Graph of Longitudinal Deceleration, Test SDC-3

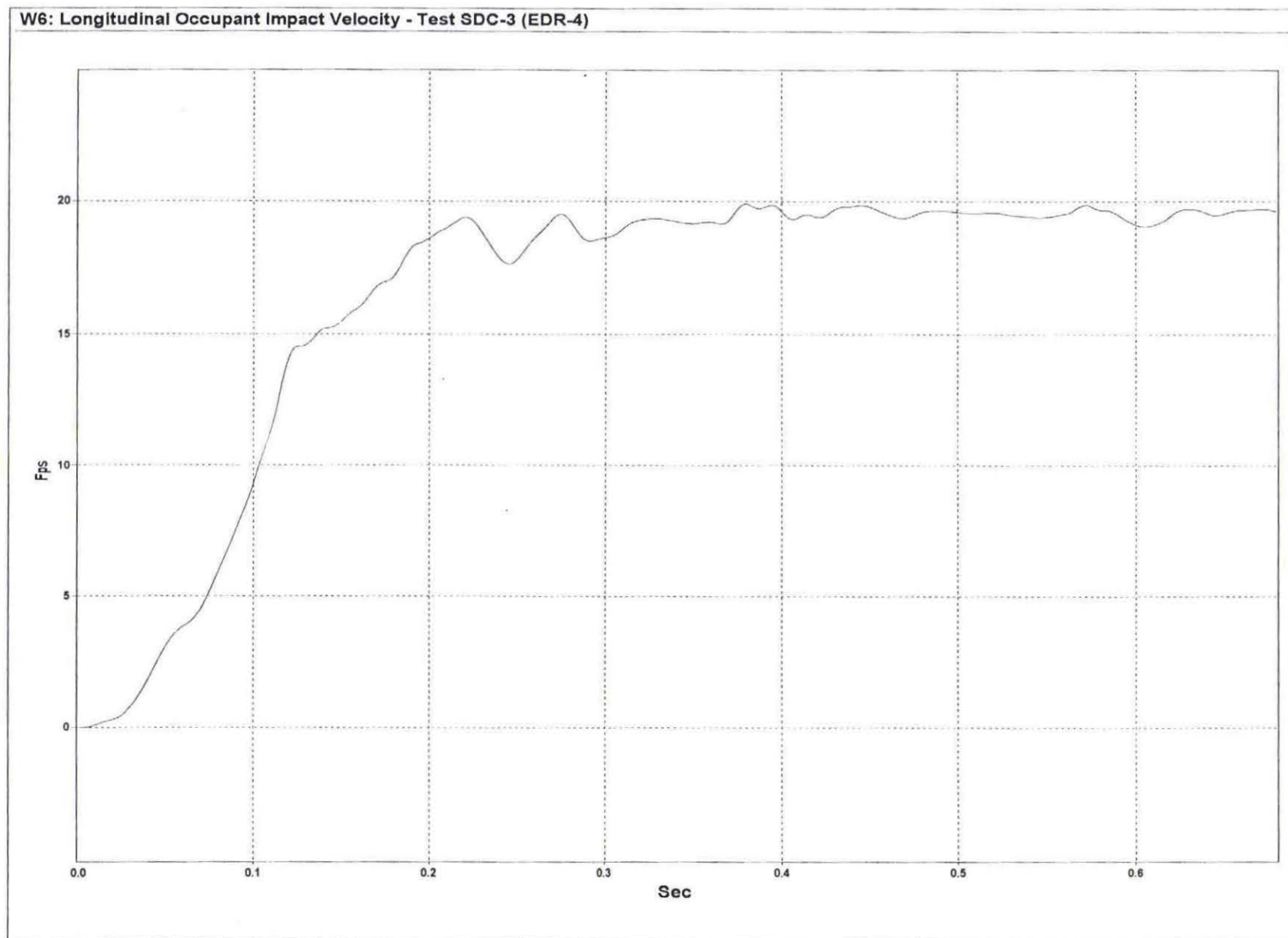


Figure F-2. Graph of Longitudinal Occupant Impact Velocity, Test SDC-3

W12: Longitudinal Occupant Displacement - Test SDC-3 (EDR-4)

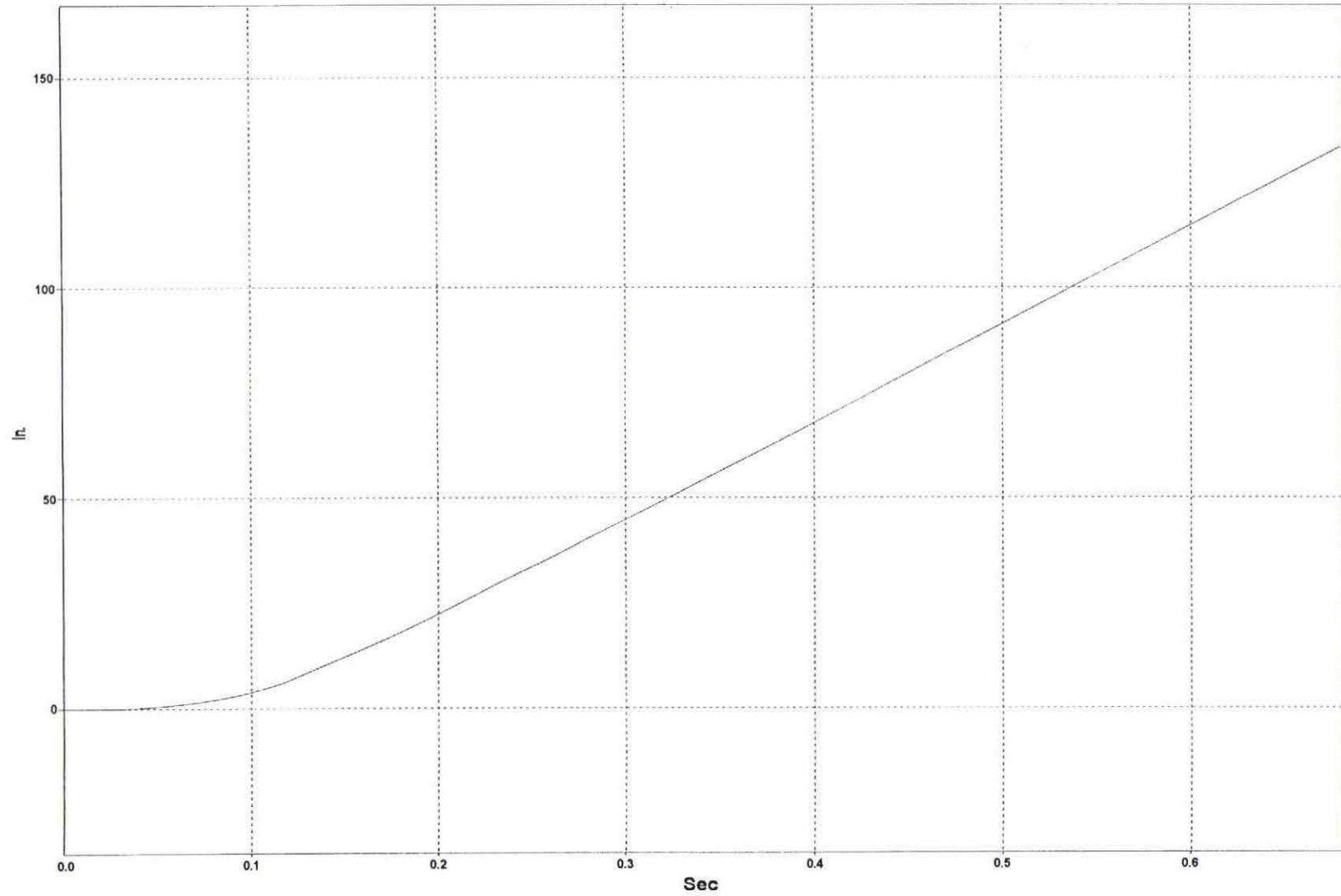


Figure F-3. Graph of Longitudinal Occupant Displacement, Test SDC-3

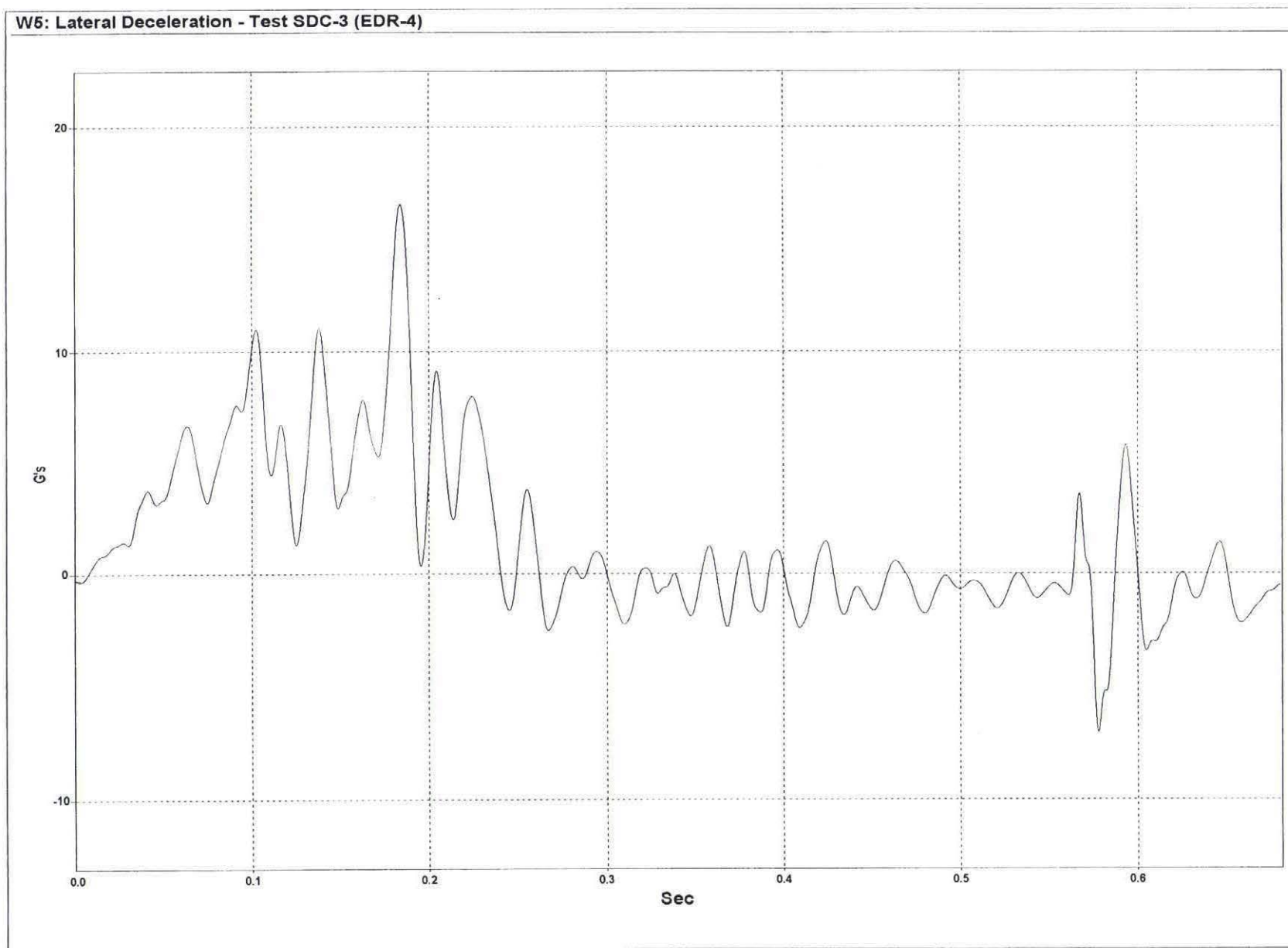


Figure F-4. Graph of Lateral Deceleration, Test SDC-3

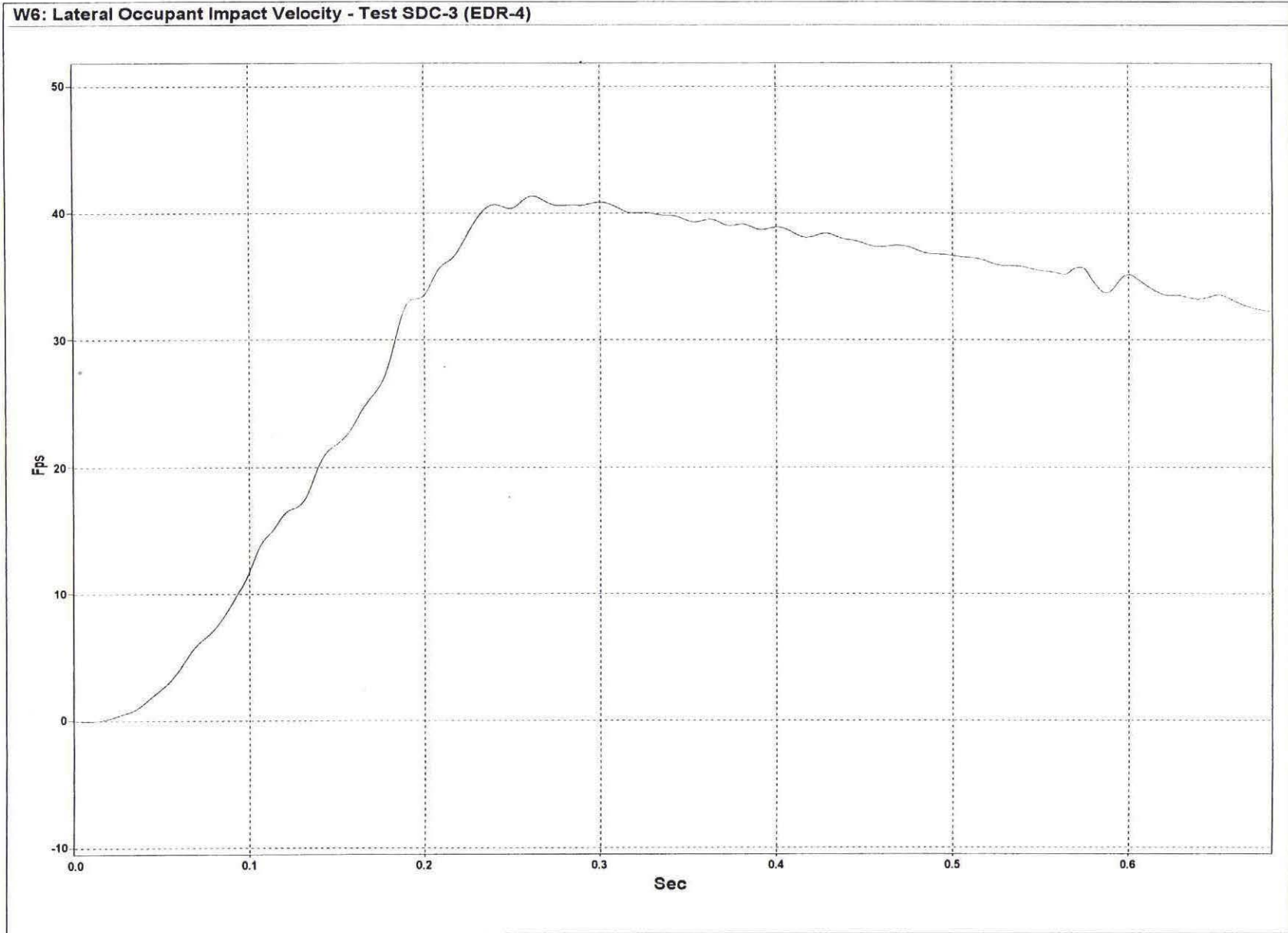


Figure F-5. Graph of Lateral Occupant Impact Velocity, Test SDC-3

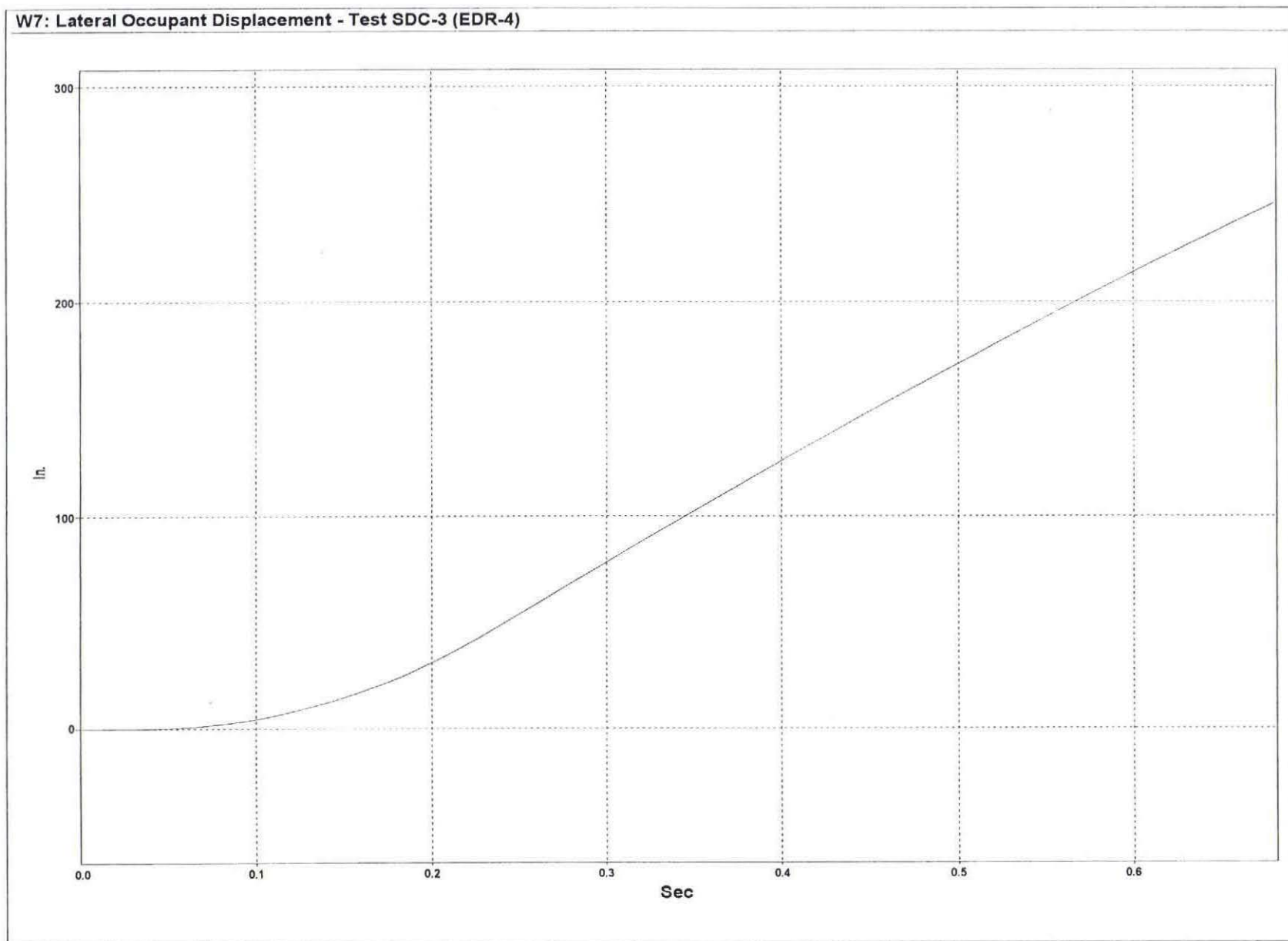


Figure F-6. Graph of Lateral Occupant Displacement, Test SDC-3

APPENDIX G

RATE TRANSDUCER DATA ANALYSIS, SDC-3

Figure G-1. Graph of Roll, Pitch, and Yaw Angular Displacements, Test SDC-3

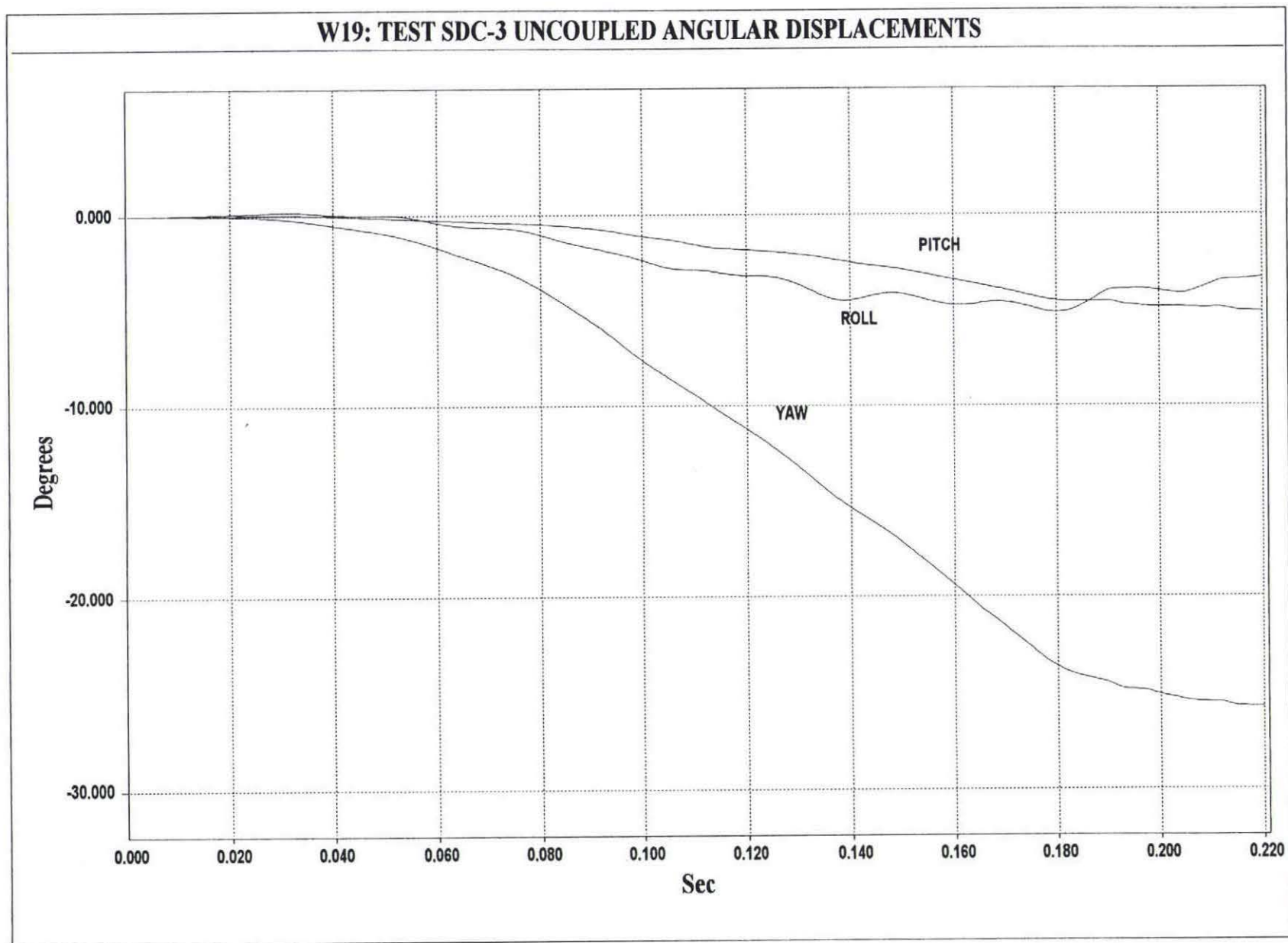


Figure G-1. Graph of Roll, Pitch, and Yaw Angular Displacements, Test SDC-3